UV NEWS

The official newsletter of the Thematic Network for Ultraviolet Measurements

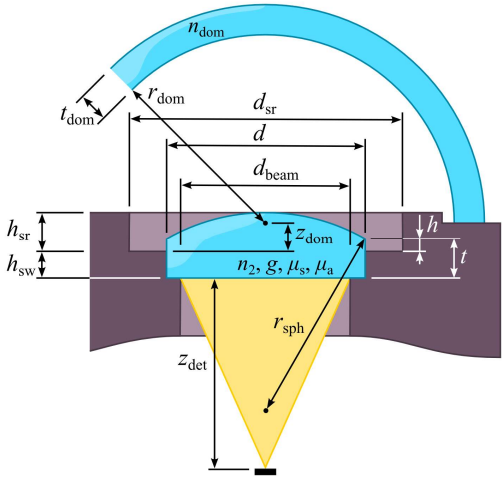

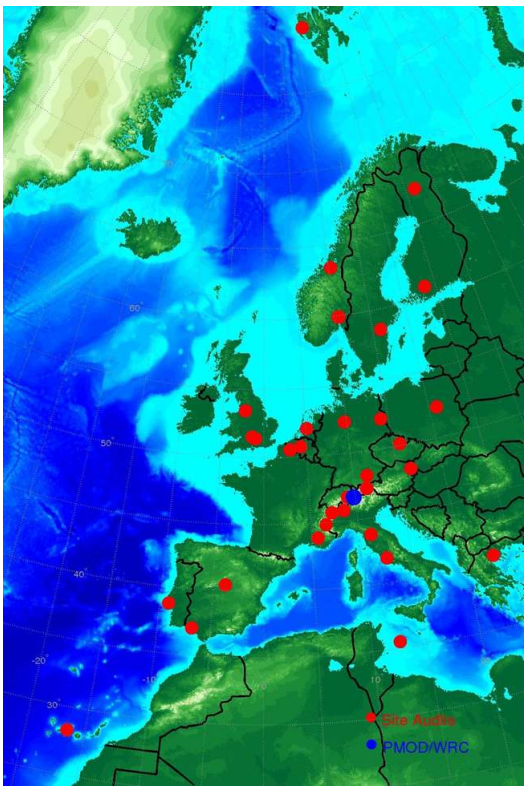

Issue 9 / January 2013

Aalto University

EMRP
European Metrology Research Programme
Programme of EURAMET

The EMRP is jointly funded by the EMRP participating countries within EURAMET and the European Union

Contents

ISSN 1456-2537

Unigrafia, Espoo 2013

UVNews is the official newsletter of the Thematic Network for Ultraviolet Measurements. The Network was originally funded by the Standards, Measurements and Testing programme of the Commission of the European Communities, as project number SMT4-CT97-7510. During 2011 – 2014 the Network gets financing from the Euramet through project EMRP ENV03 "Traceability for surface spectral solar ultraviolet radiation." *UVNews* is published at irregular intervals. It is aimed to exchange knowledge between the participants of the Network and to disseminate information on the forthcoming and past activities of the Network. The newsletter also contains scientific and technical articles on UV measurements and a news-section about activities in the field of UV measurements. The newsletter welcomes all announcements and articles that might be of importance for the readers. The editor of the Newsletter may be reached by:

Aalto University
Metrology Research Institute
Petri Kärhä
P. O. Box 13000
FIN-00076 Aalto, Finland

http://metrology.hut.fi/uvnet/

E-mail: petri.karha@aalto.fi

In case of all material to publish, submission by E-mail is preferred. The next issue will be published in July 2014.

Photographs: Cover: Selected Figures from the articles. Page 3: Participants of the Kick-off meeting of project EMRP ENV03 "Traceability for surface spectral solar ultraviolet radiation," (Picture by PMOD) Page 55: Restored main building of PMOD / WRC (Picture by PMOD).

Editorial

Petri Kärhä
Aalto University School of Electrical Engineering, Finland

The Thematic Network for Ultraviolet Measurements has been rather quiet since 2006. Now it is my pleasure to announce that we have received funding from the European Union to continue our operation for a while.

The funding takes place within the European Metrology Research Program (EMRP) Project ENV03 "Traceability for surface spectral solar ultraviolet radiation." More information on this project is given in the article starting on page 4, written by Julian Gröbner of PMOD/WRC, the coordinator of the project. *UVNet* will be used to disseminate information on the achievements in the project, among other UV-related news we distribute.

Our most visible activities will be a workshop, a solar UV intercomparison at Davos in summer 2014, and two issues of the newsletter *UVNews*, of which this is the first one. The second one is scheduled for July 2014.

This *UVNews* 9 has a dedicated section for presenting activities of the project on pp. 4 – 24. The project is in its midway. As you may see, some activities have progressed quite far already; some are still in advanced planning stage. It is still possible to take part in the activities. The project is open for collaboration (projects.pmodwrc.ch/env03/index.php/collaboration).

UVNews 10 will be issued near the final stage of the project. It will thus naturally include a special section for presenting the results of the project. If successful, we will have plenty of novel and improved instrumentation to use in solar UV measurements.

This *UVNews* includes 30 pages of regular articles starting on p. 25. It is nice to see that many interesting things are taking place in the field. *UVNews* 10 will include regular articles as well. This newsletter will be collected in spring 2014. To receive the call for articles, please register to the *UVNet* mailing list (http://metrology.tkk.fi/uvnet/lists.htm) if you do not receive our E-mails already. The same page can be used to unsubscribe from the mailing list.

More information on the coming workshop can be found on p. 55.

Finally, I would like to wish you all a nice spring and hope to see you in the coming UV activities!

EMRP ENV03 Traceability for surface spectral solar ultraviolet radiation

The EMRP Project "Traceability for surface spectral solar ultraviolet radiation"

Julian Gröbner and the SolarUV consortium

Physikalisch-Meteorologisches Observatorium Davos, World Radiation Center, Davos, Switzerland

Introduction

Long-term trends in surface solar radiation due to atmospheric induced changes (termed global dimming and global brightening), have demonstrated decadal changes of the order of 2% per decade over Europe [1]. These changes are currently explained by changes in the transparency of the atmosphere (aerosols) and possibly long-term changes in clouds (cloud fraction and cloud opacity). The effects on UV radiation have not yet been quantified due to the difficulty of observing these small changes over such long time scales. Future scenarios of UV radiation changes have been estimated using Global Climate Models (GCM).

Solar UV changes were estimated for the period 1960 to 2100 using the coupled chemistry and climate model SOCOL [2]. As is shown in this study, solar UV levels tend to decrease during the 21st century by 5 to 15% in middle latitudes, corresponding to a change of less than 2% per decade (see Figure 1).

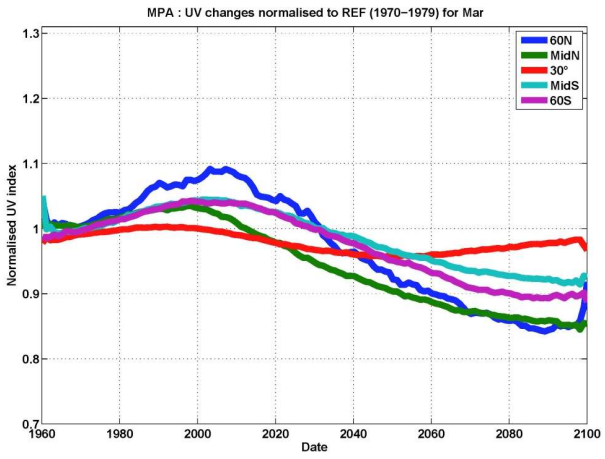

Figure 1. Evolution of monthly averaged erythemaly weighted irradiances relative to the 1970-1979 average in March and at 5 latitudinal bands.

Another study obtained with a different GCM shows contradicting results, with UV increases or decreases of 5 to 10% over the same time period depending on the assumed climate scenario used to feed the calculations [3]. Thus, projected UV radiation changes are expected to be significant, but neither magnitude nor sign of the UV radiation changes can be estimated with reliability, demonstrating the necessity for a concerted global long-term UV monitoring effort.

Detecting UV changes of this magnitude over such long time scales requires substantial efforts on the quality management of a monitoring station. Assuming a linear change in erythemal weighted UV irradiance of 15% between now and the end of the century would result in a change of 1.5% per decade. Unfortunately, such changes are not detectable with current instruments having measurement uncertainties of about 5%. Thus, a primary goal for detecting future changes in solar UV radiation requires not only significant improvements in the characterisation and operation of solar UV instruments, but also in the traceability of solar UV radiation from the primary reference standard operated by National Metrology Institutes to the measurements of a field instrument deployed at a UV monitoring site.

The Project SolarUV

The project ***Traceability for surface spectral solar ultraviolet radiation*** will address these issues in the frame of the European Metrology Research Programme which is jointly funded by the European Union and the member states of EURAMET. The three-year project has a budget of approximately 4 M€ and started in August 2011. It has 8 partners from National Metrology Institutes (NMI), 2 from industry and 4 from academic or research centres.

Its primary goal is to considerably decrease uncertainties of spectral solar UV radiation measurements from the current level of ±5% to values of ±1% to ±2%. A second major activity will consist in optimising and developing characterisation methods and operational procedures for array spectroradiometers in order to deploy them as cost effective network instruments for solar UV radiation measurements, eventually replacing current filter radiometers.

The main task of this project will be to improve and upgrade the portable reference spectroradiometer QASUME in order to provide traceable UV irradiance measurements to UV monitoring sites in Europe and World-Wide [5]. This will be achieved by developing

- a detector-based spectral irradiance calibration chain using PTB's tuneable laser suite to achieve traceable UV measurements with considerably lower uncertainties,
- stable, compact and portable UV LED based transfer standards suitable for field calibrations,

- new solid-state based detectors (SSDS) as replacements for current photomultiplier tubes (PMT) using a switched integrator amplifier,
- Global entrance-optics with angular response errors of ±1% down to 80° zenith angle,
- Wavelength scale characterisation devices to determine the wavelength-grating drive relation with ±0.01 nm uncertainty.

With regard to array spectroradiometers, the main activity concerns the development of a comprehensive stray-light correction procedure in order to correct for in-range and out-range straylight as well as homogenising the resulting spectra in terms of wavelength and spectral bandwidth. As an initial task, a guideline document describing best-practice methods for operating array spectroradiometers measuring solar UV radiation was prepared and presented at the international radiation symposium in August 2012 [4].

Results

This edition of *UVNews* features several contributions from consortium members describing recent developments in several key aspects of the SolarUV project. As an example, we will describe here preliminary results we obtained in view of designing a SSDS detector as replacement for photomultiplier tubes [6]. While the expected benefits are improved stability and linearity, the challenge of using SSDS is to achieve sufficient sensitivity for detection of the very low radiation levels in the UV-B range of the solar spectrum.

The following figures shows preliminary results from a prototype SSDS detector based on a silicon detector placed at the exit slit of QASUME. The spectral response of the PMT was determined by installing a calibrated photodiode at the exit slit of QASUME instead of the PMT. From previous solar measurements, the expected output power for a nominal solar spectrum was estimated to be between 1 fW and 1 nW, resulting in an expected detector noise of 1% at 298 nm, as shown in Figure 2.

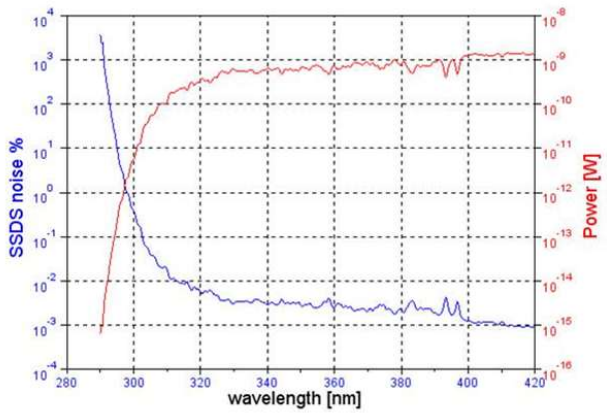

Figure 2. Estimated output power at the exit slit of QASUME and the corresponding detector noise from a silicon detector connected to a low-noise switched integrator amplifier.

This estimation was verified during a field campaign at Davos in October 2012 by measuring solar spectra with the prototype SSDS connected to QASUME. As shown in Figure 3, the standard deviation of the measurements remains below 1% for wavelengths longer than 307 nm, rising to 10% at around 301 nm, for diode currents of the order of 10 fA. While the measurements demonstrate the feasibility of using SSDS as potential replacements for PMT, significant improvements in the sensitivity are expected by the use of novel detector materials such as ZnO detectors being manufactured within the project.

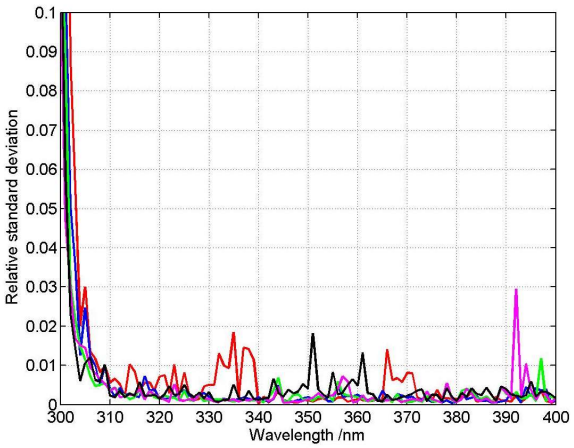

Figure 3. Relative standard deviation of several solar measurements using a prototype silicon solid state device as detector at the exit slit of the QASUME spectroradiometer. The noise peaks are due to changing weather conditions unrelated to the SSDS performance, while at short wavelength below 320 nm one can see a gradual increase of the noise due to the low signal levels.

Conclusion and outlook

The current status of the project, as well as a description of the devices and methods being developed within this project can be found on the project homepage at http://projects.pmodwrc.ch/env03/

The project results will be mainly disseminated through standard channels such as peer-reviewed publications and presentations at dedicated workshops and international conferences.

The next workshop will be held on 27 and 28 August 2013 at PMOD/WRC, Davos to present the latest results of this project to the UV community. If you are interested in participating at this workshop, or plan to submit a presentation, please contact either Julian Gröbner (julian.groebner@pmodwrc.ch) or Petri Kärhä (petri.karha@aalto.fi) for additional information or check for news on the project home-site.

Finally, an intercomparison campaign with adjoined workshop will be organised in early July 2014 at PMOD/WRC in order to demonstrate the devices and tools developed within the project. Operators of solar UV spectroradiometers (scanning and array spectroradiometers) are invited to participate at this event with their instrument to benefit from a direct traceability of solar UV measurements with reduced uncertainties of ±1% to ±2%.

Acknowledgement. This report was compiled within the EMRP ENV03 Project "Traceability for surface spectral solar ultraviolet radiation." The EMRP is jointly funded by the EMRP participating countries within EURAMET and the European Union.

References

[1] M. Wild, "Global Dimming and brightening: A review," *J. Geophys. Res.* **114**, doi: 10.1029/ 2008JD011470 (2009).

[2] Egorova, T., Rozanov, E., Gröbner, J., Hauser, M., and Schmutz, W., "Montreal Protocol benefits simulated with CCM SOCOL," *Atmos. Chem. Phys. Discuss.* **12**, 17001-17030, doi:10.5194/acpd-12-17001-2012 (2012).

[3] Watanabe, S., K. Sudo, T. Nagashima, T. Takemura, H. Kawase, and T. Nozawa, "Future projections of surface UV-B in a changing climate," *J. Geophys. Res.* **116**, D16118, doi:10.1029/2011JD015749 (2011).

[4] Blumthaler M., J Gröbner, L Egli and S Nevas, "A Guide to Measuring Solar UV Spectra using Array Spectroradiometers," IRS (in press).

[5] Gröbner, J., J. Schreder, S. Kazadzis, A. F. Bais, M. Blumthaler, P. Görts, R. Tax, T. Koskela, G. Seckmeyer, A. R. Webb, and D. Rembges, "Traveling reference spectroradiometer for routine quality assurance of spectral solar ultraviolet irradiance measurements," *Appl. Opt.* **44**, 5321-5331 (2005).

[6] Porrovecchio G., M Smid, J. Gröbner, M Rajteri, C. Portesi, K M Nield, and L. Egli, "New detection Systems for UV solar reference scanning spectroradiometers," IRS (in press).

The SolarUV consortium is composed of:

Julian Gröbner, Luca Egli, and Gregor Hülsen, Physikalisch-Meteorologisches Observatorium Davos, World Radiation Center, Davos, Switzerland (julian.groebner@pmodwrc.ch)

Petri Kärhä and Tomi Pulli, Aalto University, Espoo, Finland

Marek Smid and Geiland Porrovecchio, Czech Metrology Institute, Prague, Czech Republic

Peter Blattner, Federal office of Metrology, Bern-Wabern, Switzerland

Mauro Rajteri and Marco Pisani, Istituto Nazionale di Ricerca Metrologica, Torino, Italy

Jimmy Dubbard, Laboratoire national de metrologie et d'essais, Paris, France

Peter Meindl, Saulius Nevas, Stefan Nowy, Peter Sperfeld, and Martin Wähmer, Physikalisch-Technische Bundesanstalt, Germany

Omar El Gawhary, Dutch metrology Institute, Delft, the Netherlands

Josef Schreder, CMS-Ing. Dr. Schreder GmbH, Kirchbichl, Austria

Joop Mes, Kipp&Zonen, Delft, the Netherlands

Mario Blumthaler, Medical Univ. of Innsbruck, Innsbruck, Austria

Software for designing solar UV diffusers

Tomi Pulli[1], Petri Kärhä[1,2], Joop Mes[3] and Josef Schreder[4]

1. Metrology Research Institute, Aalto University School of Electrical Engineering, Espoo, Finland
2. Centre for Metrology and Accreditation MIKES, Espoo, Finland
3. Kipp & Zonen, Delft, The Netherlands
4. CMS - Ing. Dr. Schreder GmbH, Kirchbichl, Austria

Introduction

Large portion of the UV radiation that reaches the surface of the Earth is scattered. Therefore, an instrument that measures the total UV irradiance needs to collect radiation from the entire hemisphere. The angular response of such an instrument should be proportional to the cosine of the zenith angle and independent of the azimuth angle of the radiation. Deviations from the ideal cosine response can cause significant errors in the results. These errors can be corrected if the angular distribution of the radiation at the time of the measurement is well known, but only to an extent.

Diffusers are commonly used at the entrances of solar UV measuring instruments to reach near-ideal cosine response. As the angular response obtained with a flat sheet of diffusing material always deviates from the ideal cosine response, some form of diffuser shaping is required to reach low cosine errors. Optimizing the shape of the diffuser through trial-and-error can be time-consuming and expensive. Therefore, it would be beneficial to be able to model and optimize the structure of the diffuser before manufacturing. For this purpose a Monte Carlo software for simulating light transport inside the diffuser was developed. The software was validated by comparing the simulated results with measured angular responses. The software was then used to design an improved solar UV diffuser.

Diffuser structure

The diffuser geometry assumed by the simulation software is shown in Figure 1. The diffuser itself is characterized by the diameter d, the edge thickness t, the refractive index n_2, the scattering coefficient μ_s, the absorption coefficient μ_a, and the scattering anisotropy parameter g. The software can simulate flat diffusers as well as spherically shaped diffusers with a radius of curvature r_{sph}. The height of the diffuser is defined as $h = t - h_{sw}$, where h_{sw} is the height of the sidewall. The diameter of the visible area of the diffuser is d_{beam}. The distance between the detector and the back surface of the diffuser is z_{det}.

The diameter and the height of the shadow ring – whose purpose is to block radiation at incident angles equal to and larger than 90° – are d_{sr} and h_{sr}, respectively. The protective weather dome has an inner radius of r_{dom}, a thickness of t_{dom} and a refractive index of n_{dom}. The offset of the weather dome is determined by z_{dom} as shown in Figure 1.

Simulation algorithm

The diffuser simulation software is based on the Monte Carlo ray tracing. To ensure simulation efficiency, the particles are traced from the detector towards the sky – not vice versa – and are collected after they exit the detector head. Furthermore, instead of individual photon-like particles, large groups of particles are considered to allow for partial absorption and reflection of the weight of the particle. In the following discussion, these packages of particles traveling in the opposite direction to the photons are referred to simply as "particles."

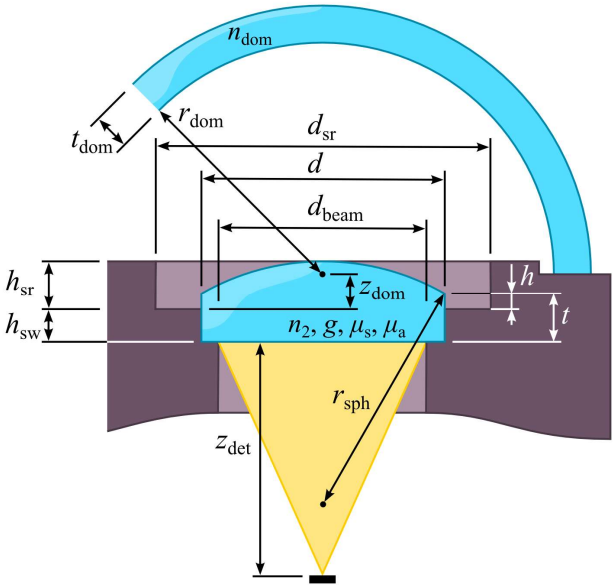

Figure 1. Structure of the diffuser. For explanation of the symbols, see text.

The workflow of the simulation software is presented in Figure 2. At the first stage of the tracing process, a particle emanating from the detector enters the diffuser. The particle is refracted at the material interface, and part of its weight is lost due to reflection. These processes are governed by Snell's law and Fresnel equations, respectively.

Inside the diffuser, the propagation follows the framework laid out in an article [1] by Wang et al. concerning the light transport in tissues. At the beginning of each propagation step, the distance to travel is determined by a random number that follows the appropriate probability distribution. If the new coordinates are inside the diffuser, the position of the particle is updated. The weight of the particle decreases due to absorption. Scattering is governed by Henyey–

Greenstein scattering phase function where scattering anisotropy parameter g determines the probability distribution of the deflection angles [2]. The propagation–absorption–scattering cycle is repeated until the weight of the particle has decreased below a user-set threshold value, or until the particle hits a material interface. Once the termination threshold is reached, the tracing process is repeated again for a new particle.

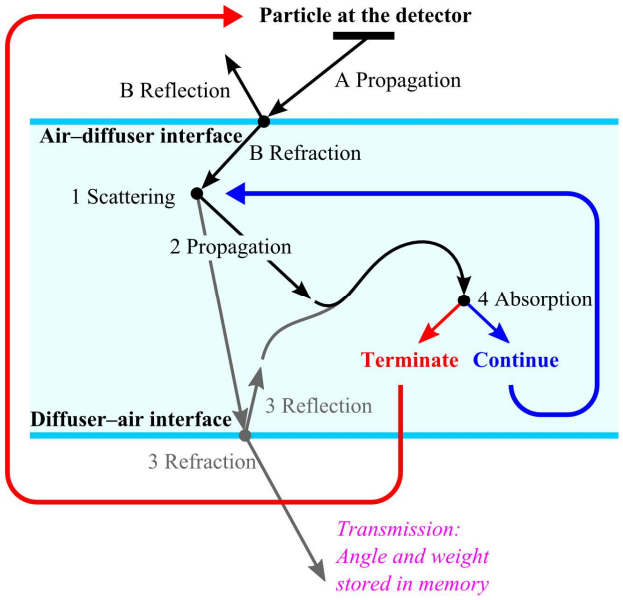

Figure 2. Workflow of the simulation software.

To find out the refraction and the reflection angles as well as the transmittance and the reflectance at the material interface, one must first calculate the coordinates at which the particle crosses the interface and the surface normal vector at those coordinates. When this is done, the law of reflection and the Snell's law of refraction in combination with the Fresnel equations can then be used to determine the necessary quantities. The reflected particle will continue to propagate inside the diffuser in a new direction and with diminished weight. If the transmitted particle hits either the shadow ring or the sidewall of the diffuser, it is absorbed. If not, then its weight will contribute to the overall angular response of the detector.

The protective weather dome, if present, has an effect on both the propagation direction and the weight of the transmitted particle. Furthermore, a particle that is reflected at the inner surface of the weather dome can still exit the detector structure at some other point of the weather dome, thus increasing the overall angular response at large zenith angles. However, this effect is only perceived when the diameter of the diffuser is close to that of the weather dome.

Simulation software

The graphical user interface of the simulation software, shown in Figure 3, was written in *Python* programming language. *Numpy* and *Matplotlib* libraries were used for array handling and data plotting, respectively. The Monte Carlo algorithm was implemented in *Cython* which is used to compile fast C extensions from a modified *Python* code.

During a typical simulation of one billion particles, roughly one hundred billion uniformly distributed pseudo-random numbers – equivalent to 800 GB of double precision floating point numbers – are generated. To draw these numbers, a fast, high quality pseudo-random number generator is required. An enhanced version of the popular Mersenne Twister algorithm, namely *SIMD-oriented Mersenne Twister* (*SFMT*) [3], was chosen for this purpose. A typical simulation of one billion particles takes roughly 10 to 15 minutes to complete with a new quad-core processor.

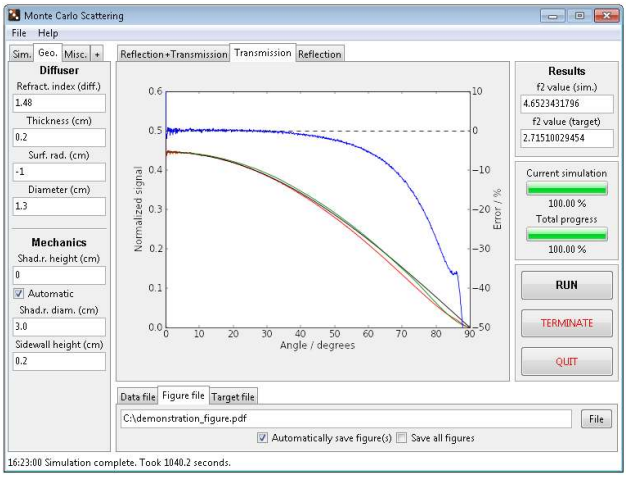

Figure 3. Graphical user interface of the simulation software.

All of the detector parameters shown in Figure 1 can be adjusted in the software, along with various simulation settings, such as the total number of particles and the termination threshold for tracing. The user can perform single simulations as well as parameters sweeps. New simulations can be queued while the current simulation is still running so that the user needs not be constantly present when a large number of simulations are performed sequentially.

Once the simulation has completed, the software plots the angular response as well as the cosine error and calculates the integrated cosine error f_2 as defined in [4]. To reduce the noise in the figures, the user can choose between different smoothing functions and adjust the span of averaging. The user can also load up a file with a target angular response that is plotted in the same figure with the simulation results. This feature is particularly useful when matching the simulated angular responses with the measurement results by adjusting one of the material parameters, e.g. the scattering coefficient μ_s.

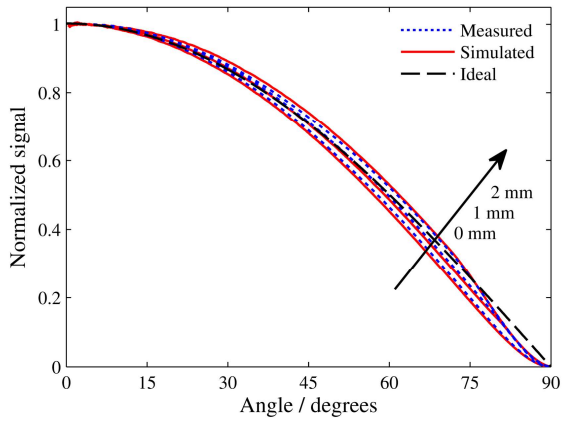

Figure 4. Comparison between the measured (dotted blue lines) and simulated (solid red lines) angular responses at three different diffuser heights h = 0 mm, 1 mm, and 2 mm. Also plotted is the ideal angular response (dashed black line).

The raw simulation data is automatically stored into a text file for further analysis along with the simulation parameters. The figures can be saved in various formats, including PDF, SVG, PNG and TIFF.

Software validation

The diffuser optimization software was validated by comparing the simulated and the measured angular responses of a prototype detector. The simulation results were first matched with the results of a measurement with a non-raised diffuser (h = 0 mm) by tuning the scattering coefficient μ_s. The assumption of uniform scattering (g = 0) turned out to yield the best results for the selected diffuser material. The height of the diffuser was then increased to 1 mm and 2 mm in both the simulations and the measurements, and the angular responses were compared again. Figure 2 shows good agreement between the measured and the simulated angular responses.

Conclusions

A software for optimizing diffusers was developed. The software utilizes Monte Carlo ray tracing to model light transport inside the diffuser. Apart from the shape of the diffuser, the software also takes into account the various surrounding structures that affect the overall angular response, such as the sidewalls of the detector, the shadow ring, and the protective weather dome. A comparison between the simulated and the measured angular responses confirmed that the software can be used to model light transport in the detector structure. Therefore, the software can be used to guide the diffuser optimization process.

Acknowledgement. This report was compiled within the EMRP ENV03 Project "Traceability for surface spectral solar ultraviolet radiation." The EMRP is jointly funded by the EMRP participating countries within EURAMET and the European Union.

References

[1] L. Wang, S. Jacques and L. Zheng, "MCML — Monte Carlo Modeling of Light Transport in Multi-layered Tissues," *Comput. Meth. Programs. Biomed.* **47**, 131–146 (1995).

[2] L. Henyey and J. Greenstein, "Diffuse Radiation in the Galaxy," *Astrophys. J.* **93**, 70-83 (1941).

[3] M. Saito, An *Application of Finite Field: Design and Implementation of 128-bit Instruction-Based Fast Pseudorandom Number Generator*, Master's thesis (Graduate School of Science, Hiroshima University, Japan, 2007) 20 p.

[4] CIE 53 - 1982, *Methods of Characterizing the Performance of Radiometers and Photometers* (International Commission on Illumination, Vienna, Austria, 1982) 27 p.

Impact of dynamic range limitations on solar UV radiation weighted irradiances

Luca Egli[1], Julian Gröbner[1] and Mario Blumthaler[2]

1. Physikalisch-Meteorologisches Observatorium Davos, World Radiation Center, Davos, Switzerland
2. Medical University Innsbruck, Biomedical Physics, Innsbruck, Austria

Introduction

Solar UV radiation has an influence on biological ecosystems and its measurement is in particular important for human health prevention. Shortwave radiation in a wavelength range between 280 to 400 nm interacts with the human body, generating e.g. sunburn on the skin or photokeratitis in the eye. UV radiation also causes DNA damage or produces Vitamin D3. The latter may have positive human health benefits.

In global solar UV radiation monitoring networks, broadband or filter radiometers are commonly used to derive the dose rate of UV radiation for biological purposes [1]. These instruments are typically optimized for one particular case (e.g. Erythema – Sunburn) or can be used for other biological applications with a limited accuracy. However, array spectroradiometers (ASRM) can measure an entire solar UV spectrum with a spectral resolution of less than a few nanometers, which enables to apply the data to different biological weighting functions (action spectra) to derive its dose rate. ASRMs are single monochromators, which are small, cost and maintenance effective and robust [2]. However, these instruments suffer from the impact of stray light in the one grating setup of the device and exhibit a limited detection threshold of the array detector [2]. A typical detection threshold for ASRM is quantified as about 1 $mWm^{-2}nm^{-1}$ [2, 3]. These limitations can lead to substantial biases of the UV measurement in particular in the UV-B range (280-315 nm). In order to describe methods for the practical operation of ASRMs measuring solar UV radiation a guideline was prepared within the EMRP project ENV03 ("Traceability for surface spectral solar ultraviolet radiation") and presented at the International Radiation Symposium (IRS) in August 2012 [3]. In this guideline the requirements of measuring solar UV with ASRM are summarized. The recommendations of the guideline are based among other investigations on a sensitivity study on potential biases from the ASRM measurements. This article aims to present and discuss the main part of the theoretical sensitivity analysis, which investigates the impact of the uncertainty of solar UV irradiance measurements from ASRM on the following action spectra:

- CIE Erythema (280 to 400 nm) [4]
- Vitamin D3 generation (280 to 330 nm) [5]
- Total UVB (280 to 315 nm)
- DNA damage (280 to 370 nm) [6]

The sensitivity analysis addresses the specific question: What is the required dynamic range in solar UV irradiance measurements to achieve an integration of a solar UV spectrum with a selected action spectrum within 1% of the full solar spectrum under clear sky conditions? Any uncertainty contributions from e.g. calibration, angular response, temperature and stability are explicitly excluded in this analysis. The dynamic range of solar UV measurement also determines the minimal wavelength (*wl-cut*) and minimum intensity (min_{irr}), defined by a signal to noise ratio of 1, which should be measured with ASRM to achieve an uncertainty of less than 1% of the weighted dose rates. The knowledge of these specific parameters is of practical interest to use ASRM for biological applications and the following results may lead to determine the applicability of a specific ASRM intended to be used to monitor solar UV radiation for human health prevention.

Data and Method

Modelled solar UV spectra were used for this study. The spectra were obtained with the "LibRadtran" radiative transfer package [7] assuming clear sky conditions. The main variables for the model calculations were the solar zenith angle (SZA) and the total column ozone (TO_3). A total of 288 (=18 SZA x 16 TO_3) spectra were computed over the wavelength range 280 to 450 nm for the SZA range 0° to 85° and TO_3 from 200 to 500 DU. Figure 1a shows 4 modeled spectra for the extreme cases of atmospheric conditions, while Figure 1b indicates the different biological weighting functions applied to the solar spectra.

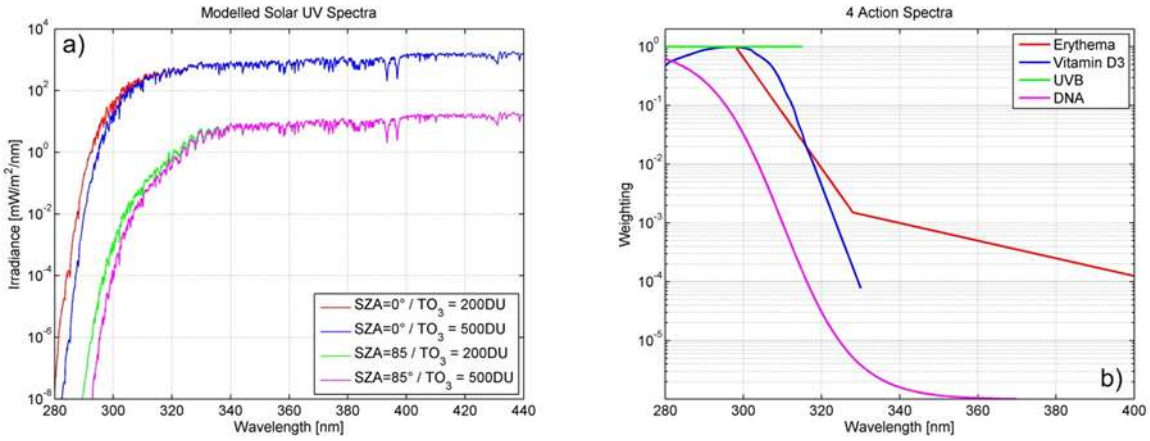

Figure 1. a) Modelled solar UV spectra for 4 different atmospheric conditions represented by the variable solar zenith angle (SZA) and total ozone column (TO_3). b) Four different action spectra used for the weighting of the solar spectra to calculate the integral value.

To calculate the minimum required order of magnitude of the dynamic range, the following procedure was applied:

1) The maximum irradiance (max_{irr}) of a specific modelled solar spectrum is determined. The order of magnitude is predefined as: $10^{\text{m-order}}$. From the ratio of these two values the minimum irradiance (min_{irr}) is calculated using equation 1, assuming that the ASRM is able to accurately measure the irradiance from the maximum intensity to the minimum intensity (min_{irr}):

$$min_{irr} = max_{irr} / 10^{\text{m-order}} \quad (1)$$

2) It is further assumed that irradiances below the critical min_{irr} and shorter than the wavelength *wl-cut* at min_{irr} are not reliable due to the impact of stray light and poor detectability of the array detector (e.g. signal to noise lower or equal to one). Therefore these values are set to 0.

3) The obtained modified spectrum and the original modeled spectrum are weighted with the action spectra for Erythema, Vitamin D3, UVB and DNA (see Figure 1b) and the integral of the weighted spectra is calculated for all SZA and TO_3. The ratio between the original model data and the modified spectra is determined as

$$\text{Fractional deviation} = \frac{\text{Uncertain measurent}}{\text{TRUE}} = \frac{\int_{wl-cut}^{450nm} E(\lambda, SZA, O_3) * C(\lambda) d\lambda}{\int_{280nm}^{450nm} E(\lambda, SZA, O_3) * C(\lambda) d\lambda} \quad (2)$$

where $E(\lambda,SZA,O_3)$ is a specific modeled solar UV spectrum, $C(\lambda)$ denotes the normalized weighting function for the different action spectra (see Figure 1b) and *wl-cut* indicates the cut-off wavelength derived from min_{irr} as defined in 1). The fractional bias of the weighted spectra for all possible combinations of SZA and TO_3 was determined for different orders of magnitude (*m-order*).

4) With the procedure 1-3 the order of magnitude depending on all SZA and TO_3 combinations, was selected if the deviation is less than 0.01 (=1 %). This order of magnitude also defines the specific wavelength (*wl-cut*) and the corresponding minimum absolute irradiance where the weighted integral biases are <1%.

Results and Discussion

The procedure described above results in 3 different surface plots for each biological weighting function (Figure 2-5). The results reveal that the minimum required order of magnitude to achieve an uncertainty of the weighted integral of less than 1% varies significantly between all 4 weighting functions. The same procedure yields the cut-off wavelength and the corresponding minimum detectable intensity as a function of SZA and TO_3, assuming clear sky conditions.

a) Erythemal action spectrum

Theoretically, the minimum requirement for an ASRM to determine erythemal weighted global irradiance for all atmospheric conditions is the ability of the instrument to cover 3.74 orders of magnitude relative to the maximum irradiance intensity. Figure 2a indicates that this benchmark of 1% is reached under the extreme conditions at high zenith angles (~85°) and low TO_3 (~200 DU) concentrations. In this region the measurements below about 295 nm (see Figure 2b) can be set to 0 resulting in an integral percental bias of <1%. Figures 2b and 2c show that in priciple ASRM need to be able to measure irradiances of ~2.5 $mWm^{-2}nm^{-1}$ at 300 nm (for high SZA=85° and low TO_3=200 DU) and ~0.05 $mWm^{-2}nm^{-1}$ at 309 nm (for high SZA=85° and high TO_3=500 DU). Note that detecting 0.05 $mWm^{-2}nm^{-1}$ is a demanding requirement for the detectability of the detector in ASRMs [3].

However, an intensity of about 1 $mWm^{-2}nm^{-1}$ may be practically detected with typical array detectors by applying the procedure describes in the guideline [3]. This level of intensity is reached in case of lower SZA (< 50°) and for moderate concentrations of TO_3 (~350 DU) with a cut-off wavelength around 300 nm (Figure 1 b).

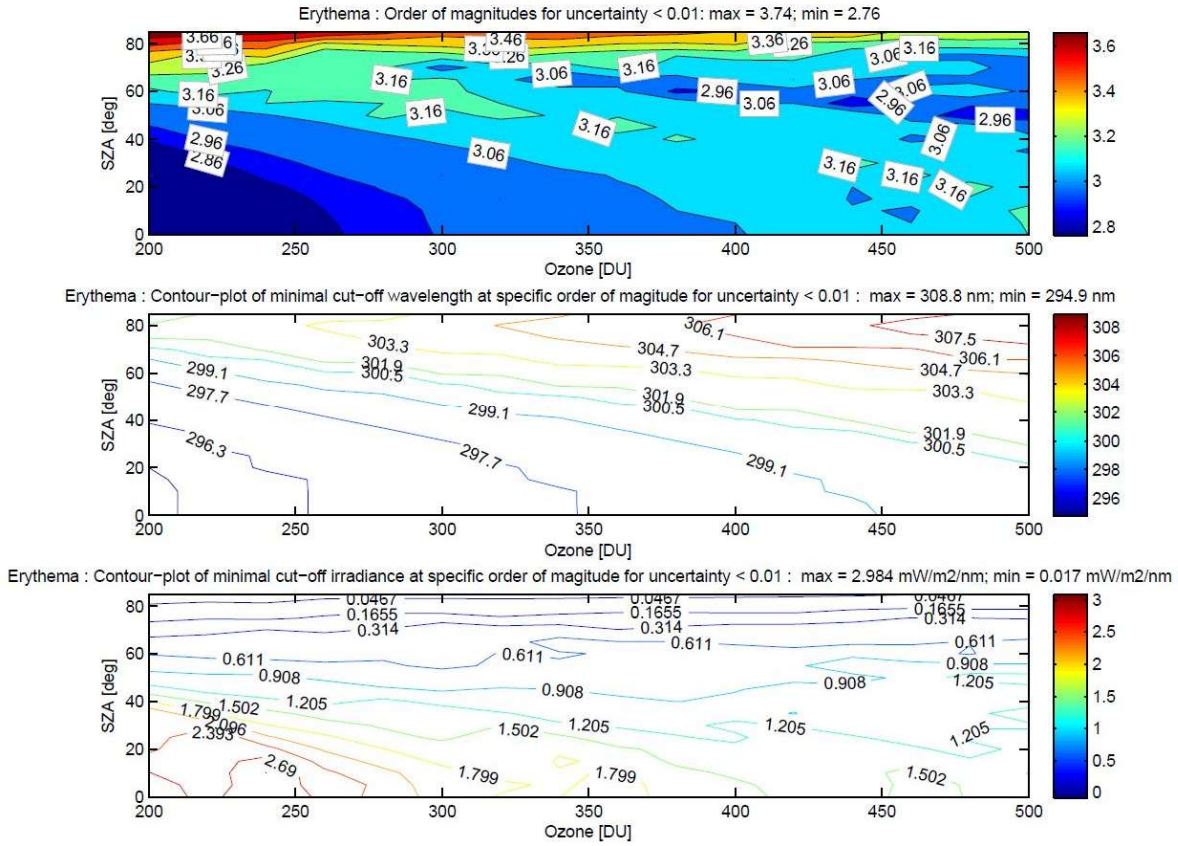

Figure 2 a-c. Erythema weighted dose rate for uncertainty < 1%: a) orders of magnitude (upper panel), b) minimal wavelength (middle panel) and c) minimal detection threshold of absolute irradiance (lower panel).

b) Vitamin D3 action spectrum

The minimum requirement for an array spectrometer is to cover 4.4 orders of magnitude when investigating Vitamin D3 related biological effects, which is more than half an order higher than required for erythemal weighted dose rates. Figure 3a demonstrates that due to the theoretical considerations the critical benchmark of 1% is also reached under the extreme conditions at high zenith angles (~85°) but in contrast to erythemal weighted global irradiance, at high TO_3 (=500 DU) concentrations. Remarkably, in this region the measurements below about 304 nm (see Figure 3b) can be set to 0, if the irradiance of ~0.005 $mWm^{-2}nm^{-1}$ can be measured with a signal to noise ratio of 1, which is very below a typical detection threshold of array detectors.

However, related to practice at SZA < 50° irradiance of ~1 $mWm^{-2}nm^{-1}$ can be measured at wavelengths around 300 nm. The required level of intensity is almost independent on the TO_3 concentration (200-500 DU). This irradiance can be detected with typical monochromators presumed that a stray light reduction until 300 nm can be achieved.

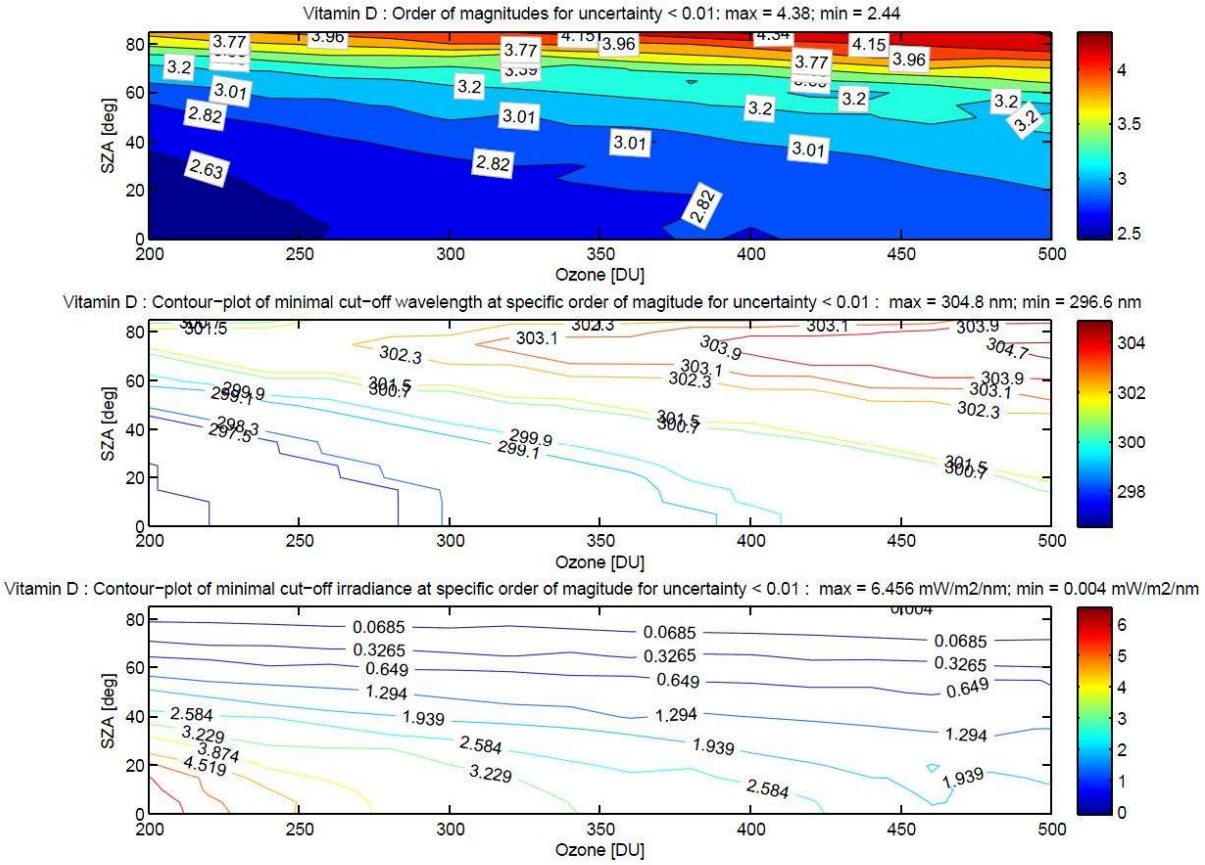

Figure 3 a-c. Vitamin D weighted dose rate for uncertainty < 1%: a) orders of magnitude (upper panel), b) minimal wavelength (middle panel) and c) minimal detection threshold of absolute irradiance (lower panel).

c) Total UVB global Irradiance

To accurately estimate the total UVB, an ASRM should cover at least 3.95 orders of magnitude of the dynamic range of the UV-irradiance for all atmospheric conditions and SZA. Figure 4a show that similar to Vitamin D3 the benchmark of 1% is reached under the extreme conditions at high zenith angles (~85°) and high TO_3 (=500 DU) concentrations. In this region the measurements below about 306 nm (see Figure 4b) can pragmatically be set to 0 to reach the predefined accuracy.

In contrast to Erythema and Vitamin D3 the fractional deviation of the weighted integral is less than 1% for SZA < 70° if the irradiance can be accurately measured at a level of 1 $mWm^{-2}nm^{-1}$. This means that it is practically feasible to measure accurate total UVB for SZA below 70°, where only around 2.5 orders of magnitude have to be captured at a wavelength around 303 nm. Therefore the requirements to operationally estimate total UVB global irradiance is less demanding then for Erythema or Vitamin D3.

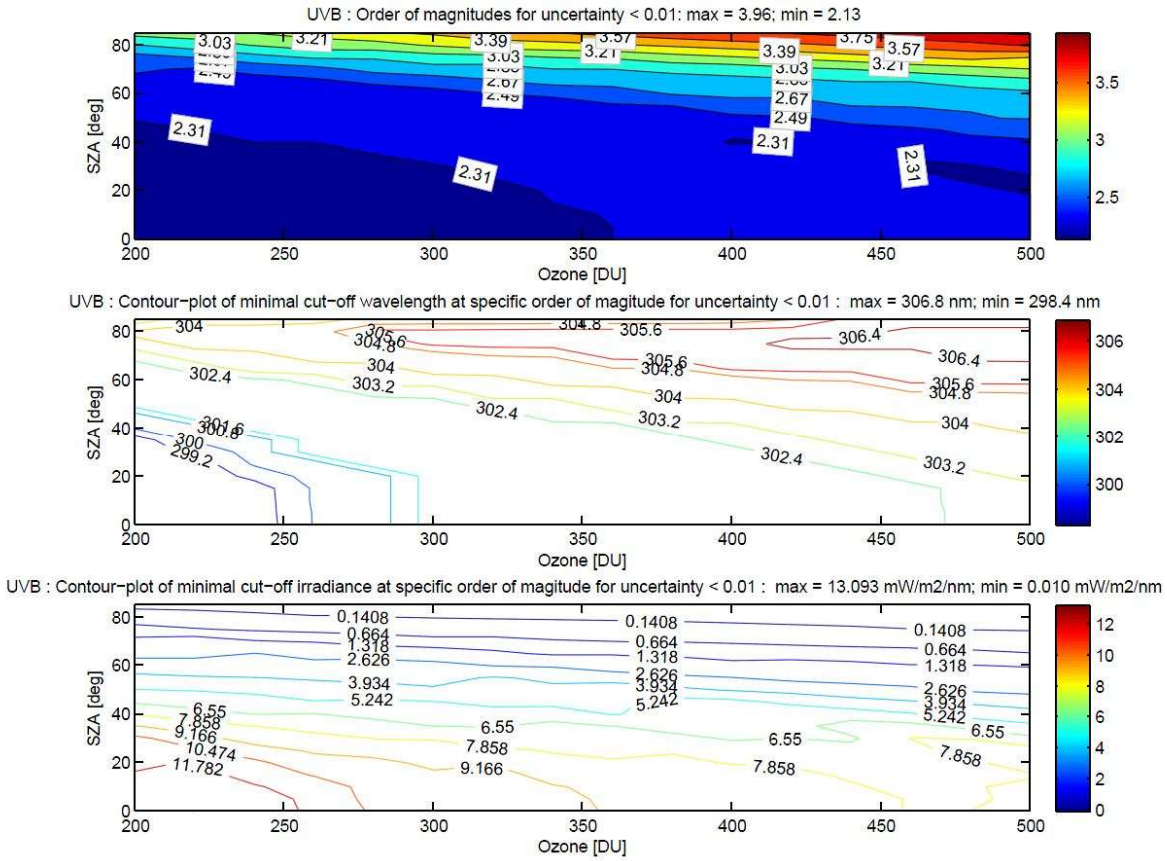

Figure 4 a-c: UVB weighted dose rate for uncertainty < 1%: a) orders of magnitude (upper panel), b) minimal wavelength (middle panel) and c) minimal detection threshold of absolute irradiance (lower panel).

d) DNA

Considering DNA weighted solar UV irradiance, the ASRM should cover in principle about 3.5 – 5 orders of magnitude of the dynamic range for integral fractional biases of less than 1% (Figure 5a). Covering such a high order of magnitude, the cut-off wavelength varies from 290 nm to 302 nm (Figure 5b), which is significantly below the wavelength found in the first 3 cases. Also differently to all others biological weighting functions, Figure 5c indicates that the required detection threshold varies between 0.001 – 0.5 $mWm^{-2}nm^{-1}$, which is a very challenging requirement for typical array detectors, even if a stray light reduction until 3.5-5 orders of magnitude can be achieved.

If an intensity ~0.3 $mWm^{-2}nm^{-1}$ can be detected practically by a specific instrument and procedure (e.g. with cooled array detectors), the DNA weighted integral is less than 1% at SZA around noon (SZA ~20°). In this case the required orders of magnitude and the minimal intensity are weakly correlated with TO_3 concentration in the atmosphere, but the signal should be accurately detected to wavelength between 293 – 298 nm.

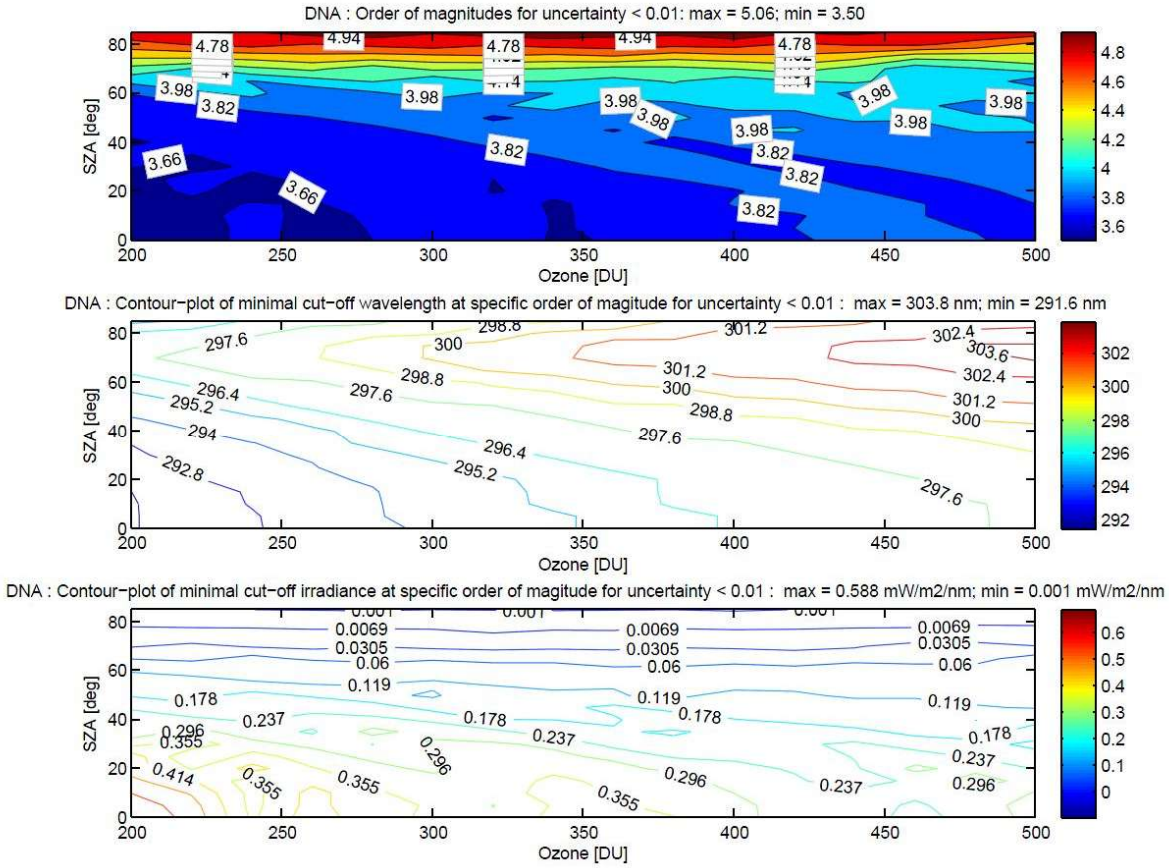

Figure 5 a-c: DNA weighted dose rate for uncertainty < 1%: a) orders of magnitude (upper panel), b) minimal wavelength (middle panel) and c) minimal detection threshold of absolute irradiance (lower panel).

Conclusion

For spectrally weighted solar irradiances, such as Erythema, Vitamin D3, UVB or DNA action spectra, at least 3.8 – 5 orders of magnitude of the dynamic range of solar UV irradiance should be theoretically captured by array spectrometers if an accuracy of 1% should be achieved at all atmospheric conditions. The resulting orders of magnitude imply that a stray light reduction of the array spectroradiometer until wavelength between 290 to 298 nm with an irradiance detectability of 0.001 – 0.017 $mWm^{-2}nm^{-1}$ should theoretically be achieved for all SZA and TO_3 concentrations.

However, practically assumed that an array spectroradiometer is able to detect an intensity of around 1 $mWm^{-2}nm^{-1}$ with a signal to noise ratio of 1, the factional biases of the weighted integral are less than 1% for SZA smaller than 60° (Erythema, Vitamin D3, UVB-Index) and are less dependent on TO_3 concentration than on SZA. Under the condition of small SZA the irradiance of 1 $mWm^{-2}nm^{-1}$ is typically reached around 300 nm where the solar UV measurement should not be influenced by stray light in the instrument.

However, due to the considerations above we cannot assume that detecting 1 $mWm^{-2}nm^{-1}$ is sufficient to obtain DNA weighted integrals with an accuracy < 1%. To practically estimate the potential of DNA damage with solar UV radiation, require instrumentations which are highly sensitive and perform a stray light reduction to cover at least 4-5 orders of magnitude of the dynamic range.

Acknowledgement. This report was compiled within the EMRP ENV03 Project "Traceability for surface spectral solar ultraviolet radiation." The EMRP is jointly funded by the EMRP participating countries within EURAMET and the European Union.

References

[1] Schreder, J., Gröbner, J., Los, A. and Blumthaler, M., "Intercomparison of monochromatic source facilities for the determination of the relative spectral response of erythemal broadband filter radiometers," *Opt. Lett.* **29** (2004).

[2] Seckmeyer, G., Bais, A., Bernhard, G., Blumthaler, M., Drüke, S., Kiedron, P., Lantz, K., McKenzie, R. and Riechelmann, S., *Instruments to measure solar ultraviolet radiation Part 4: Array Spectroradiometers*, *WMO/GAW No.191* (World Meteorological Organisation, Geneva, 2010).

[3] Blumthaler, M., Gröbner, J.,Egli, L. and Nevas, S., "A Guide to Measuring Solar UV Spectra using Array Spectroradiometers," IRS (in press).

[4] Webb, A. R., Slaper, H., Koepke, P. and Schmalwieser, A. W., "Know Your Standard: Clarifying the CIE Erythema Action Spectrum," *Photochem. Photobiol.* **87,** 483–486. doi: 10.1111/j.1751-1097.2010.00871.x (2011).

[5] Bouillon, R., Eisman, J., Garabedian, M. et al. *Action spectrum for the production of pre-vitamin D3 in human skin*, Technical Report CIE;174:1-12 (Commission Internationale de l'Eclairage, 2006).

[6] Setlow, R.B., "The wavelengths of sunlight effective in producing skin cancer: a theoretical analysis," *Proc. Natl. Acad. Sci. USA* **71**, 3363-3366 (1974).

[7] Mayer, B. and Kylling, A., "Technical note: The libRadtran software package for radiative transfer calculations - description and examples of use," *Atmos. Chem. Phys.* **5**, 1855-1877, doi:10.5194/acp-5-1855-2005 (2005).

Stray light correction of array spectroradiometer data for solar UV measurements

Saulius Nevas[1], Julian Gröbner[2] and Luca Egli[1]

1. Physikalisch-Technische Bundesanstalt, Braunschweig, Germany
2. Physikalisch-Meteorologisches Observatorium Davos, World Radiation Center, Davos, Switzerland

Introduction

Compact array spectroradiometers are used to monitor surface spectral solar ultraviolet radiation. In order to ensure measurements with acceptable uncertainties the instruments have to be carefully characterised and calibrated. One of the highest uncertainty components in the measurements by the array spectroradiometers is caused by a poor suppression of the spectral stray light, known also as the out-of-band response or spectral leakage. Their stray light properties are inferior to those of the scanning systems due to a compact design and the principle of operation of the instruments. Nevertheless, numerical correction methods exist enabling a correction of the stray light effects using a correction matrix determined with the help of spectrally tuneable monochromatic radiation [1, 2]. Provided that the stray light properties of an array spectroradiometer, i.e. the spectral response of the instrument to a monochromatic excitation, are known for any wavelength within the spectral range of the array spectroradiometer, a numerical improvement of the stray light suppression by one to two orders of magnitude is possible. The correction is, however, effective only as long as the spectral range of the instrument coincides with the spectral range of the array detector in use. Thus, a stray light correction matrix determined for an array spectroradiometer is limited to its spectral range to, e. g., 250 nm to 400 nm. Having a silicon CCD detector, that typically is able to detect optical radiation up to 1100 nm, the matrix would be little effective unless additional measures are taken in order to account for the stray light that is created outside of the spectral range of the spectroradiometer, i.e. within 400 nm to 1100 nm, which can still be detected by the Si-detector. The effect of the long-wavelength stray light is amplified due to the fact that thermal sources (e.g. halogen lamps) are used for the calibration of the instruments and the responsivity of the Si detectors is higher for the radiation at longer wavelengths than for shorter wavelengths. The simplest way of taking care of this stray light, let's call it out-of-range (OoR) in order to differentiate from the in-range (InR) stray light that is included in the correction matrix, would be by using bandpass filters or other spectral pre-selection techniques that block the OoR radiation at the entrance of the instrument [3]. It is also possible to characterise the effects of the OoR stray light using tuneable laser sources. In contrast to the normal stray light characterisation procedure, however, an additional calibrated instrument is needed as reference for the OoR radiation measurements during the characterisation. In this *UVNews* issue we present such a work started within the EMRP project "Traceability for surface spectral solar ultraviolet radiation" and show preliminary results obtained for a solar UV spectroradiometer operated by the PMOD/WRC in Davos.

Correction of out-of-range and in-range spectral stray light

We start with the equation (4) in the original stray light correction method by Zong. et al. [1]. Using a matrix notation, the spectral stray light signal vector $\mathbf{Y}_{s\_spec}$ can be written as

$$\mathbf{Y}_{s\_spec} = \mathbf{D} \cdot \mathbf{Y}_{IB} + \mathbf{\Delta} \quad (1)$$

where $\mathbf{D}$ is the spectral stray light distribution matrix, $\mathbf{Y}_{IB}$ is the in-band signal vector and $\mathbf{\Delta}$ is a vector with the OoR stray light contribution for every pixel of the detector. The OoR stray light vector $\mathbf{\Delta}$ can be found as

$$\mathbf{\Delta} = \mathbf{s}_{OoR} \cdot \mathbf{E}_{OoR} \cdot \delta\lambda , \quad (2)$$

provided that the responsivity of every detector pixel to the radiation at different wavelengths outside the spectral range of the instrument, put in a matrix $\mathbf{s}_{OoR}$, and the spectral irradiance outside the spectral range of the spectroradiometer, contained in a vector $\mathbf{E}_{OoR}$, are known. $\delta\lambda$ represents the OoR wavelength step with which the OoR stray light data are available. The dimension of the matrix $\mathbf{s}_{OoR}$ is *N*x*M*, where *N* is the number of pixels in the array detector and *M* is the number of the OoR stray light data vectors distribute on a uniform wavelength grid throughout the OoR of the instrument, say every 1 nm. Then we can follow the matrix formalism of [1] and write down the measured signal vector as

$$\mathbf{Y}_{meas} = \mathbf{Y}_{IB} + \mathbf{D} \cdot \mathbf{Y}_{IB} + \mathbf{\Delta} , \quad (3)$$

and finally the spectroradiometer data vector corrected for both the InR and OoR spectral stray light as

$$\mathbf{Y}_{IB} = [\mathbf{I} + \mathbf{D}]^{-1} \cdot [\mathbf{Y}_{meas} - \mathbf{\Delta}] = \mathbf{A}^{-1} \cdot [\mathbf{Y}_{meas} - \mathbf{\Delta}] . \quad (4)$$

Hence, the OoR stray light contribution $\mathbf{\Delta}$ first needs to be subtracted from the measured signal vector $\mathbf{Y}_{meas}$, before applying the stray light correction matrix. It has also to be noted that the spectral irradiance $\mathbf{E}_{OoR}$ outside of the spectral range of the array spectroradiometer, for the wavelengths up to 1100 nm, needs to be known for both the source used to calibrate the instrument and the source under test in order to be able to apply the correction of (4). For calibration sources such data is typically available. The OoR stray light estimation for a test source, i.e. the solar radiation, however, requires either measurements by an auxiliary spectroradiometer or

some kind of prediction (e.g., with radiative transfer model calculations) for the spectral content in the OoR based on the InR measurement data by the instrument. An example of such a procedure is provided in the following section.

The stray light properties of array spectroradiometers, i.e. the Line Spread Functions (LSFs), can be determined by means of wavelength tunable lasers. At PTB, Pulsed Laser for Advanced Characterisation of Spectroradiometers (PLACOS) setup is routinely used for this purpose [4]. To determine the OoR stray light responsivity matrix $\mathbf{s}_{OoR}$ the setup was slightly modified. Figure 1 shows schematically the PLACOS setup adapted for the OoR stray light measurements. Here, a microlense array-based laser beam homogenizer was used to generate a uniform field irradiating subsequently the input optics of the solar UV array spectroradiometer and of a calibrated reference spectroradiometer with its spectral range extending from 200 nm to 1100 nm. The reference instrument enables to quantify the spectral irradiance to which the test instrument is exposed outside of his spectral range. The monitor instrument helps to compensate for the variation in the laser output power during the measurements.

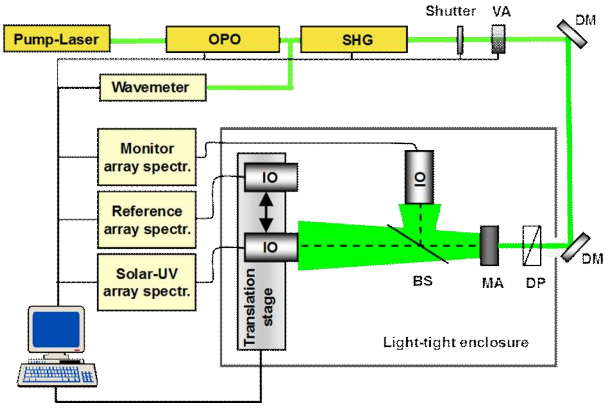

Figure 1. PLACOS setup adapted for the out-of-range stray light characterisation of array spectroradiometers. OPO: optical parametric osicilator; SHG: second harmonic generator; IO: input optics (diffuser head) connected via a fibre link to an array spectroradiometer; BS: beam splitter; MA: microlense array-based beam homogeniser; DP: depolariser; DM: dichroic mirror; VA: variable attenuator.

Preliminary results

As a first artifact selected for studies within the project, an AvaSpec-ULS array spectroradiometer owned by the PMOD/WRC, named AVOS, was characterized both for InR and OoR stray light properties at the PLACOS setup of PTB. The Instrument has a nominal spectral range of 280 nm to 440 nm, 0.7 nm bandpass and a Hamamatsu back-illuminated Si CCD with 2048 pixels. As a reference instrument for the OoR stray light characterization, another AvaSpec-ULS array spectroradiometer with its spectral range from 200 nm to 1100 nm was used. The determined InR stray light properties of the AVOS are shown in Figure 2. Figure 3 displays the responsivity of the spectroradiometer to the OoR stray light at several selected wavelengths. By examining Figure 3 one can notice that the response of the instrument to the OoR stray light is changing within the spectral range of the spectroradiometer mostly for the OoR wavelengths of up to about 600 nm. The response to the OoR radiation at wavelengths above 600 nm is relatively monotonous over the spectral range of the AVOS spectroradiometer meaning that the data can be safely interpolated based on the measurements at several OoR wavelengths.

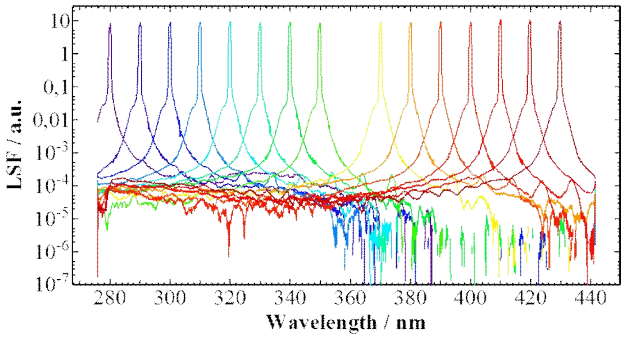

Figure 2. In-range stray light properties of the AVOS spectroradiometer.

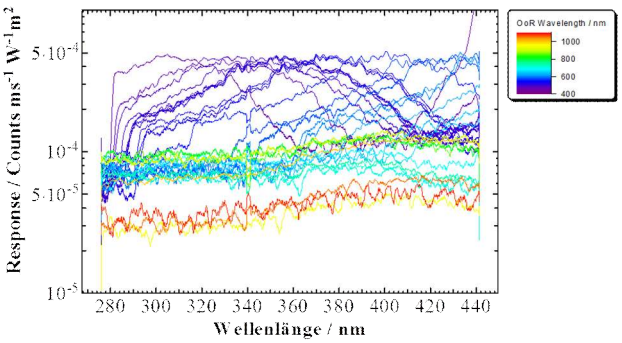

Figure 3. AVOS spectroradiometer response to the out-of-range stray light caused by the radiation at 440 nm to 1100 nm wavelengths.

The stray light characterisation data of the AVOS spectroradiometer was used to determine a correction matrix for the InR stray light. The OoR stray light contribution (2) during the spectral irradiance responsivity calibration of the instrument was estimated from the lamp spectral irradiance values. Thus, the responsivity of the spectroradiometer including the correction for the InR and OoR stray light could be determined with the help of (4). In the next step, solar UV irradiance data obtained by the AVOS spectroradiometer in a clear sky measurement campaign in Davos were treated. Here, the biggest challenge in applying the OoR stray light correction was to determine the solar OoR irradiance $\mathbf{E}_{OoR}$ during the measurements as no auxiliary instrument measuring the solar radiation up to 1100 nm was available during these measurements. For this purpose the OoR solar irradiance was estimated with the "Libradtran radiative transfer model" [5]. The model was initialized with measured input parameters (ozone, aerosols) and the radiative transfer was obtained

under clear sky conditions. The modeled spectra showed accurate congruence to the InR UV measurements and it is, thus, assumed that the modeled OoR spectra reflect a realistic solar input from this wavelength range. Figure 4 shows results obtained with the OoR and OoR&InR stray light correction applied to AVOS measurement data compared with the double monochromator reference data and the solar irradiance determined by AVOS without any stray light correction.

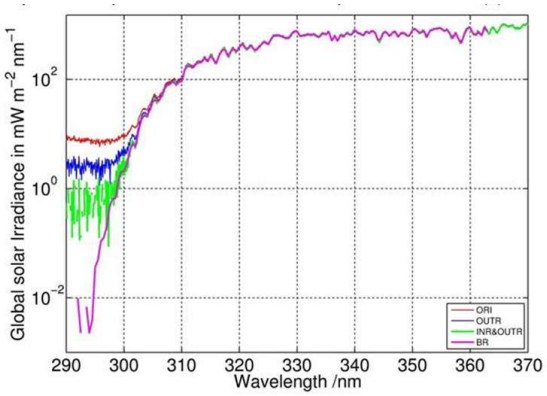

Figure 4. Stray light correction of AVOS spectroradiometer. Magenta Curve is the solar spectrum measured with a scanning double monochromator. The red curve is the calibrated solar spectrum from AVOS without any stray light correction applied. The blue and green curves are the solar spectra corrected for the OoR and the OoR&InR stray light, respectively.

Conclusion and outlook

Stray light characterisation of array spectroradiometers using wavelength tuneable lasers provides fundametal information on the instrument performance under any spectral distribution of a source being measured and enables to correct the data numerically in terms of a correction matrix. The determined correction matrix, however, is efficient as long as the spectral range of the instrument covers the spectral range of the built in detector. In the case of Si array detectors, the longest wavelength that the detector is able to register extends up to 1100 nm. Thus, solar UV spectroradiometers designed for a narrow spectral range need additional efforts to account for the out-of-range stray light. Within the EMRP project Traceability for surface spectral solar ultraviolet radiation laser-based characterisation method was considered in order to enable a numerical correction not only of the InR but also of the OoR stray light. The preliminary data obtained with the array spectroradiometer of PMOD/WRC show that this approach works. The biggest challenge in applying the OoR stray light correction is quantifying the spectral irradiance that is not measured directly by the instrument itself but still causes a stray light contribution to the measured signal. We showed also a way of estimating it based on an extrapolation of the solar UV measurement data by the instrument. A suitable filtering technique blocking the radiation outside the spectral range of the spectroradiometer, though, may be simpler in application.

It is planned to characterise a number of array spectroradiometers of stakeholders and participants in the project for the stray light properties. The efficiency of the stray light rejection methods will be tested in an intercomparison campaign with adjoined workshop in June 2014 at PMOD/WRC. A full article is also planned to be published on the stray light correction methodology for taking into account both the OoR and InR stray light.

Acknowledgement. This report was compiled within the EMRP ENV03 Project "Traceability for surface spectral solar ultraviolet radiation." The EMRP is jointly funded by the EMRP participating countries within EURAMET and the European Union.

References

[1] Y. Zong, S. W. Brown, B.C. Johnson, K. R. Lykke and Y. Ohno, "Simple spectral stray light correction method for array spectroradiometers," *Appl. Opt.* **45**, 1111–1119 (2006).

[2] S. Nevas, G.Wübbeler, A. Sperling, C. Elster and A. Teuber, "Simultaneous correction of bandpass and stray light effects in array spectroradiometer data," *Metrologia* **49**, S43–S47 (2012).

[3] L. Egli, J. Gröbner, M. Smid, G. Porrovecchio, T. Burnitt, K. Nield, S. Gibson, J. Dubard, S. Nevas and M. Tormen, "New Technologies to Reduce Stray Light for Measuring Solar UV with Array Spectroradiometers," IRS (in press).

[4] S. Nevas, M. Lindemann, A. Sperling, A. Teuber and R. Maass, "Colorimetry of LEDs with Array Spectroradiometers," *MAPAN—J. Metrol. Soc. India* **24**.

[5] B. Mayer and A. Kylling, "Technical note: The libRadtran software package for radiative transfer calculations - description and examples of use," *Atmos. Chem. Phys.* **5**, 1855-1877, doi:10.5194/acp-5-1855-2005 (2005).

Development of monitoring sources based on UV light-emitting diodes

Stefan Nowy[1], Nguyen Van Hung[1], Saulius Nevas[1], Peter Blattner[2] and Julian Gröbner[3]

1. Physikalisch-Technische Bundesanstalt (PTB), Braunschweig, Germany
2. Bundesamt für Metrologie (METAS), Bern-Wabern, Switzerland
3. Physikalisch-Meteorologisches Observatorium, World Radiation Center, Davos, Switzerland

The development of compact, stable, portable, and robust monitoring sources based on state-of-the-art, commercially available UV light-emitting diodes (LEDs) is one of the tasks within the European Metrology Research Programme (EMRP) Project "Traceability for surface spectral solar ultraviolet radiation". It is aimed towards shortening the traceability chain and reducing the uncertainties of spectral solar UV radiation measurements in the wavelength range 280 nm to 400 nm. These monitoring sources will be used to maintain the spectral calibration of spectroradiometers while deployed at solar UV measurement sites.

As a first step, commercially available LEDs with flat emission windows in TO-18 housing have been selected in such a way that the wavelength range from 280 nm to about 450 nm is covered. The peak wavelengths of the investigated LEDs (three per wavelength) have been determined to be 285 nm, 299 nm, 310 nm, 323 nm, 333 nm, 342 nm, 352 nm, 369 nm, 401 nm, and 437 nm, see Figure 1.

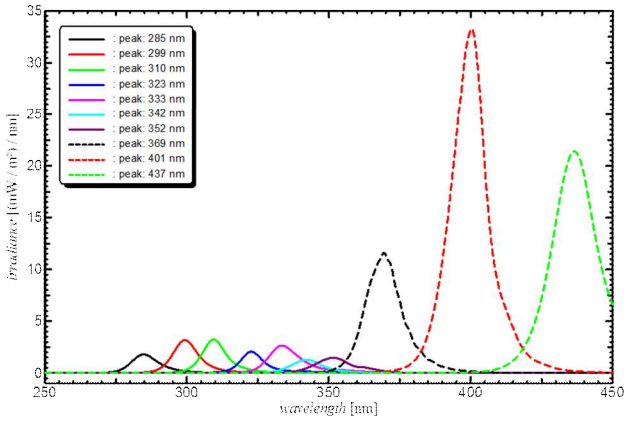

Figure 1. Estimated spectral irradiance of ten different LEDs after aging. Distance of LEDs to entrance optics of a spectroradiometer approximately 5 cm.

In order to study the aging behavior, the irradiance of each LED was monitored in a fully automated measurement setup with a Si photodiode and a calibrated UV array-spectroradiometer. The LEDs were driven in constant current mode. All LEDs were mounted in separate holders, each equipped with a thermostat. The aging of the LEDs has been performed until the drift in irradiance was less than 0.05% per hour (as required for the project goals) or no further change could be expected in reasonable time. Consequently, the operating times ranged between about 100 to over 600 hours. Please see Table 1 for details.

Table 1. Drift in irradiance after operating the LEDs in constant current mode.

peak wavelength	operating time	operating temperature	drift in irradiance
285 nm	565 h	25°C	-0.08% / h
299 nm	402 h	25°C	-0.05% / h
310 nm	476 h	25°C	-0.05% / h
323 nm	120 h	25°C	-0.01% / h
333 nm	101 h	25°C	-0.03% / h
342 nm	134 h	35°C	-0.04% / h
352 nm	120 h	25°C	-0.02% / h
369 nm	134 h	35°C	-0.01% / h
401 nm	120 h	25°C	< -0.01% / h
437 nm	120 h	25°C	0.02% / h

While aging the devices, the spectral irradiance has been monitored and a change in the centroid wavelength towards longer wavelengths has been observed, however, this shift has been calculated to be well below 10-3 nm per hour (Table 2). Also, the full width half maximum (FWHM) value of the emission peak is slightly increasing over time.

Table 2. Shift in centroid wavelength and FWHM for selected UV-LEDs.

peak wavelength	operating temperature	shift in centroid wavelength	shift in FWHM
285 nm	25°C	$1.7 \cdot 10^{-4}$ nm / h	$0.9 \cdot 10^{-4}$ nm / h
299 nm	25°C	$0.8 \cdot 10^{-4}$ nm / h	$0.3 \cdot 10^{-4}$ nm / h
310 nm	25°C	$0.4 \cdot 10^{-4}$ nm / h	$<0.1 \cdot 10^{-4}$ nm / h
333 nm	25°C	$5.1 \cdot 10^{-4}$ nm / h	$6.1 \cdot 10^{-4}$ nm / h
342 nm	35°C	$5.4 \cdot 10^{-4}$ nm / h	$3.5 \cdot 10^{-4}$ nm / h
369 nm	35°C	$1.3 \cdot 10^{-4}$ nm / h	$7.8 \cdot 10^{-4}$ nm / h

Another requirement for the monitoring sources are irradiance levels of at least 1 mW m^{-2} nm^{-1} for wavelengths between 280 nm and 330 nm, and 5 mW m^{-2} nm^{-1} for longer wavelengths. A prototype monitoring source has been designed to hold 10 LEDs, which were selected after analyzing their aging behavior. Unfortunately, the irradiance levels of the available LEDs around 340 nm have proved to be not very high (see Figure 1); to compensate, two LEDs emitting at peak wavelengths of 352 nm have been selected instead of a LED with the peak emission at 342 nm, as this has a more favourable effect for the expected total irradiance of the monitoring source. The total spectral irradiance expected from the 10 selected LEDs in a distance of 5 cm to the entrance optics of a spectroradiometer is shown in figure 2, along with the required irradiance levels, and the irradiance of a tungsten lamp (FEL, distance 50 cm). The irradiance levels probably will not meet the requirements over the whole spectral range; however, the

LEDs will offer higher levels than the FEL in the low wavelength range.

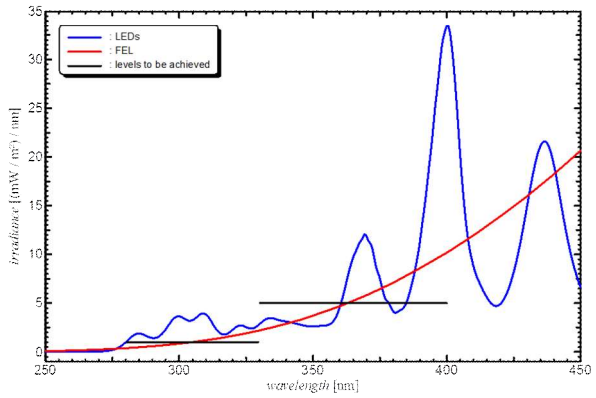

Figure 2. Blue curve: expected spectral irradiance from the ten selected LEDs. Red curve: spectral irradiance from a tungsten lamp (FEL, distance 50 cm). Black lines: desired irradiance levels.

A prototype of a monitoring source has already been constructed. The ten selected LEDs are mounted into an aluminum block, along with a SiC monitoring photodiode. A Peltier element is used for temperature controlling. A spacer - a cylinder of stainless steel - is mounted between the aluminum/LED block and interchangeable flanges. These flanges are used as mechanical interface to different types of entrance optics of spectroradiometers, ensuring a reproducible geometry between the LEDs and the diffuser heads. The cylinder is, however, thermally isolated from the aluminum block by a Teflon spacer. See figure 3 for a picture of the prototype. At the moment, this prototype is being tested for temperature stability. Further investigations will provide the level and stability of irradiance, its reproducibility and the time needed to reach steady state conditions after switching on the LEDs. If these tests are successful, field measurements with this prototype will be undertaken in the near future.

Figure 3. Assembled prototype of the monitoring source based on UV-LEDs.

Acknowledgement. This report was compiled within the EMRP ENV03 Project "Traceability for surface spectral solar ultraviolet radiation." The EMRP is jointly funded by the EMRP participating countries within EURAMET and the European Union.

Characterization of a Fourier transform spectrometer for solar UV irradiance measurements

Peter Meindl, Christian Monte and Martin Wähmer

Physikalisch-Technische Bundesanstalt (PTB), Berlin, Germany

Primary radiometric standards like e.g. black body radiators [1] or cryogenic radiometers [2] are not suitable for the dissemination of radiometric units to remote measuring sites that are used for solar irradiance measurements. For this reason, portable reference instruments have to be used as transfer standards. Within the European Metrology Research Project EMRP ENV03 "Traceability for surface spectral solar ultraviolet radiation" the feasibility of using a commercially available Fourier transform spectrometer (FTS) as an alternative reference spectroradiometer will be examined. For that purpose, a Bruker FTS VERTEX 80v has been adapted for measurements in the ultraviolet spectral range from 280 nm to 400 nm by adding a UV detector and a UV beam splitter. Furthermore, the modified FTS has been characterized with respect to the suitability for solar UV irradiance measurements with low uncertainties. A global entrance optics will be fitted in order to perform irradiance measurements, and an absolute calibration of the instrument against a black body radiator with known temperature will be performed. Furthermore, the uncertainty budget with regard to solar UV irradiance measurements in the wavelength range from 280 nm to 400 nm will be determined, and a comparison of the performance of the modified FTS against a portable scanning spectroradiometer will be made.

Up to now, scanning spectroradiometers are in use as reference instruments [3]. This type of radiometer has a couple of disadvantages. For example, the solar spectrum is scanned sequentially which needs several minutes of time for each spectrum and limits the temporal resolution of the radiometer. This is a big disadvantage considering varying atmospheric conditions. The standard uncertainty of these instruments for solar irradiance measurements is around 2.3% to 4.4% depending on wavelength and solar zenith angle [3].

It is the goal of the European Metrology Research Project ENV03 to enhance the reliability of spectral solar UV radiation measurements at the Earth's surface by developing new techniques and devices that enable a traceability of solar UV irradiance measurements of better than 2%. For this reason, wavelength accuracies of better than 50 pm are required to reach nominal uncertainties of 1% to 2% due to the steep decrease of solar UV irradiance below 330 nm over many orders of magnitude. For the same reason, a high dynamic range over at least five orders of magnitude is necessary to cover the wavelength range between 280 nm and 400 nm. Furthermore, the rapid temporal variation of solar UV radiation due to varying atmospheric conditions (e.g. fast moving clouds) requires fast spectroradiometers.

Considering these demands, the usage of Fourier transform spectroradiometers may improve the dissemination of absolute irradiance scales due to the specific advantages of these instruments [4, 5]:

- Fourier transform spectrometers have a high throughput which is caused by the circular aperture of these instruments (Jacquinot or throughput advantage). This gives a comparable high signal-to-noise ratio.
- There are no diffraction losses to higher-order spectra as it is the case in grating spectrometers. This also enhances the signal-to-noise ratio.
- The whole spectrum is measured simultaneously which allows fast measurements (multiplex advantage). This is important in the case of rapid temporal variations of solar UV radiation due to atmospheric conditions (e.g. fast moving clouds).
- Fourier transform spectrometers have a wide free spectral range and therefore cover broad spectral ranges with high resolution and high wavenumber accuracy.
- Modern FT spectrometers often use integrated HeNe lasers for the measurement of the position of the moveable mirror of the FTS interferometer. This laser can be used for the wavenumber calibration of the FTS. In this way, the wavenumber scale of the FTS is inherently traced to the SI.
- Instrumental distortions are often calculable and correctable.

Traceability of the wavelength scale

The knowledge of the position of the movable FTS interferometer mirror is necessary to calculate the absolute wavenumber scale of the measured spectra. The Fourier transform spectrometer Bruker VERTEX 80v uses the radiation of a HeNe laser at 633 nm to determine the sampling positions of the interferogram [6]. The HeNe laser beam is coupled into the interferometer nearly coaxial to the radiation under investigation and generates an additional sinusoidal interferogram which is measured by a separate detector. Following a recommendation of the CIPM (International Committee for Weights and Measures), the frequency (respectively the wavelength) of unstabilized HeNe lasers has been added to the list of standard frequencies of the *mise en pratique* of the definition of the meter [7, 8]. For this reason, the SI unit *meter* can be realized by using the wavelength of an unstabilized HeNe laser as a primary standard. Consequently, the wavenumber scale of the FTS can be assumed to be traceable to the SI provided that:

- the laser is a non-tuneable helium–neon laser operating on the 3s2 → 2p4 transition (633 nm) without contamination by radiation from other transitions (e.g. 640 nm) [8],
- the built-in laser is perfectly in line with the beam under test because any misalignment leads to a wavenumber error.

Both conditions may be checked by performing an FTS measurement of the wavenumber of an external HeNe laser with well known properties. Several measurements concerning the wavenumber calibration and the spectral resolution have been performed with two Fourier transform spectrometers of the same type (Bruker VERTEX 80v). In particular, the wavelength uncertainties have been measured by using the radiation of a well known external HeNe laser and of the spectral lines of a mercury pencil lamp (Oriel Model 6034). The wavelengths of the mercury lines are well known from literature [9, 10].

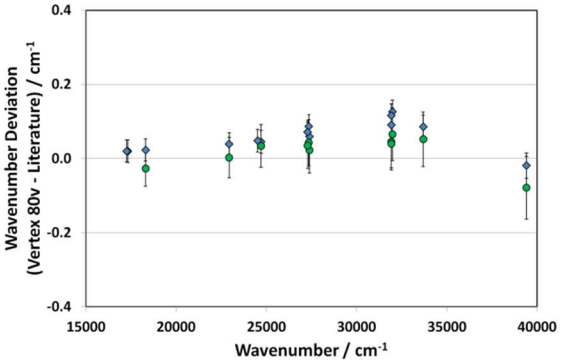

Figure 1. Deviations of measured mercury peak wavenumbers from the literature data after performing an SI-traceable wavenumber calibration of the FTS against an external HeNe laser at 633 nm.

It has been found that the measured wavenumber of the external HeNe laser can slightly deviate from the SI value (up to 0.12 cm^{-1}). This deviation is probably caused by a marginal misalignment of the internal HeNe laser. However, it has to be noted that the deviation is rather small compared to the demands of the JRP ENV03 and can simply be added to the wavenumber uncertainty of the FTS. And, if smallest possible wavelength uncertainties are desired, the misalignment error can easily be corrected either by an optimized adjusting of the internal HeNe laser or more easily by using an external HeNe laser to set the FTS' wavenumber scale (Fig. 1).

The combined wavelength standard uncertainty of the Bruker VERTEX 80v is between 3 pm and 6 pm in the spectral range from 250 nm to 500 nm. These wavelength uncertainties are an order of magnitude below the demanded 50 pm which are required to reach irradiance uncertainties of 1% to 2%. The wavelength uncertainty will therefore not limit the uncertainty of solar UV irradiance measurements.

Responsivity and stability

The spectral responsivity of the FTS is mainly determined by the responsivity of the used detector (Si or GaP) and by the properties of the beam splitter. All FTS mirrors are aluminum coated and do not limit the desired wavelength range from 280 nm to 400 nm. The irradiance calibration of this spectroradiometer will be performed by using the calculable radiation of a black body radiator [11, 12, 13]. A main influence on the stability of the FTS is given by the temperature dependence of the detectors that are used within the FTS. The temperature sensitivity of the Bruker VERTEX 80v has therefore been investigated for Si and GaP detectors. As a result, the temperature of the FTS should be stable within about ± 1 K with respect to the temperature during the irradiance calibration in order to confine the uncertainty contribution of the temperature dependence to the uncertainty of solar irradiance measurements which should be less than 2%.

Results

The usage of Fourier transform spectroradiometers may improve the dissemination of absolute irradiance scales due to the specific advantages of these instruments. The investigated Fourier transform spectrometer Bruker VERTEX 80v has a comparatively small wavelength uncertainty of less than 6 pm in the wavelength range from 250 nm to 500 nm. This is well below the 50 pm which are demanded to obtain an uncertainty of irradiance measurements of less than 2%. Furthermore, the wavelength scale can be assumed to be traceable to the SI via the built-in HeNe laser or via a wavenumber measurement of an external HeNe laser. This property is a big advantage compared with scanning spectroradiometers.

Acknowledgement. This report was compiled within the EMRP ENV03 Project "Traceability for surface spectral solar ultraviolet radiation." The EMRP is jointly funded by the EMRP participating countries within EURAMET and the European Union.

References

1. J. Hartmann, "High-temperature measurement techniques for the application in photometry, radiometry and thermometry," *Physics Reports* **469**, 205-269 (2009).
2. J.E. Martin, N.P. Fox and P.J. Key, "A Cryogenic Radiometer for Absolute Radiometric Measurements," *Metrologia* **21**, 147-155 (1985).
3. J. Gröbner, J. Schreder, S. Kazadzis, A.F. Bais, M. Blumthaler, P. Görts, R. Tax, T. Koskela, G. Seckmeyer, A.R. Webb, and D. Rembges, "Traveling reference spectroradiometer for routine quality assurance of spectral solar ultraviolet irradiance measurements," *Appl. Opt.* **44**, 5321-5331 (2005).
4. S.P. Davis, M.C. Abrams and J.W. Brault, *Fourier Transform Spectrometry* (Academic Press, 2001).
5. Herres, Gronholz, "Understanding FT-IR Data Processing, Part 1 – 3," *Comp. Appl. Lab.* **2**, p.216 (1984).
6. *Bruker VERTEX 80v User Manual*
7. 96th Meeting of the CIPM (International Committee for Weights and Measures, Recommendation 2 (CI-2007): "On the value and uncertainty of unstabilised He-Ne lasers."
8. J.A. Stone, J.E. Decker, P. Gill, P. Juncar, A. Lewis, G.D. Rovera and M. Viliesid, "Advice from the CCL on the use of unstabilized lasers as standards of wavelength: the

helium–neon laser at 633nm," *Metrologia* **46**, 11–18 (2009).

9. C.J. Sansonetti, M.L. Salit, and J. Reader, "Wavelengths of spectral lines in mercury pencil lamps," *Appl. Opt.* **35**, 74-77 (1996).
10. C.J. Sansonetti, J. Reader, "Spectrum and energy levels of singly-ionized mercury (HgII)," *Phys. Scripta* **63**, 219-242 (2001).
11. J. Hollandt, R. Friedrich, B. Gutschwager, D.R. Taubert, J. Hartmann, "High-accuracy radiation thermometry at the National Metrology Institute of Germany, the PTB," *High Temperatures - High Pressures* **35/36**, 379-415 (2003/2004).
12. J. Hartmann, K. Anhalt, R.D. Taubert, J. Hollandt, "Absolute Radiometry for the MeP-K: The Irradiance Measurement Method," *Int. J. Thermophys.* **32**, 1707-1718 (2011).
13. J. Gröbner and P. Sperfeld: "Direct traceability of the portable QASUME irradiance scale to the primary irradiance standard of the PTB," *Metrologia* **42**, 134–139 (2005).

Regular articles

Spectrophotometer for deep ultraviolet measurements

Erik Schoeffel[*]

McPherson, Chelmsford MA, USA, www.McPhersonInc.com

Ultraviolet (UV) spectrophotometry has a well-deserved niche. Very few instruments optimize for the region between 120 and 400 nm. Development and manufacture of ultraviolet lasers, optics, crystalline materials, phosphors for more efficient lighting, resonance Raman instruments, and other applications including fundamental research require a broadly useful instrument for analysis, optical characterization, and test. McPherson's new Vacuum Ultraviolet Analytical Spectrophotometer VUVAS-PL depicted in Figure 1 provides capability to measure transmission, reflection and excitation \ emission for samples that exhibit luminescence or fluorescence.

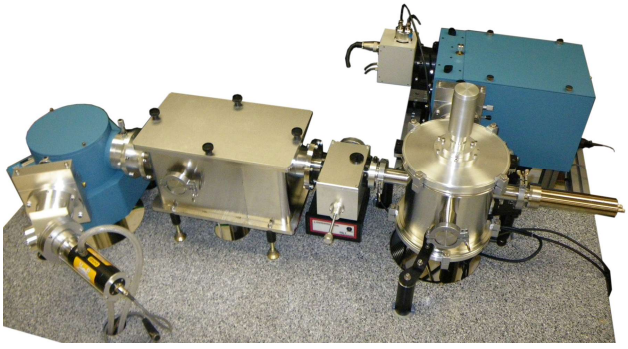

Figure 1. VUVAS-PL Spectrophotometer.

The McPherson VUVAS-PL instrument meets the requirements of deep and vacuum ultraviolet analysis in the 120 to 400 nm range. It offers a clean, particulate free and tight, purge or vacuum capable enclosure. UV enhanced optics, sources, detectors, and a computer optimized optical system. All VUVAS-PL elements are selected to improve analytical results and simplify measurement tasks for the user.

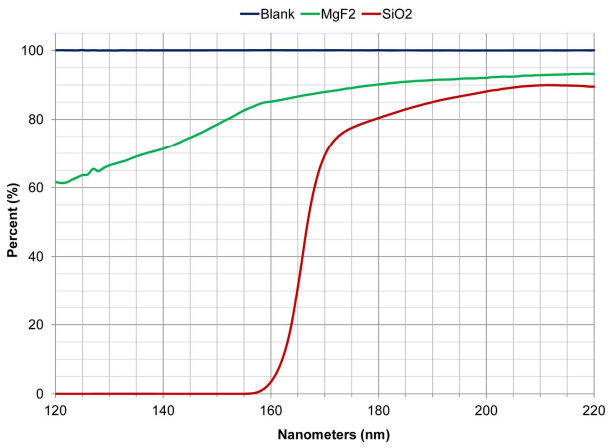

Figure 2. Measurements demonstrating precision; the VUVAS makes 0.05%T RSD measurements at a fixed wavelength, e.g. 157 nm. Wavelength scanning over the 120 to 320 nm region results in data better than 0.3%T RSD. Overall instrument stability is better than 0.5%T per hour.

The VUVAS-PL spectrophotometer works with solid samples and can be equipped with gas or liquid sample cells. Most users employ optic-like substrates coated with sample for transmission measurements (Figure 2). A three-position sample holder is standard. Cryogenic single-sample mounts and raster-mapping attachments for large samples are available as specials. Reflectance is readily measured, and angle of incidence to the sample surface is easily altered. Detector angle is also adjustable. It can maintain theta/2-theta geometry for specular reflectance measurements, or deviate from this, to measure scatter or dispersive samples.

The wavelength region below 350 nm has very few, if any, standard reference materials. [1] One reason is the energetic ultraviolet light materials must tolerate. There is also the sensitivity of samples to contamination. Contamination by monolayers of water, oxygen or oil has reportedly been responsible for transmission losses of 15% at 157 nm. [2] By design, VUVAS-PL delivers absolute measurements. A single detector collects reference data as well as the final transmission or reflectance measurement. This approach enables users to qualify instrument performance, anytime and without extra accessories. The ability of the VUVAS-PL to prove spectral and photometric precision in-situ provides data with confidence.

[*] Erik.Schoeffel@McPhersonInc.com

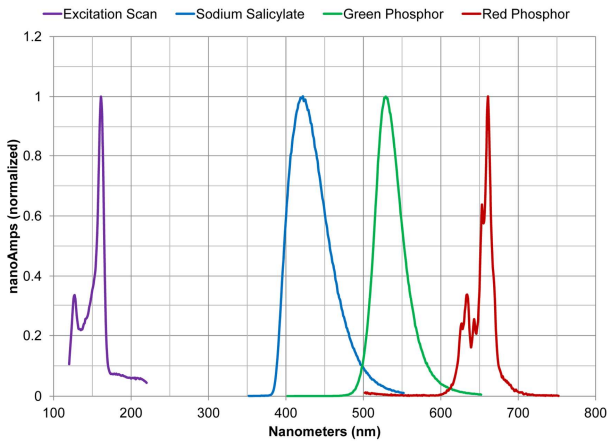

Figure 3. Excitation scan in 120 to 220 nm region together with normalized emission of three samples; sodium salicylate, green phosphor and red phosphor.

The VUVAS-PL emission spectrometer operates from 140 nm to 2600 nm depending on the selected model; vacuum and atmospheric versions are available. It uses all reflective optics to collect emission at ninety degree angle and deliver signal – free from chromatic aberration – to the entrance slit of the emission spectrometer. The emission spectrometer may be optimized to detect signals into the near Infrared. Signal acquisition of the 400 to 800 nm visible spectral region (Figure 3) with resolution on order 0.2 nm full-width-half-maximum can occur in milliseconds using the charge-couple device (CCD) detector. Accessories for persistence measurements are available too.

The VUVAS-PL system [3] is an integrated and total solution. The one-touch vacuum (purge) control system and software allow users to perform high quality deep and vacuum ultraviolet measurements more easily and with higher confidence. It complements high performance UV/Vis instruments found in many laboratories and provides solid performance for the deep and vacuum ultraviolet region.

References

1. John P. Hammond C.Chem MRSC, "New Certified Reference Materials for the determination of photometric accuracy in UV spectrophotometry," *Spectroscopy Europe* **13**(4) (2001).
2. W. Pantely and D. Collier, "Taking the UV Challenge," *OE Magazine*, October (2001).
3. www.McPhersonInc.com/systems/vuvas2000/vuvas2000.htm

One decade of Qasume site audits: 2002-2012.

Gregor Hülsen and Julian Gröbner

Physikalisch-Meteorologisches Observatorium Davos, World Radiation Center, Davos, Switzerland

Introduction

More than one decade ago, in 2001, the Q.A.S.U.M.E. project was initiated. The aim of the project was the development of a new approach for facilitating Quality Assurance of solar Spectral Ultraviolet irradiance Measurements carried out in Europe (Bais et al., 2002).

The first task of the project was the development of a transportable reference spectroradiometer, later called "QASUME" (Gröbner et al., 2005). Secondly this instrument was used for measurements at external UV monitoring sites with stationary UV spectroradiometers (Gröbner et al. 2006). Through these site audits the data submitted to the GAW World UV data Centre (WOUDC) could be quality assured to meet the needs of the scientific community. Furthermore, the project aimed at improving the data quality at European UV monitoring sites and at harmonizing the results from different stations and monitoring programs in order to ensure representative and consistent UV radiation data on a European scale.

The core of Qasume is a commercial DM150 double monochromator (Bentham) mounted in a temperature stabilized box. The fiber coupled and temperature controlled input optic was optimized for a low cosine error.

As a byproduct of the project activates the irradiance reference of the Qasume spectroradiometer was formed by six transfer standards traceable to the PTB.

After the end of the project in 2005, the duties were carried over to the European UV Calibration Center (EUVC), operated by the Physikalisch-Meteorologisches Observatorium Davos (PMOD/WRC). The transportable spectroradiometer became the European UV reference spectroradiometer.

After one decade the status of the harmonization can be presented by the comparison of the data collected by UV monitoring stations in Europe relative to the European reference spectroradiometer.

Results

Since 2002 53 site audits were performed in 16 European countries (Fig. 1). During the measurement campaigns UV irradiance data from 59 instruments were traced back to the European irradiance reference. The results of each site visit were summarized in a report publicly available at www.pmodwrc.ch/euvc/euvc.php?topic=qasume_audit.

Figure 1. Map of all sites visited by the Qasume reference spectroradiometer in the last decade.

In total 137 comparisons (including multiple visits) relative to Qasume were used to calculate the average deviation of the solar UV measurements by the UV monitoring instruments relative to QASUME (Fig. 2). The statistics are listed in table 1. A subset 1 can be selected which includes only the last comparison to the instruments, excluding multiple visits. The last subset consists only of Brewer spectrophotometers, which are the majority of instruments in the Qasume database.

Table 1. Statistics of the site audits results performed with Qasume from 2002 till 2012. Displayed are the ratios of test instrument to Qasume filtered in the UVB range.

Subset	*N*	Med	Mean	Min	Max
All	137	0.982	0.988	0.809	1.221
S1:Unique	59	0.984	0.995	0.809	1.221
S2:Brewer	37	0.974	0.992	0.924	1.221

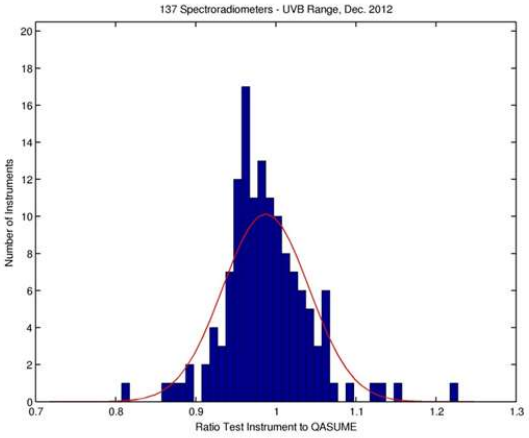

Figure 2. Histogram of the performance of all UV spectroradiometers which have been compared to the Qasume reference instrument (bar width of the histogram is 1 %).

Some examples of observed instrument features are discussed in the next section. Figures 3 to 5 illustrate typical errors of the entrance optics. The large cosine error is visible by the symmetric diurnal change in the ratio of the instrument to the reference (Fig. 3). This error is caused by a non-ideal input optic and is a function of the solar zenith angle and the wavelength. Figure 4 shows a large azimuth error which was caused by a misalignment of the fiber within the input optic. The error could be detected by turning the input optic of the test instrument (ID 1) by 180 deg for a few scans. The last example (Fig. 5) shows a temperature dependence effect, which is most common for Brewer spectrophotometers. A correction algorithm can reduce this diurnal variability.

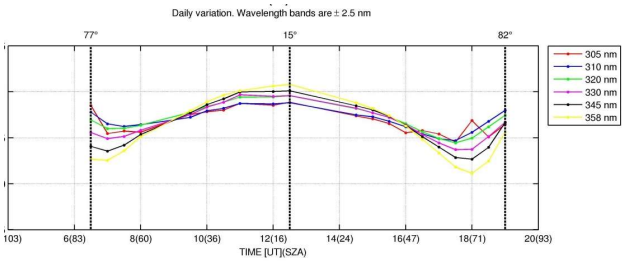

Figure 3. Symmetric diurnal variability of the ratio test instrument to Qasume. This is an indication for a cosine error which is a function of the solar zenith angle and the wavelength.

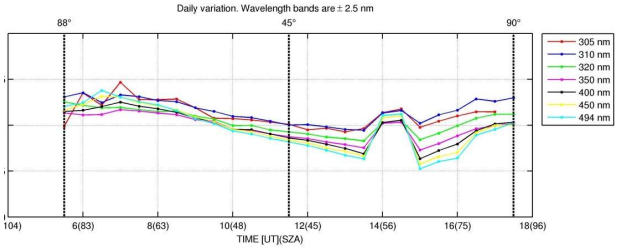

Figure 4. An azimuth error of an instrument (ID 1) can be tested by turning the input optic by 180 deg during the comparison as done here for two scans at 14 and 14:30 UT.

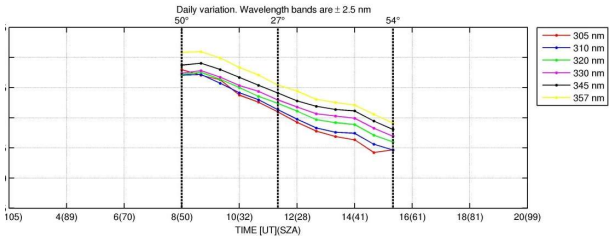

Figure 5. The drift of the test instrument is a function of the internal temperature of the spectroradiometer and can be largely removed by an appropriate correction algorithm.

Finally, figure 6 shows the ratios of the UV data of a spectroradiometer relative to Qasume recorded in August 2011. The average ratio is close to unity, no diurnal variability could be observed and the noise is less than 1%. The data originates from a second site visit to the instrument ID1. The large azimuth error has been repaired and the performance of the instrument is in very close agreement to the QASUME reference spectroradiometer.

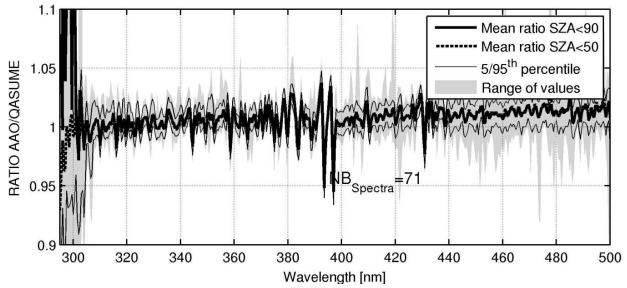

Figure 6. Result of the site audit to instrument shown in Figure 4 after the repair of the input optic.

Conclusion

The Qasume project is a powerful tool to investigate the consistency of spectral UV measurements across Europe. The task of the project was continued by the European UV calibration center of PMOD/WRC. Most UV monitoring stations in Europe could be compared to the Qasume reference instrument. Through continuous visits and multiple audits the homogenization of spectral UV data across Europe has shown significant improvements in the data quality.

Recently, the WMO has recognized the PMOD/WRC as a World Calibration Center for solar UV radiation for the World Meteorological Organization, Global Atmosphere Watch Programme. The PMOD/WRC performs, within this framework, the following activities:

a) assist WMO Members operating WMO/GAW stations to link their UV radiation observations to the WMO/GAW Reference Scale through comparisons of the station instruments with the standard instruments operated by PMOD/WRC,

b) assist the WMO/GAW Scientific Advisory Group (SAG) on UV radiation in the development of the

quality control procedures required to support the quality assurance of UV observations and ensure the traceability of these measurements to the corresponding primary standard,

c) maintain and operate a transportable reference spectroradiometer for the routine quality assurance and calibration of spectroradiometers measuring spectral solar UV irradiance through regular site visits,

d) maintain and operate instrumentation to provide calibration facilities for UV radiation radiometers (spectral and broadband).

e) Provide traceability to the primary spectral irradiance standards of NMIs by calibrating spectral irradiance standards of UV monitoring laboratories (Gröbner and Sperfeld, 2005).

References

Bais, M. Blumthaler, J. Gröbner, G. Seckmeyer, A. R. Webb, P. Gorts, T. Koskela, D. Rembges, S. Kazadzis, J. Schreder, P. Cotton, P. Kelly, N. Kouremeti, K. Rikkonen, H. Studemund, R. Tax, and S. Wuttke, "Quality Assurance of Spectral Ultraviolet Measurements in Europe Through the Development of a Transportable Unit (QASUME)," *Proc. SPIE*, 14-18 October, Shanghai, China (2002).

Gröbner, J., J. Schreder, S. Kazadzis, A. F. Bais, M. Blumthaler, P. Görts, R. Tax, T. Koskela, G. Seckmeyer, A. R. Webb, and D. Rembges, "Traveling reference spectroradiometer for routine quality assurance of spectral solar ultraviolet irradiance measurements," *Appl. Opt.* **44**, 5321-5331 (2005).

Gröbner, J., M. Blumthaler, S. Kazadzis, A. Bais, A. Webb, J. Schreder, G. Seckmeyer, and D. Rembges, "Quality Assurance of spectral solar UV measurements: results from 25 UV monitoring sites in Europe, 2002 to 2004," *Metrologia* **43**, 66-71, doi: 10.1088/0026-1394/43/2/S14 (2006).

Gröbner J., and P. Sperfeld,, "Direct traceability of the portable QASUME irradiance scale to the primary irradiance standard of the PTB,'' *Metrologia* **42**, 134—139 (2005).

Characterization of instruments for the measurement of optical radiation

S. Saudino Fusette[1],S. Facta[1], A.Bonino[1], M.Vaccarono[2], L.Anglesio[2] and G.d'Amore[1]

1. ARPA Piemonte, Ivrea, Torino, Italy
2. Università degli studi di Torino, Corso di laurea in Fisica, Torino

Abstract

Optical radiation measurements are rather difficult because of the following two aspects: most of the part of sources investigated for human exposure assessment emit radiation within a wide spectral range; human exposure assessment is based on radiometric quantities weighted according to different action spectra. In this work the response characteristics of some UV meters, obtained by laboratory measurements, will be discussed. Particular attention will be paid to the accuracy evaluation based on the comparison between real and ideal wavelength response of the meters.

INTRODUCTION

Broadband radiometers or spectroradiometers can be used to measure ultraviolet (UV) radiation. The radiometers give the value of a radiometric quantity, as for example, irradiance or radiance, integrated over their spectral region of sensitivity, while spectroradiometers allow to obtain its spectral distribution. Spectroradiometers are constituted by a single or a double monochromator in order to separate the radiation at various wavelengths and they can be divided into two categories: scanning spectroradiometers and spectroradiometers with CCD array detectors.

The choice of the instrument to be used should be made considering the characteristics of the source, such as emission spectrum and time variability, and the need of measuring effective radiometric quantity, that is weighted according an action spectrum. The scanning spectroradiometers with double monochromator allow to obtain more accurate results, but they can be used just if the radiation to be measured is not time-variable. Indeed the measurement is not instantaneous but it takes a time, up to several minutes, to scan the range of interest. Otherwise, if the source emission is variable in the time, array ccd spectroradiometers can be used, but care should be taken in the UV spectral range where stray light may cause high errors in measurements.

If it is not necessary to know the spectrum of the source, broadband radiometers can also be used. They are easy to use instruments with a fast response time, but significant mistakes may occur in the measurement, because of the poor matching of radiometer spectral response to the ideal one. The ideal response can be a biological action spectrum, for measurements of effective quantities, or equal to one within a specific spectral region and zero elsewhere, for measurements of physical not weighted quantities. If the matching of the radiometer response and the ideal response is not good, the measurement results depend also on the calibration spectrum and on the spectrum emitted by the measured source.

To evaluate the accuracy and the reproducibility of the radiometric measurements, the response characteristics of three radiometers were analysed in laboratory. This analysis allowed to know the error associated to the radiometric measurement and to obtain some factors to correct it. Then some sources with different emission spectra were measured with the radiometers and the measured values were compared to those obtained by means of a double monochromator spectroradiometer, considered as reference meter.

The analysis reported in this paper are carried out according to the CIE 53-1982 technical report [1].

MATERIAL AND METHODS

The radiometric measurement accuracy depends on the matching of the spectral and angular responses to the ideal ones. Furthermore other parameters, like the dynamic range, the out-of-band response, the aging of the optical elements of meters, the temperature and the humidity conditions, may have influence on the measurement results. However, these parameters will not be discussed in this paper.

In this work, three instruments were investigated: a UVA radiometer (280-315 nm), a UVB radiometer (315-400nm) and an erythemal UVE radiometer (effective irradiance weighted according to the erythemal action spectrum over 280-400 nm). All these meters were calibrated in irradiance mode.

Firstly the spectral and angular responses were characterized in laboratory. The laboratory characterization was aimed to evaluate the uncertainty associated to the radiometric measurements of sources with emission spectra different from that emitted by the calibration lamp.

Measurements on different sources by broadband radiometers were compared to those obtained by means of a double monochromator spectroradiometer, as reference instrument for UV radiation measurements.

The comparison allowed to evaluate the accuracy of the radiometric measurement. The spectroradiometric measurements were carried out with a portable double monochromator spectroradiometer, Optronic Laboratories mod. OL756, used with OL IS-270 integrating sphere having a 10 mm knife-edge entrance aperture and with a 2 m fiber optic cable. Spectral measurements were carried out over the 250 nm to 800 nm wavelength range with a stray light rejection lower than 10^{-8} at 285 nm.

The instrument is regularly calibrated in the Laboratory of Optics of ARPA Piedmont using a 250W tungsten halogen lamp traceable to National Institute of Standards

as a reference source. The wavelength scale is calibrated to match known emission lines of a low pressure mercury argon fluorescent lamp.

The spectral response

The relative spectral response facility consists of a Bentham double monochromator DM 150. The radiation source is a 150 W Xe lamp positioned in front of the entrance slit and adjusted thus to maximise the radiation at the exit slit. Behind the exit slit, the radiometer and a calibrated photodiode was alternately placed.

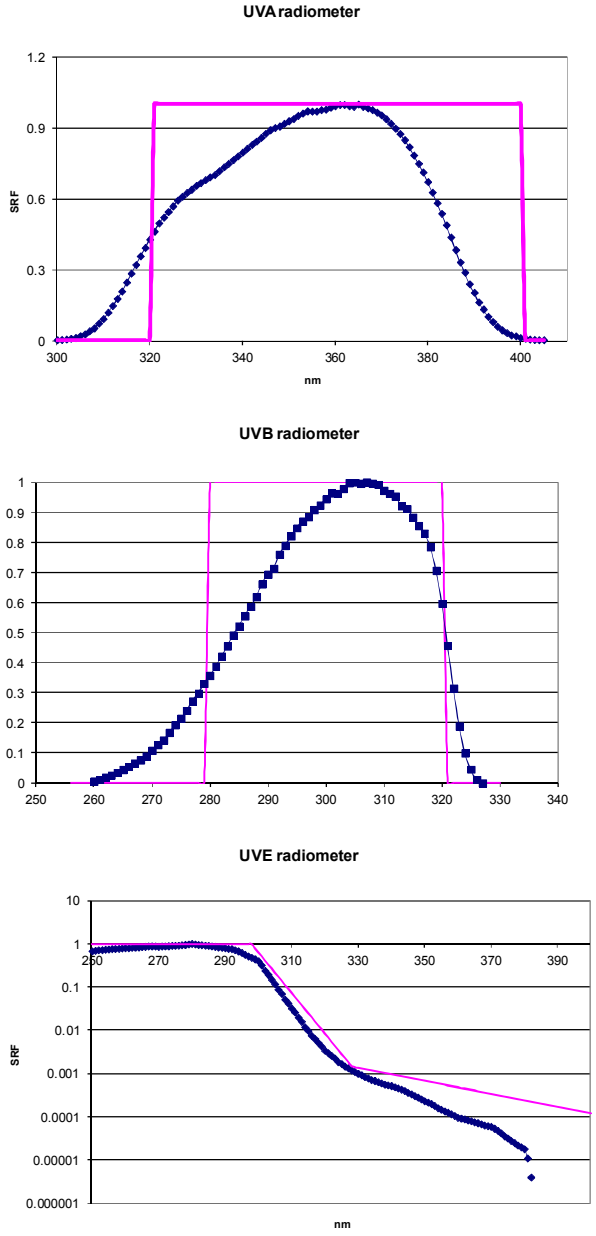

Figure 1. Measured radiometer SRF (blue symbols) compared to ideal responses (pink solid lines).

The spectral response function $s(\lambda)$ is obtained from:

$$s(\lambda) = \frac{E(\lambda)}{P(\lambda)} \qquad (1)$$

where $P(\lambda)$ is the power measured by the photodiode and $E(\lambda)$ is the irradiance measured by the radiometer, both at wavelength λ.

Then the spectral response function was normalized to its maximum. The relative uncertainty of the function was estimated equal to 10%.

The measured spectral response functions of the analyzed radiometers are reported in Fig.1, and are compared to the ideal responses. There are strong differences between the measured and ideal responses of all radiometers, as shown in Fig.1.

The knowledge of $s(\lambda)$ and of the calibration spectrum allows to evaluate the f_1' error associated to the measurement of sources having emission spectrum different from the spectrum of the calibration source. In particular, according to the CIE 53-1982, f_1' is given by equation

$$f'_1 = \frac{\int \left| s_x(\lambda)' - s_T(\lambda) \right| d\lambda}{\int s_T(\lambda) d\lambda}, \qquad (2)$$

where $s_x(\lambda)'$ is given by

$$s_x(\lambda)' = \frac{\int S(\lambda)_A s_T(\lambda) d\lambda}{\int S(\lambda)_A s(\lambda) d\lambda}, \qquad (3)$$

where $s_T(\lambda)$ is the ideal spectral function and $S(\lambda)_A$ is the calibration spectrum.

Table 1. The radiometric measurement uncertainties associated to the spectral and angular responses.

Radiometer type	Uncertainty	
	Spectral response f_1'	Angular response f_2
UVB	47 %	74%
UVA	34 %	65%
UVE	30 %	41%

The f_1' values were estimated for all three radiometers. The calibration of each radiometer was carried out at a specific wavelength: 365 nm for UVA radiometer and 295 for both UVB and UVE radiometers. The monochromatic radiation was obtained coupling a 1000 W Xe lamp to a single monochromator Zolix Omni λ150. The size of the monochromator slits was set so as to have a throughput FWHM equal to 16 nm

The f_1' error values are reported in Table 1, together with the values of f_2 error, which will be discussed further in this document.

If the measured source spectrum $S(\lambda)_Z$, the calibration source spectrum and the radiometer spectral response are known, a multiplicative correction factor $a(Z)$ may be calculated, according to the CIE 53-1982. This factor, which allows to correct the radiometric measurement, is given by

$$a(Z) = \frac{\int S(\lambda)_Z s(\lambda) d\lambda}{\int S(\lambda)_Z s_T(\lambda) d\lambda} \times \frac{\int S(\lambda)_A s_T(\lambda) d\lambda}{\int S(\lambda)_A s(\lambda) d\lambda}. \qquad (4)$$

The correction factors were calculated for different lamps and are reported in Table 2. Subsequently these factors will be compared to those obtained as ratio of radiometric to the spectroradiometric measurements.

Table 2. The corrective factors to be applied to radiometric measurements of different kinds of sources.

Type of source	Corrective factors $a(Z)$		
	UVA	UVB	UVE
Deuterium lamp	1.4	0.83	0.82
Halogen lamp	1.64	0.7	0.88
Xe lamp	1.5	0.77	0.83
Low pressure domestic tanning device	1.16	0.49	1.44

The angular response

The angular response was obtained by fully irradiating the radiometer probe with radiation from a 1000 W Xenon lamp and turning the probe around its center.

The correct measurement of the irradiance requires the contribution of the incident radiation to be proportional to the incidence angle cosine calculated with respect to the normal of the receiving surface (cosine response). The measured angular responses of the investigated radiometers are reported in Fig.2 and are compared to the cosine response. The UV radiometer angular responses decrease faster than the cosine function. This fast decrease may cause some mistakes if the measurement geometrical conditions are different by the geometry of calibration. Calibration is usually carried out far from the source enough to assume all radiation to be perpendicular to the probe surface. The measurements near the source may be underestimated, since the radiation invests the probe surface from different angle.

The error associated to the deviation of radiometer angular response from the ideal one may be evaluated in terms of f_2, according to the CIE 53-1982. The f_2 value is given by equation

$$f_2 = \int_{\varepsilon=0}^{85} \left| f_2(\varepsilon) \right| \times \sin(\varepsilon) d\varepsilon \,, \qquad (5)$$

where $f_2(\lambda)$ is the ratio of the radiometer angular response to the cosine response, at the angle ε, decreased by a unit. f_2 is the error associated to the radiometric measurement carried out in geometrical conditions different from those of calibration.

The f_2 values obtained for the investigated radiometer were reported in table 1. They are always higher than 40%, since the radiometer angular response are strongly different from the cosine response.

RESULTS

The radiometer response characteristics were analyzed in laboratory and six sources with different emission spectra or different power were measured. The radiometric measurement results were compared to those obtained with a double monochromator spectroradiometer.

The spectroradiometer is equipped by an integrating sphere, so that its angular response is very close to the cosine response.

The results of the measurements are reported in Table 3.

Generally the differences between radiometric and spectroradiometric measurements were lower than the error associated to the poor matching of radiometric angular and spectral responses to the ideal response (Table 1).

Indeed the measurements were carried out far from the source enough to assume the incident beam to be normal to the probe surface, taking into account also the size of source. Therefore the non-ideal spectral response is most important cause of measurement errors.

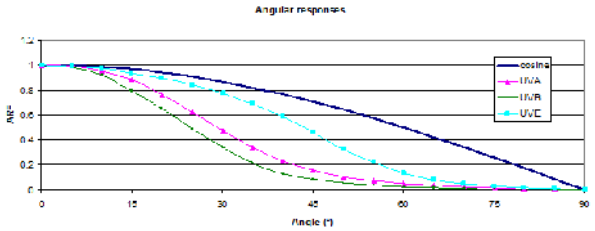

Figure 2. Measured radiometer ARF compared to the cosine response.

Analyzing data reported in Table 3, the measured correction factors are in good agreement with those calculated. So the radiometric measurements may be corrected if the measured source spectrum and the radiometer spectral response are known.

Moreover, the reported data show that for UVB and UVE radiometers, the differences between the calculated and measured correction factors are greater in the measurement of 250 W halogen lamp emissions than in the measurement of 1000 W halogen lamp emissions. In the first case, the signal is rather low, close to the instrument sensitivity (0.1 $\mu W/cm^2$), so the higher difference may be due to the imperfect linearity response of the radiometers. In addition the correction factor measured for deuterium lamp is significantly lower than the calculated one. The reason is the different spectral range the spectroradiometer and the radiometer are sensitive within: the radiometer measures UV radiation between 250 and 400 nm, while the UVE radiometer measures also radiation below 250 nm, which is a high spectral component in the emission spectrum of deuterium lamp.

CONCLUSIONS

The broadband radiometers are instruments widely used for optical radiation measurements, being cheap and easy to use with a fast response time. However radiometric measurements by these instruments may be inaccurate, in particular if the measurement conditions are different from that of calibration. This inaccuracy is mainly due to the poor matching of radiometric spectral and ideal responses and to the deviation of the angular response from the cosine response.

In laboratory the response characteristics of three radiometers, UVA, UVB and UVE, were evaluated. The knowledge of spectral and angular response allowed to calculate the error associated to the measurement in conditions different by those of calibration, according to the CIE 53-1982. The highest estimated value of the

error was equal to 47% for the spectral response and was equal to 74% for the angular response. Moreover, on the basis of the spectral response measured in laboratory, the corrective factors which have to be applied to the radiometric measurement were estimated.

Six sources with different emission spectra or different power were measured by the three radiometers. The obtained results were compared to those obtained by means of a spectroradiometer. The difference between radiometric and spectroradiometric measurements resulted in agreement with the uncertainty values estimated by the laboratory analysis. Moreover the knowledge of the measured source spectrum allowed verifying the agreement between the calculated and measured corrective factors.

The obtained results show that the radiometric measurement can be affected by a high inaccuracy. Anyway the knowledge of meter response characteristic allows estimating the error associated to the measurement and, if the spectrum of the measured source is known, to correct the radiometric value by the corrective factor $a(z)$.

REFERENCE

[1] CIE Technical report 53, *Methods of characterizing the performance of radiometers and photometers* (1982).

Table 3. Comparison between radiometric and spectroradiometric measurements.

Deuterium lamp	Radiometer	Spectroradiometer	Difference (%)	Measured corrective factor	Calculated corrective factor $1/a(z)$
UVA radiometer [μW/cm^2]	5.8	8.4	30.9%	1.45	1.4
UVB radiometer [μW/cm^2]	8.8	6.7	-30.5%	0.76	0.83
UVE radiometer [μW/cm^2]	17.6	12.8	-37.6%	0.72	0.82
250W halogen lamp					
UVA radiometer [μW/cm^2]	2.4	3.8	36.2%	1.58	1.64
UVB radiometer [μW/cm^2]	0.3	0.3	-19.6%	0.82	0.7
UVE radiometer [μW/cm^2]	0.2	0.2	1.6%	1.02	0.88
1000W halogen lamp					
UVA radiometer [μW/cm^2]	55.6	93.1	40.2%	1.68	1.64
UVB radiometer [□W/cm^2]	9.9	6.8	-46.0%	0.68	0.7
UVE radiometer [μW/cm^2]	5.4	4.6	-15.3%	0.86	0.88
Low pressure tanning devices					
UVA radiometer [μW/cm^2]	550.2	679.0	19.0%	1.24	1.16
UVB radiometer [μW/cm^2]	20.9	10.0	-109.0%	0.48	0.49
UVE radiometer [μW/cm^2]	0.9	1.3	35.4%	1.55	1.44
1000 W Xe lamp					
UVA radiometer [μW/cm^2]	36.0	51.5	30.0%	1.44	1.5
UVB radiometer [μW/cm^2]	16.4	12.0	-36.4%	0.73	0.77
UVE radiometer [μW/cm^2]	13.0	10.9	-19.0%	0.84	0.84
150W Xe lamp					
UVA radiometer [μW/cm^2]	9.3	14.0	33.4%	1.51	1.5
UVB radiometer [μW/cm^2]	4.3	3.3	-30.3%	0.77	0.77
UVE radiometer [μW/cm^2]	3.9	3.1	-24.4%	0.8	0.84

Standardization of broadband UV measurements

George P. Eppeldauer

National Institute of Standards and Technology, Gaithersburg, MD, USA

Abstract

The CIE standardized rectangular-shape UV response functions can be realized only with large spectral mismatch errors. The spectral power-distribution of UV sources is not standardized. Accordingly, the readings of different types of UV meters, even if they measure the same UV source, can be very different. In order to solve this problem, available UV detectors and UV meters used for irradiance measurement from 365 nm sources were evaluated. The spectral product of the source-distribution and the meter's spectral-responsivity were calculated for different combinations to estimate broad-band signal-measurement errors. Standardization of both the UV source-distribution and the measurement procedure is recommended here in an example where 365 nm sources are measured with UV-A meters. The goal is to perform uniform broad-band UV measurements with low uncertainty. It is shown what spectral responsivity function(s) is needed for new and existing UV irradiance meters to perform low-uncertainty broadband (with ~365 nm peak) measurements.

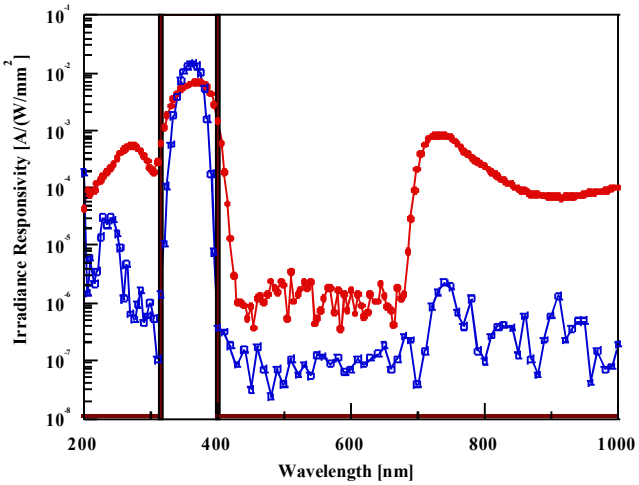

Figure 1. The CIE standardized UV-A (square-shape) and two realized spectral responsivity functions.

Introduction

UV irradiance meters measure optical radiation from broad-band UV sources. In the example shown here, UV sources that peak at 365 nm are used for non-destructive testing of metal parts. Available UV-A irradiance meters read different irradiance values when they measure the same 365 nm source. The differences in the readings can increase to higher than 20 % when different UV radiometer models are involved in the irradiance measurements. The reason for the large measurement errors is lack of standardization for UV measurements. The CIE standardized UV-A function has a square shape between 320 nm and 400 nm. Since filter combinations are to be used to realize this square-shape band-pass function, the spectral mismatch errors are large. The function-realizations of two commercial UV-A meters are illustrated in Fig. 1 [1].

The full dots show a typical realization and the open-squares represent a better realization. It is shown clearly that both realizations have large spectral mismatch errors relative to the CIE (square shape) standard function. Table 1 shows the measurement errors obtained with the better realization when four types of (commonly used) calibration sources are reused as test sources [1]. When the test source is different than the calibration source, the measurement error can increase to 60 % or higher. The measurement errors, using the typical meter, can increase to 300 %.

Table 1. Errors in broad-band UV measurements with a commercial UV meter having a better-than-average response function.

	Test Source			
Calibration Source	FEL	Mercury	Deuterium	Xenon
FEL	0.0 %	50.8 %	-6.7 %	2.7 %
Mercury	-33.7 %	0.0 %	-38.2 %	-31.9 %
Deuterium	7.2 %	61.7 %	0.0 %	10.1 %
Xenon	-2.7 %	46.8 %	-9.2 %	0.0 %

A reasonable calibration (correction) factor for broadband UV measurements cannot be assigned based on the CIE UV-A standard responsivity function. Also, the spectral power distribution of the excitation 365-nm sources has not been standardized which is a must if the realized spectral responsivity function of the UV meter is different from the standard function. The wavelength range of the presently used CIE standard function is too broad for the required tests where 365 nm excitation sources are used. At present, the 365 nm Hg line is used for non-destructive material tests. The neighboring Hg-lines (such as the 334 nm line) are attenuated using glass filters. As shown in Fig. 2, the blocking is usually not perfect and the UV irradiance meters with their different spectral responsivity functions can measure the radiation produced by the remaining neighboring line(s). Also, the continuum of the source spectral distribution can produce different output signal components in the different broadband UV irradiance meters.

In this example, the test detector measured 14 % higher than the reference (called standard) detector. The reason of this large error is that the different spectral responsivities of the UV meters produce different spectral products with the source distribution. At present, manufacturers are unable to improve their UV meters because of the lack of standardization of broad-band UV

measurements. The UV sources have not been standardized either.

In order to phase out mercury from future tests (primarily because of safety reasons) and to eliminate out-of-band radiation from the UV source, LED sources with similar irradiance distribution to the filtered Hg-lamps are introduced here.

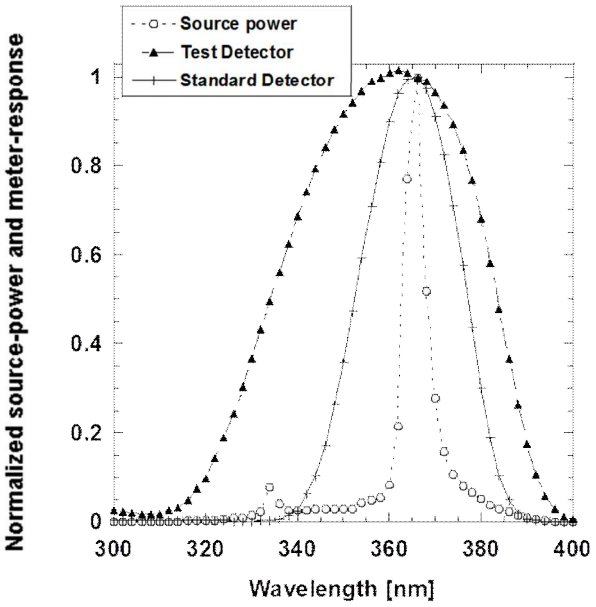

Figure 2. Relative spectral distribution of a filtered 365 nm Hg source and the responses of two different UV meters normalized at 366 nm.

The goal of this work is to make the broadband UV measurements uniform and to lower the broad-band UV (with a typical emissivity peak of 365 nm) irradiance measurement uncertainties. To achieve this goal, the realization issues of the meter's spectral responsivity and the 365-nm source distributions have been studied and a new definition for standardized measurements is developed to decrease the large errors in existing broadband UV measurements.

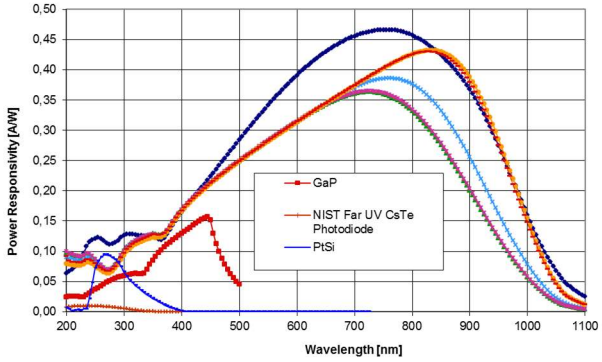

Figure 3. Spectral power responsivities of UV detectors. The broadband detectors (without labels) are different Si photodiodes.

UV detectors

The spectral power responsivities of several commercially available UV detectors have been measured. The obtained responsivity functions are shown in Fig. 3. The GaP detector, that has a reasonably high responsivity at 365 nm, cuts down at wavelengths longer than 500 nm. However, it is not resistant to UV damage. The PtSi detector cuts down for wavelengths longer than 400 nm. The CsTe photodiode also cuts down above 400 nm but its peak responsivity is almost a decade lower. The broadband detectors (not labeled) are mostly UV damage-resistant silicon photodiodes. Care should be taken when using these Si detectors because they measure optical radiation to about 1200 nm.

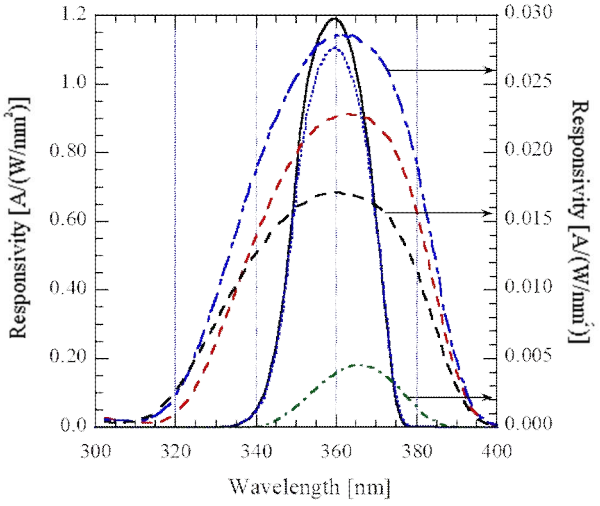

Figure 4. Spectral irradiance responsivities of different UV meters.

UV irradiance meters

Six available UV irradiance meters have been measured for spectral irradiance responsivity. Figure 4 shows how different the spectral responsivities are. Both the peak responses and the spectral bandwidths (wavelength coverage) are different.

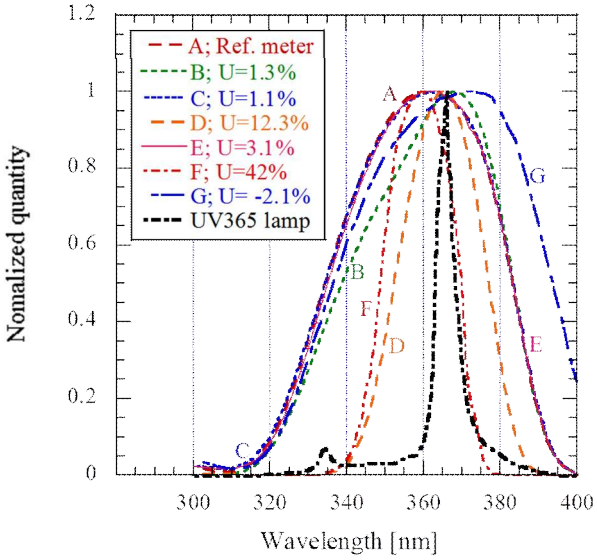

Figure 5. Normalized quantity versus wavelength includes the spectral responses of UV meters from A to G and the spectral power distribution of a filtered UV 365 nm Hg lamp.

Seven normalized (A to G) spectral responses are shown in Fig. 5. The graph also shows the spectral distribution of the filtered 365 nm (peak) Hg source. In order to determine the measurement errors of the different meters, the signal reading of each meter was divided by the signal reading of the commercial reference meter A (UDT268UVA) when they all measured the same UV365 lamp in the figure. The percent errors are shown in the legend of the graph. The meter A was arbitrarily selected here as a reference meter to compare the measurement results obtained with the different UV meters. The errors show how uniform the seven broadband UV measurements are. Some of the shown measurement uniformity errors are small but others (where the shapes of the spectral responsivity functions were not adequate) increased to 42.3 %. In this worst case, the responsivity peak was 360 nm instead of 365 nm where the source peak was. Two meters (with narrow spectral bandwidths) did not measure the 334 nm (filter-attenuated) neighbouring Hg line and also part of the source continuum but the others with the broad spectral coverage measured both the 334 nm (attenuated) line and the continuum of the Hg source.

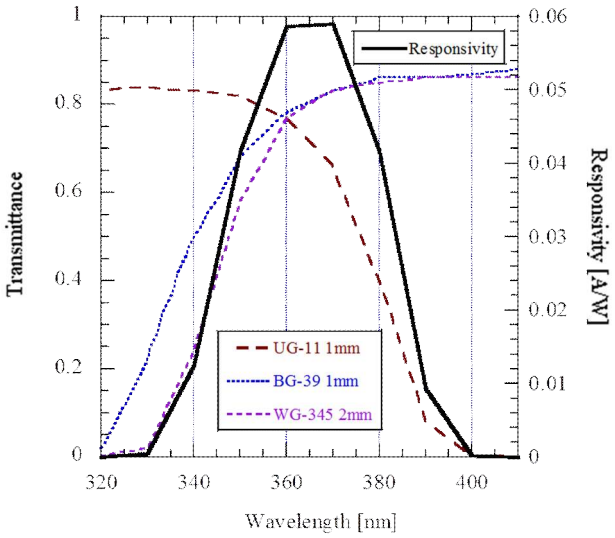

Figure 6. Modeled 365 nm meter-response function using 3 filters and a UVG-100 silicon photodiode.

Spectral modeling

A spectral responsivity function that can be easily realized and used as a reference function has been designed using three filters and a UV-damage resistant silicon photodiode. The filter transmittance functions and the resultant responsivity function with its center at 365 nm are shown in Fig. 6. This design was made for LED sources with 365 nm ± 5 nm peaks. The model was calculated with 10 nm wavelength-increments.

The modeled and then normalized response function is also shown in Fig. 7 together with the normalized spectral response of a commercial UV meter and the spectral distributions of a UV LED-based projector built with seven LEDs and dyes (phosphors) in an array. The meter responses in Fig. 7 were normalized to unity at the peaks to compare the two functions for 365 nm LED measurements.

It can be seen that the spectral power distributions of the two LED sources (shown for 1 A and 2 A feeding currents) are well within the spectral responsivity functions for both UV meters. Also, there is no leaking responsivity for wavelengths outside of the source spectral distribution function that could be measured by the two different meters. The requirement for standardization is to receive the same spectral product for the source distribution and the meter responsivity even if different meters or different 365 nm sources are used.

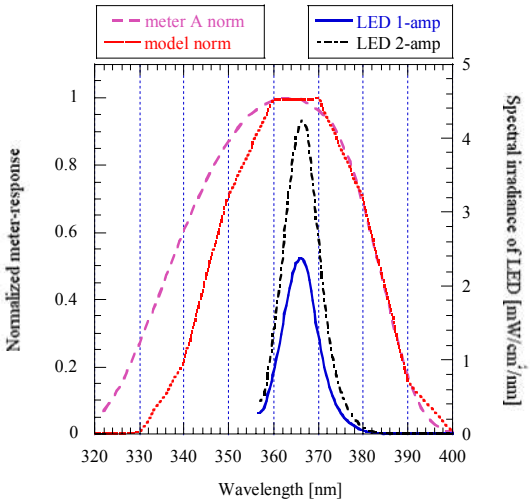

Figure 7. Comparison of the modeled 365 nm response to the commercial meter A. The distribution of the UV LED projector is shown at 1 A and 2 A currents.

LED sources

Because of environmental safety reasons, 365 nm LED sources have been selected to substitute Hg lamps. The spectral distribution of these LED sources is similar to that of Hg lamps. However, LED sources do not have neighboring emission lines and they do not have a continuum-radiation like Hg lamps. The first step in the modeling and in the following standardization is to establish the spectral band-limits and peak tolerances for the 365 nm LEDs. The suggestion here is to use LEDs with 365 nm ± 5 nm peaks and a maximum spectrum halfwidth (FWHM) of less than 15 nm to keep the spectral mismatch errors and the uncertainties of the spectral products (signals) at a reasonably low level even if different meters and/or sources are used.

Figure 8 shows the design of a high-power UV-LED source that can produce a uniform irradiance, larger than 1 mW/cm^2 [2] within a diameter of 7.5 cm at a distance of 40 cm (measured from the source). The spatial distribution of the radiance of the LED is not uniform. Therefore, a hexagonal quartz rod is used to homogenize the LED output radiation. The radiation incident into the rod, above an angle limit, is totally reflected inside of the rod-walls. The mixed reflected beams at the output of the rod will produce a uniform radiance distribution. The output beam of the homogenizer is focused by an objective lens onto the target surface. A 365 nm irradiance source like this can satisfy the requirements for standardization.

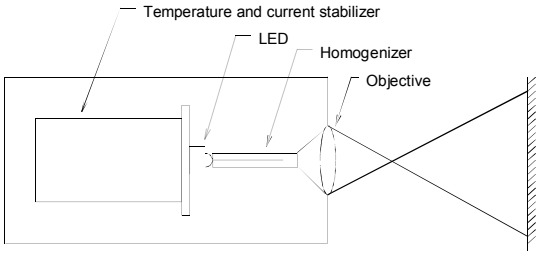

Figure 8. Input optics scheme of a UV LED irradiance source.

Definition of uniform broadband 365 nm measurements

First, satisfy the requirements for source distribution: Use LEDs with 365 nm ± 5 nm peaks and a maximum spectrum-half-width (FWHM) of less than 15 nm. In the next step, match the spectral response of the UV meters to the 365 nm source distribution function such that the spectral product of the source-distribution and the meter responsivity will produce an error less than the required measurement uncertainty when different UV meters (models) and/or different 365 nm sources are used.

The standardization of the broad-band UV measurements is needed only if more than one UV meter and/or more than one 365-nm source are used.

Conclusions

UV irradiance measurements verified that the presently applied CIE UV-A standard responsivity function is not suitable for accurate realization. Large 365 nm irradiance measurement uncertainties were obtained using the present CIE standard UV-A function. Up until now, Hg lamps were used for 365 nm excitation. The lamps were filtered but the spectral distribution of the excitation UV sources has not been standardized. Commercially available UV detectors and meters have been evaluated and compared in this paper. Also, different UV LED sources have been studied, evaluated, and suggested for standardization. A broadband UV measurement-model is described to develop an easily realizable spectral responsivity function based on the spectral power distribution of 365 nm (peak) LED sources. The 365 nm LED sources do not have environmental safety issues like mercury lamps and have continuum-free spectral distributions. Based on the model, a standard procedure is suggested that can result in uniform broadband 365 nm irradiance measurements with low uncertainty. The definition for the standard procedure is described. The first step in the procedure is to select the source according to the requirement described in the definition. In the second step, the responsivity function of the meter is selected with a spectral match to the standardized source-distribution function according to the definition. Invariant spectral products can be obtained when using the described 365-nm LED distributions and the meter responsivity functions even if different sources (with different peak wavelengths and spectral widths) are used in the measurements. Based on the definition described here, UV meter models (that satisfy the described standardization requirements) can be selected for uniform broadband 365 nm measurements. Other UV meters, where the described spectral-response requirements are not achieved, are non-ideal for uniform broadband UV measurements.

Acknowledgements. This project was funded by the U.S. Air Force AFMC AFMETCAL. The author thanks T. C. Larason for supplying the spectral responsivity data for the spectral modeling and J. D. Schanda for the design of the UV-LED source.

Disclaimer. Certain commercial equipment, instruments, or materials are identified in this paper to foster understanding. Such identification does not imply recommendation or endorsement by the NIST, nor does imply that the equipment are necessarily the best available for the purpose.

References

1. T. C. Larason, C. L. Cromer, “Sources of Error in UV Radiation Measurements,” J. Res. Natl. Inst. Stand. Technol. **106**, 649-656 (2001).
2. ASTM -E1417, *Liquid Penetrant Examination standard*.

UV-app "My sun time" for safe sun-time and to promote sun-sense

Ulf Wester[1], Hampus Brynolf[2] and Maria Stråhle[1]

1. Swedish Radiation Safety Authority
2. Intellecta AB, Sweden

Summary

In the era of smartphones and mass tourism to sunny destinations all over the globe the Swedish Radiation Safety Authority (SSM) has developed an "app" for estimating safe time in the sun under clear sky. It is free to download and it works without costly phone-internet connections practically everywhere on earth at any season or time of the day (Figure 1). The UV-app is available for iphone and android smartphones. It is used to disseminate sun-sense information and was introduced early in the summer 2012. At the end of the summer there had been well over 40 000 down-loads.

Figure 1. The UV-app "My sun time."

Introduction

Skin cancer incidence has been on the rise since decades – and still is - mainly due to overexposure to solar ultraviolet radiation at home during episodes of strong summer sun or abroad during vacations at southern latitudes in countries where the sunburn-intensity is unfamiliar to northern visitors and proper protection precautions too often are neglected. However skin cancer is a preventable disease and over the years information campaigns by health authorities have provided advice for protection and also tools to estimate solar UV strength. In the 1980´s simple computer programs appeared for small desktop computers (Diffey 1984). The 1990´s saw the advent of stratospheric ozone depletion resulting in public and media concerns and eventually the UV-index as a standardized global information resource (WHO/ICNIRP 1995). In Sweden noon-time UV-index forecasts were distributed with weather reports by media and from the summer 1995 a "sun-disc", a card-board dial disc (Figure 2), could be used by persons with skin types I – III to calculate safe sun-time during the course of the day (Wester, Boldemann; 1996). Still in present days solar UV- and sun sense information is needed and in this era of smartphones an "app-version" of the sun-disc was envisaged. SSM´s communication department hired a company (Intellecta AB) specialized in making and designing smartphone apps to make an electronic sun-disc.

Figure 2. The "sun-disc" 1995 for "sun time" from the UV-index.

Material and methods

A modern smartphone knows it´s position´s GPS-coordinates and it knows the date and time. These are parameters needed to calculate solar zenith angle – and eventually UV-intensity – either directly with a radiation transfer model or with a look-up table of data generated from an RT-model. Apart from "weather" and cloud optical depth, stratospheric ozone is the most important of several more parameters (albedo, aerosols etc) also needed for calculation models. In the 1990´s global data for the UV-index had been calculated from an RT-model (provided 1993 by Dr. E. Weatherhead, NOAA) and using the ozone´s normal dependence on latitude and season as an input (Figure 3, Wester, Josefsson; 1997).

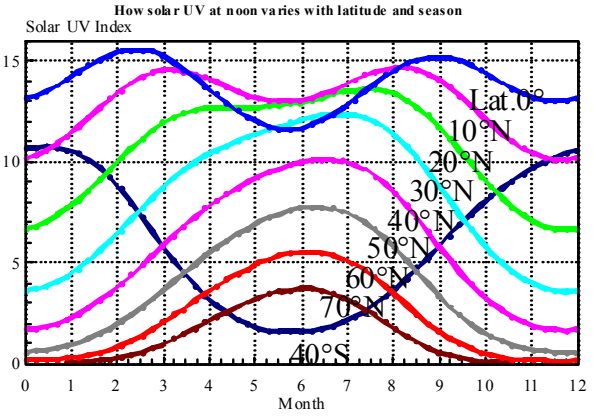

Figure 3. Estimated global solar UV-index in the 1990´s.

Available from the calculations was a table of noon-time UV-index data for all latitudes and seasons. The "app company", Intellecta AB, under guidance of SSM, used these data, information from the COST 726 project

(http://www.cost726.org/, final report, sect. 2,1 "UV-modeling") and a radiation transfer model available on the internet (http://www.libradtran.org/doku.php) to generate a more detailed table of data fine-tuned to fit the previous. Calculated data from the 1990´s on diurnal UV-index variations for a few latitudes in spring and summer together with the sun-disk was used to estimate how the UV-index varies under a clear sky from early in the morning until late in the afternoon. In the UV-app these detailed tables are used to interpolate a UV-index value from the phone´s GPS coordinates, date and time. The UV-index value is displayed on a vertical bar scale on the phone. The user of the phone can select his/her sun sensitivity from three choices (skin type I, II or III) and the app calculates estimated safe time in the sun from the UV-index and a value of erythemal dose set for the respective skin types (200, 300 and 500 J/m^2). Exposure times are calculated for situations with unobstructed horizon under clear sky, but also estimated for shade by a small parasol (50% shade) and on a shaded terrace (75%). Sun protection advice is given for these and a few other situations. Special advice is given concerning infants and small children. Instead of using the phone´s GPS-position, it is also possible to choose among common tourist travel destinations from a list and have the UV-app calculate the UV-index for a given date and indicate appropriate sun protection measures.

Dissemination of the UV-app, market communication efforts and download results

On Tuesday the 26th of June 2012, the app "My sun time" was launched. SSM released the news via a press release to traditional and social media. SSM also spread the news by sending letters and e-mails to around 450 communication agents, for instance travel agencies, other Swedish authorities and associations (Figure 4).

After the day of launch, the app had reached a total of 8,400 downloads. The app was placed in 1st place in App Store's category "health and exercise" in Sweden. The news about "My sun time" generated around 120 articles in Swedish local media and more than 230 posts on Twitter and Facebook. One of the biggest charter travel agencies in Sweden decided to on a regular basis inform their travelling customers about "My sun time" in its newsletter communication.

Over the summer, SSM used Google advertisements in mobile apps and on the Internet. SSM also released several news items on its external website and performed telephone follow-ups of letters to travel agencies. The app was highlighted by App Store and ranked 4th on the iTunes home page.

By the end of the summer, the app had a total of 46,000 downloads, approximately 800 people who wanted to participate in an evaluation of the app and a user rating of 4 on Google Play.

The app "My sun time" raised some interest in other countries. In Finland, for example, the app was placed 5th in App Store's category "health and exercise" on the day of launch. It was also awarded as a "Must-have app" for leisure craft users.

Figure 4. The UV-app "my sun time" as a planning tool for vacation trips. Photo: Bosse Alenius, SSM.

The UV-app so far is available in the Swedish language. Information in Swedish and down-load addresses are available via the SSM-website:

http://www.stralsakerhetsmyndigheten.se/start/Sol-och-solarier/njut-av-solen/minsoltid/

References

Diffey B., "Using a microcomputer program to avoid sunburn," *Photodermatology* **1**, 45-51 (1984).

ICNIRP 1/95, *Global solar UV-index,* A joint recommendation of WHO, WMO, UNEP, ICNIRP (1995).

Wester U, Boldemann C., "Safe suntime 'sundisk' – and UV-index," In *Environmental UV-radiation, Risk of Skin Cancer and Primary Prevention*, Veröffentlichungen der Strahlenschutzkommission, Conference reports 6-8 Mai 1996 Hamburg, SSK Band 34, p.427.

Wester, Josefsson, "UV-index and Influence of Action Spectrum and Surface Inclination," In *WMO, Global Atmosphere Watch*, No 127, 63-66 (1997)

The Spectro 320D double monochromator for fast and accurate measurements in the ultraviolet and beyond

G. Leschhorn

Instrument Systems GmbH, Munich, Germany

The Spectro 320D scanning double monochromator is based on Instrument System`s Fast-Scan-Technology. Up to three different gratings are mounted on a common turret, share the same rotation axis and are continuously driven by a DC motor. A precision angle encoder synchronizes the data acquisition during rotation. This technology ensures an unprecedented wavelength accuracy and linearity. Furthermore, it makes the Spectro 320D a very fast (measurement of UV-B range up to 450 nm within 1 minute) and precise instrument.

Figure 1. The Spectro 320D double monochromator is a compact and all-in-one instrument that can be configured according to the needs of the customer. All functions and measurement routines are controlled via the software SpecWinPro and no manual hardware changes are needed. All accessories and measurement adapters are coupled via a fiber link.

Researchers can configure the spectroradiometer according to their individual needs and can still rely on a convenient turn-key system (see Figure 1). The instrument is completely software controlled and no manual changes are needed. This includes the choice of three different gratings and detectors. The Spectro 320D automatically positions the integrated entrance and exit slit wheels as well as the density and order-sorting filter wheels depending on the setting or measurement task. The user interface of the software SpecWin Pro allows for a manifold of possibilities to analyze or illustrate the measurement results. Furthermore, the configuration of the measurement is easily changed to ensure ideal measurement conditions. For example, the wide spectral range of 190 to 5000 nm in maximum can be divided into sub-ranges that can be scanned with different detectors, scanning times, bandwidths, scan increments etc. Additionally, an integration of the Spectro 320D into a customer-specific measuring system is supported. DLL and LabVIEW drivers are available for creating proprietary programs.

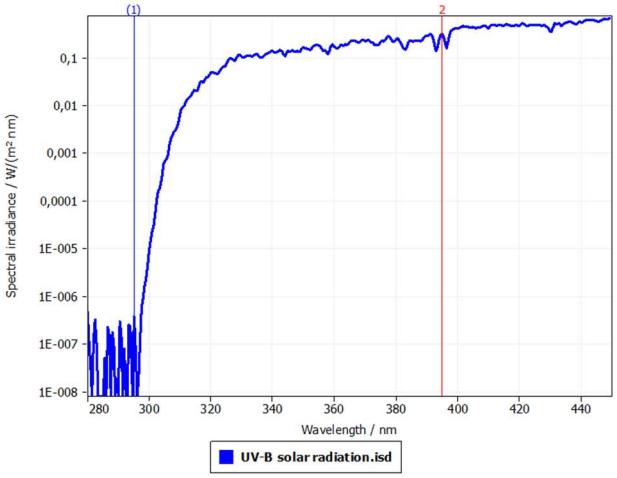

Figure 2. Measurement of the UV-B solar spectral irradiance over 7 decades with the Spectro 320D. The signal noise is by far smaller than 10^{-6} W/m^{2}nm.

The Spectro 320D is ideally suited for measurements in the ultraviolet. Instrument Systems offers UV-researchers diverse options and possibilities. This includes, for example, the choice of a cooled photomultiplier detector that is optimized for the UV spectral region and can be used together with two other detectors. Furthermore, a direct-fiber input (DFI) option is available to enhance the sensitivity of the instrument dramatically. The DFI uses a cross-section converted fiber bundle that adapts to the shape of the entrance slit apertures. Bypassing the focusing input optics and the density filters, the DFI is positioned right in front of the entrance slit and therefore avoids the inherent input losses. For measurements like UV-B monitoring the device must provide several key attributes. The high wavelength accuracy and low stray light of the double monochromator design makes the Spectro 320D ideally suited for this kind of research. Furthermore, the instrument is optimized for high signal sensitivity in combination with very short measurement times. The fast changing solar UV radiation can therefore be measured with very high precision (refer to Figure 2 for a UV-B measurement example).

New facility for spectral irradiance and radiance calibrations

Germar Bernhard and Charles R. Booth

Biospherical Instruments, San Diego, USA

Biospherical Instruments (BSI) has recently upgraded its calibration laboratory to a state-of-the-art facility in support of the NASA project Optical Sensors for Planetary Radiant Energy (OSPREy) [Hooker et al., 2012]. The design of the new facility is based on recommendations established by the National Institute of Standards and Technology (NIST) [Walker et al. 1987; Yoon et al. 2010] and supports irradiance (Fig. 1) and radiance calibrations (Fig. 2) over the spectral range of 290 - 1,640 nm. Materials (e.g., paints, divider walls, and baffles) with low IR reflection were selected to reduce uncertainties from stray light. The whole laboratory is temperature stabilized to ±1°C. Lamp and transfer radiometer alignment is performed by means of lasers (Fig. 3). BSI also maintains a roof-top calibration facility where radiometers can be vicariously calibrated against an SUV-100 spectroradiometer, which measures global spectral irradiance between 290 and 600 nm with a bandwidth of 1.0 nm.

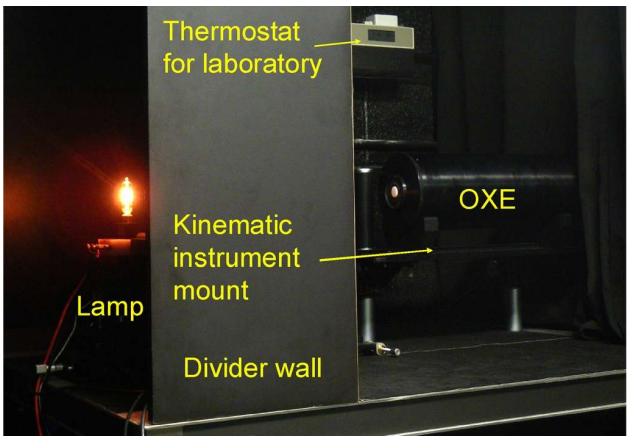

Figure 1. The irradiance calibration bench. Lamp and radiometer compartment are divided by a wall equipped with a computer-controlled shutter.

Starting with support from NASA, BSI maintains a Lamp Library consisting of more than 30 tungsten-halogen 1000 Watt FEL lamps operating in vertical orientation (FEL-V), 5 FEL lamps operating in horizontal orientation (FEL-H), and several 200 Watt lamps (Model Q6.6AT4/5CL from General Electric). Three FEL-V lamps have been calibrated by NIST to the NIST spectral irradiance scale of 2000 [Yoon et al., 2002] and five additional FEL-V lamps have NIST calibrations relative to the previous NIST scale realization of 1990 [Walker et al. 1987]. The remaining FEL-V lamps have been calibrated against these NIST primary standards at the new facility and divided into several categories (e.g., working standards for daily operations, medium-term and long-term standards). By using this hierarchical approach, the run-time of the NIST primary standards is kept at a minimum (e.g., once per year). This strategy assures the long-term stability of irradiance scales maintained at BSI.

Four of the five FEL-H lamps have been calibrated by NOAA's Central UV Calibration Facility (CUCF; http://www.esrl.noaa.gov/gmd/grad/calfacil/cucfhome.html) and are traceable to NIST's irradiance scale realization of 2000. These lamps are operated in a special apparatus, which was designed and built in accordance to CUCF recommendations. The 200 Watt lamps are traceable to the NIST 1990 scale, which is the scale used by the solar UV radiation monitoring project supported by the U.S. National Science Foundation (http://uv.biospherical.com).

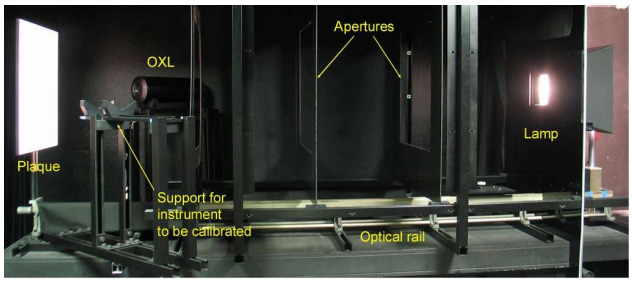

Figure 2. The radiance calibration bench with the lamp mounted 290 cm away from a Spectralon plaque. Several apertures made of black acrylic plastic are mounted between the lamp and plaque to minimize stray light. Two instrument holders with kinematic mounts point to the center of the plaque from opposite sides at 45° angles. The setup permits the installation of two radiometers at the same time, with one radiometer being a monitoring device (in this case an OXL) and the other the instrument to be calibrated. The lamp is mounted on an optical rail to permit accurate determination of the calibration distances.

The system for powering the lamps uses a power supply with both digital and analog control inputs, a high-accuracy shunt (which is regularly calibrated by a dedicated external calibration laboratory and compared with other in-house shunts), a digital multimeter for monitoring the voltage across the shunt, and a high-capacity UPS to prevent sudden power losses at the lamp in case of a power outage. It is possible with this system to set and maintain the lamp current to within a precision of ±50 µA (0.0006% for a target current of 8.2 A). The accuracy of the current is only limited by the shunt's calibration uncertainty of 0.002%.

Several transfer radiometers are available to compare the scale of irradiance standards or to calibrate new lamps. Instruments include two OSPREy Transfer Radiometers (OXR), one equipped with irradiance and one with radiance front optics, and a GUV Transfer Radiometer (XGUV). The two OXR systems are "hybridspectral"

radiometers because they include both a filter component with 18 channels ranging from 320 to 1,640 nm and a spectrograph component. The filter component uses BSI's new microradiometer technology (Chapter 2 of [Hooker et al., 2012]). The irradiance version of the OXR (the OXE) was calibrated by the NIST SIRCUS facility [Brown et al., 2006], which uses tunable lasers to determine the spectral responsivity functions of radiometers in absolute terms. Together with BSI's Lamp Library, the OXE presents the opportunity to compare the NIST FASCAL irradiance scale [Yoon et al., 2002] with the NIST SIRCUS scale of irradiance. The internal spectrograph of the OXE radiometer (model MMS UV-VIS II from Zeiss) can be used to detect emission lines that may affect the spectrum of FEL lamps [Disterhoft, 2005]. The XGUV is a 12-channel version of BSI's GUV-2511 multi-channel ground-based ultraviolet radiometer system covering the wavelength range of 290 - 875 nm. The XGUV is insensitive to changes in orientation and can be used both with the irradiance bench (Fig. 1) and the apparatus for operating FEL-H lamps.

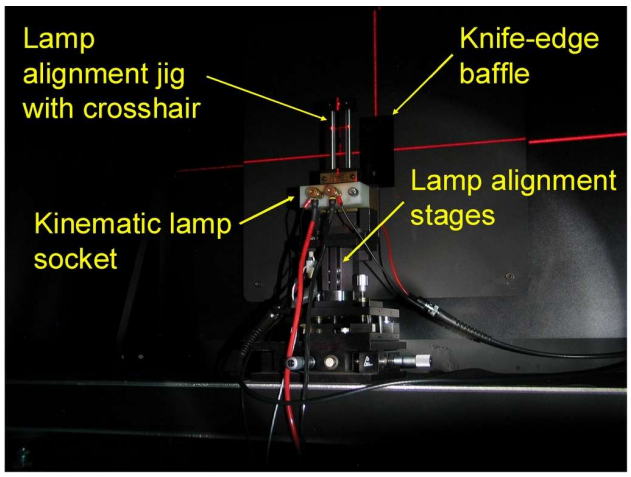

Figure 3. Lamp alignment assembly for the irradiance bench. The red lines are generated by an alignment laser. The laser defines the optical path and is used to center the crosshair of the alignment jig placed in the lamp socket and the center of the transfer radiometer.

A study was undertaken to determine the uncertainty resulting from using moderate-bandwidth radiometers rather than high-resolution spectrometers for transferring the irradiance scale of FEL lamps (Section 6.5. of [Hooker et al., 2012]). It was concluded that worst-case systematic errors arising from the relatively large bandwidth of 10 nm of the transfer radiometers' filter channels are smaller than 0.3% for wavelengths larger than 300 nm and smaller than 0.1% for wavelengths larger than 370 nm. These uncertainties are considerably smaller than the uncertainty of lamp irradiance tables issued by NIST. Compared to high-resolution (e.g., < 1.0 nm) spectrometers, filter instruments have the advantage of better short-term stability and better signal-to-noise ratio.

The spectral irradiance of a test lamp $E_T(\lambda)$ is given by $E_T(\lambda) = R(\lambda)E_R(\lambda)$. Here $E_R(\lambda)$ is the spectral irradiance of a reference lamp (e.g., a NIST primary standard), interpolated to a wavelength grid of 1 nm. $R(\lambda)$ is the ratio of the signals of test lamp and reference lamp measured by the transfer radiometer and interpolated to the same 1 nm grid. Irradiance tables of reference lamps issued by standard laboratories such as NIST are typically provided in wavelength steps ranging from 10 nm in the UV to up to 150 nm in the infrared. Accurate interpolation to intermediate wavelengths is non-trivial because the spectrum of these lamps varies over four orders of magnitude. Interpolation schemes recommended by NIST [Walker et al. 1987; Huang et al., 1998] are defined as step-wise functions, which generally leads to discontinuities at wavelengths where two functions come together. BSI has developed a new interpolation technique that uses a combination of a Planck function and approximating splines to avoid this problem. Approximating splines are also used for the calculation of $R(\lambda)$. As an example, Fig. 4A shows the ratio of net signals of test lamp V-035 and lamp F-616 (one of the NIST standards) measured by the ORE (red dots) and XGUV (blue dots), plus the ratio $R(\lambda)$ derived by interpolating these measurements (green line). Figure 4B shows that residuals of the XGUV and ORE measurements relative to $R(\lambda)$ are smaller than 0.1% at all wavelengths and have no systematic pattern. This excellent result gives confidence in the calculation of $R(\lambda)$, and ultimatively $E_T(\lambda)$.

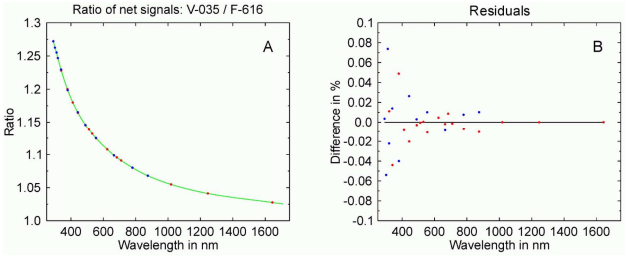

Figure 4. Comparison of net signals when measuring test lamp V-035 and reference lamp F-616. Panel A: ratio of net signal measured by the OXE (red dots) and the XGUV (blue dots) radiometer plus the associated fit function (green line). Panel B: residuals of the measurements relative to the fit function. Residuals are smaller than 0.1% at all wavelengths and there is no systematic bias between the residuals for the OXE and the XGUV.

The radiance bench (Fig. 2) uses diffuse reflectance standards made of Spectralon as a target for radiance calibrations. BSI maintains several reflectance standards (also know as plaques). One of which has been calibrated in 2012 by the NIST Spectral Tri-function Automated Reference Reflectometer (STARR) [Barnes et al., 1998] between 280 and 1,700 nm. The expanded uncertainty (k=2) of the plaque's reflectance factor calibration is smaller than 0.01 at all wavelengths. The plaque is stored in a specially-designed nitrogen-purged enclosure when not in use to minimize contamination. The

radiance emanating from the plaque is calculated based on the known irradiance of the radiation source (FEL lamp shown on the right side of Fig. 2), the distance between lamp and plaque, and the reflectance factor of the plaque. The plaque forms the calibration source for up to two radiance radiometers, which can face the plaque simultaneously (Fig. 2).

BSI can offer calibration services for the following applications using the new facility:

- Spectral irradiance calibration of incandescent lamps between 290 and 1,640 nm
- Calibration of customer-supplied irradiance or radiance radiometers between 290 and 1,640 nm.
- Transfer for calibrations from a horizontal to a vertical optical axis with the XGUV.

To request a service at the new facility, please contact support@biospherical.com or go to the website http://www.biospherical.com/ and use the 'Contact us' form.

References

Barnes P.Y, E.A. Early, A.C. Parr, *NIST measurement services: spectral reflectance*, Nat. Inst. Stand. Technol. Spec. Publ. 250-89, 253 p. (NIST, Gaithersburg, Maryland, 1998).

Brown S.W., G.P. Eppeldauer, and K.R. Lykke, "Facility for spectral irradiance and radiance responsivity calibrations using uniform sources," *Appl. Opt.* **45**, 8218-8237 (2006).

Disterhoft P., "Stability characteristics of 1000 Watt FEL-type QTH lamps during the seasoning and screening process," *Proc. SPIE* **5886**, Ultraviolet Ground- and Space-based Measurements, Models, and Effects V, 58860G; doi:10.1117/12.614584 (2005).

Hooker, S.B., G. Bernhard, J.H. Morrow, C.R. Booth, T. Comer, R.N. Lind, and V. Quang, *Optical Sensors for Planetary Radiant Energy (OSPREy): Calibration and Validation of Current and Next-Generation NASA Missions,* NASA Tech. Memo. 2012-215872 (NASA Goddard Space Flight Center, Greenbelt, Maryland, 2012). http://www.biospherical.com/images/pdf/hooker-215872-rs.pdf

Huang, L.K., R.P. Cebula, E. Hilsenrath, "New procedure for interpolating NIST FEL lamp irradiances, " *Metrologia* **35**, 381-386 (1998).

Walker, J.H., R.D. Saunders, J.K. Jackson, D.A. McSparron, *Spectral Irradiance Calibrations*, NBS Special Publication 250-20 (1987).

Yoon H.W., C. E. Gibson, and P.Y. Barnes, "Realization of the National Institute of Standards and Technology detector-based spectral irradiance scale," *Appl. Opt.* **41**, 5879-5890 (2002).

Yoon H.W. and C. E. Gibson, *NIST measurement services: spectral irradiance calibrations*, Nat. Inst. Stand. Technol. Spec. Publ. 250-89, 132 pages, (NIST, Gaithersburg, Maryland, 2011).

Measurement of spectral radiation in UV curing systems

Stefan Pieke and Mark Paravia

OpSyTec GmbH, Karlsruhe, Germany

Abstract

Measurements of spectral irradiance in laboratories are common practice. In industrial environments, broadband radiometers have been in use in UV curing systems for years. Their sensitivity functions differ widely depending on the apparatus used, as a result of which their measurement results cannot be compared. It was only the availability of a compact spectral radiometer that enabled standardized measurements to be made in such systems. This article describes the development of a mobile UV spectral radiometer for industrial use and compares its measuring principle and measurement errors with those of a broadband radiometer.

UV curing

The quality and production speed of modern printing and painting systems have improved rapidly over the last few years. The solvent-based paints and varnishes used in the past have been increasingly replaced by solvent-free coatings. These paints and varnishes are cured with UV radiation in a way that respects the environment and acquire an excellent resistance against organic solvents, chemicals and mechanical environmental factors [1].

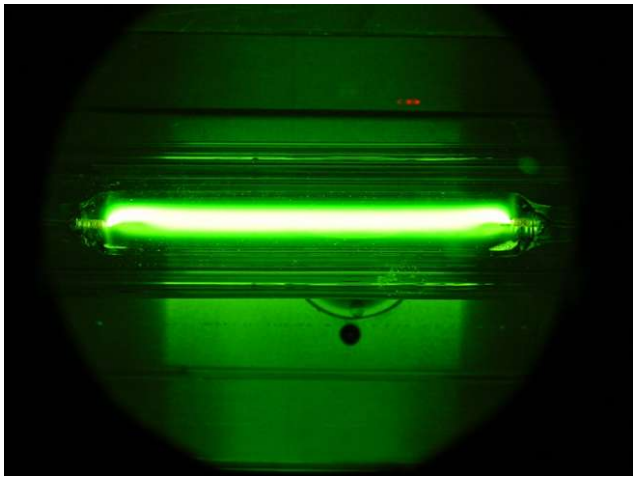

Figure 1. Medium pressure mercury lamp for use in UV curing systems.

However, the problems with this technique concern the cure monitoring of the paints and varnishes. In existing systems, the paint itself is not monitored. Rather, the quality of the curing process is monitored by referring to the measured values of the irradiance and the radiation dose. The UV lamps usually employed in such curing systems have electrical power ratings ranging from a few hundred watts up to approx. 20 kW. Figure 1 shows just such a lamp, which generates irradiances in the region of a few W/cm2 in production plants. If the lamp is doped with indium, gallium or for example iron, this allows the emission spectrum to be adjusted to the absorption of the photoinitiator. The photoinitiator, as a component of a UV paint, initiates the chemical cross-linking of the liquid paint. In addition, UV LED modules with irradiances of up to 16 W/cm^2 are suitable for thermally critical processes.

In most systems, flat articles are cured, e.g. from the furniture industry. Very often their height is only 15 mm. In order to attain high irradiances, the separation between the UV lamp and the item due to be irradiated is kept as small as possible and the articles are moved on conveyor belts at speeds of up to 35 m/min. Due to the small installation height, the measuring device employed is exposed to a high thermal load from lamps operating at temperatures of over 1000ºC.

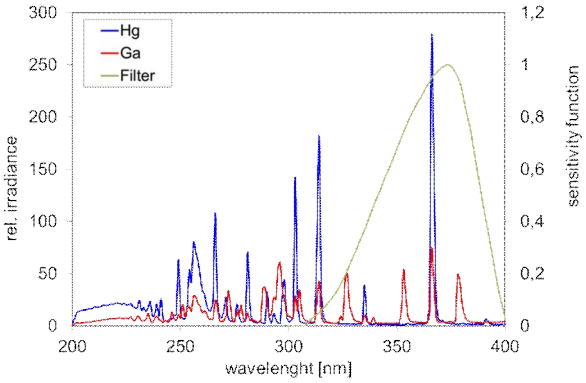

Figure 2. Emission spectra of a mercury (Hg) and a gallium (Ga) medium pressure lamp and a sensitivity function of a broadband radiometer.

Common procedures for monitoring curing systems consist of compact broadband radiometers in a robust housing with an installation height of between 10 and 15 mm. They are supplemented by mobile spectral radiometers, whose advantage lies in the traceability of the measurement of the irradiance back to national standards.

Broadband radiometer

Broadband radiometers consist of a photodiode (Si, SiC, GaP) with an optical filter placed in front. Through the careful selection of the filter, the measuring range can be roughly adjusted to a particular UV spectral range. However, standardized division [2] into UVA, UVB and UVC is not possible.

Following a simple change of lamp, say from a mercury lamp to a gallium lamp, precise measurements of the irradiance and the radiation dose with a broadband radiometer are, to a certain extent, no longer possible. By way of example, the spectra of these two lamps are shown in Figure 2 together with a sensitivity function of a broadband radiometer.

The irradiance shown on the measuring device corresponds to the weighting of the spectral sensitivity S_λ of the receiver diode-filter combination with the emission

spectrum E_λ of the UV lamp according to its optoelectronic conversion. In order to achieve this, upon calibration with a known irradiance, a calibration factor k_1 is assigned to a photovoltage U_{photo}

$$E = \int E_\lambda \cdot S_\lambda d\lambda \overset{!}{=} k_1 \cdot U_{Photo} \quad (1)$$

However, broadband radiometers are only calibrated by their manufacturers for one type of lamp and are therefore only able to reproduce correct measurement results for this type of lamp. For example, the deviation with respect to the spectral radiometric target value of the gallium lamp for the spectra shown in figure 2 is -18%.

Thus broadband radiometers are suitable for monitoring moving systems since in such cases it is only necessary to check whether the lamp is dirty or shows signs of ageing. It is also possible to compare systems of identical design. However, as soon as the lamp's spectrum changes or other lamp technologies such as UV LEDs are employed, the measured values for identical devices differ.

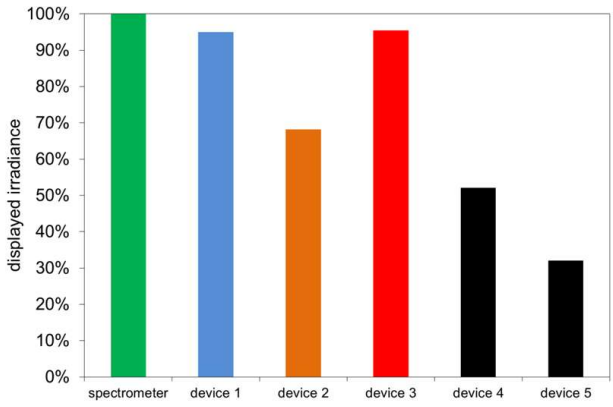

Figure 3. standardized irradiance from a comparison of measuring devices involving five broadband radiometers and a spectral radiometer.

A further problem concerns the arbitrary, manufacturer-specific sensitivity functions of such devices. If broadband radiometers from different manufacturers are compared on the same UV system, then manufacturer-specific deviations emerge that prevent a irradiance reading (as a measured figure). Figure 3 shows the standardized irradiances of five broadband radiometers and a spectral radiometer on a UV curing system with a mercury lamp. What becomes clear is that in some instances, there are deviations of up to 40%. This is why such comparisons between different types of measuring devices are carried out in practice. In order to ensure proper curing, UV systems are usually oversized. In this example, the use of precise measuring technology could reduce the lamp power consumption by 40%. This could lead to reductions in CO2 emissions for a system with a lamp power of 20 kW of around 42 t per year.

The irradiance of printing and painting systems can thus be monitored with broadband radiometers although new systems can only be set up after a comparison of measurement devices. The result is that printing and painting systems are very often oversized, which reduces their cost-effectiveness and worsens their eco-balance.

Spectral radiometer

For scientific purposes, the irradiance is measured using spectral radiometric means. Here, measurement devices consisting of a spectrometer or a monochromator, a cosine-corrected optical probe and, if necessary, an optical fiber. The simulation of a ray path between the optical components of a spectrometer in a Czerny-Turner configuration is shown in Figure 4.

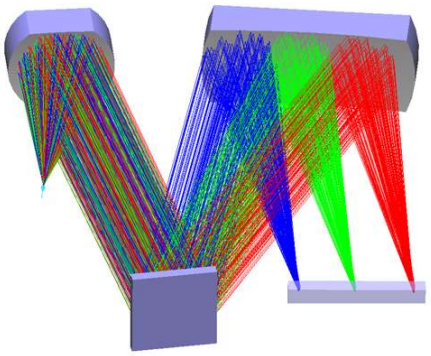

Figure 4. Simulation of a ray path in a Czerny-Turner array spectrometer.

Setup

Its functional principle can be outlined as follows: the input slit is located at the focal point of the collimating mirror on the input side. The mirror parallelizes the impinging ray of light and reflects it onto a diffraction grating, which separates the ray into its spectral components and guides it onto the focusing mirror located on the output side. The mirror then focuses the light onto the detector. The distance between the detector and the mirror on the output side is referred to as the focal length and together with the dispersion grating it defines the spectrometer's basic optical parameters. In the case of compact array spectrometers, whose array detector captures a complete spectrum in parallel, the focal length is usually between 40 and 75 mm. The advantage of the Czerny-Turner configuration is the small degree to which the scattered light is dispersed in the spectrometer, which particularly affects measurement precision in measurements in the UV range or involving highly dynamic spectra. For array spectrometers, suppressions of scattered light of approx. between 10^{-3} and 10^{-4} are attained.

A standardized value for the total irradiance can be obtained through the mathematical integration of the spectral irradiance. In addition, this class of measurement devices can be calibrated in a way that is traceable back to the national meteorological institutes (PTB, NIST).

Wavelength-resolved measurements obtained by weighting the lamp spectrum with the absorption of the photoinitiator allow a production process to optimized and monitored by also referring to the effects [3]. This is useful if doped lamps are used since such lamps increase their emission of a mercury spectrum at the end of their service life.

For mobile measurements in UV systems, a commercial device was set up as an unsymmetrical variant of a

Czerny-Turner configuration. Its overall height of 14.4 mm allows it to be used wherever space is at a premium (Fig 5).

Figure 5. Mobile spectral radiometer with an array spectrometer in a Czerny-Turner variant.

Technical requirements

If spectral radiometers are used in UV conveyor systems then the following should be observed:

The item due to be irradiated/measurement device heats up to +40ºC in the space of a few seconds and is exposed to ambient temperatures of up to 70ºC. Due to curing runs measuring in the region of a few meters, the spectral radiometer must either possess long optical fibers that are nevertheless capable of attenuating in the UVC range of the spectrum or must be capable of being deployed on a mobile basis, i.e. without any fiber optic or cable connection. The overall height of common spectrometers means that it is either difficult or impossible to use them in production plants. Even so-called mini-spectrometers with overall heights of between 25 and 40 mm are too large.

The most important requirements and boundary conditions are as follows:

1. Low overall height
2. Ambient temperatures up to 70ºC and resistance to temperature changes
3. Suppression of scattered light
4. Real time evaluation of measurement data
5. The current-carrying capacity of lithium batteries prevents the use of signal processors
6. It must be implemented in a way that ensures that untrained personnel are able to carry out spectral-radiometric measurements.

The low overall height and the suppression of scattered light were achieved through an optimized design. Amongst other things, this includes the coupling of the ray of light through the use of a miniaturized Ulbricht sphere, which combines a cosine correction and 90º deflection of the ray. In addition, the use of highly integrated electronics enabled a spectrometer to be obtained with a focal length of 76 mm.

Spectral-radiometric collection allows measurements to be performed that refer to effects by rear-mounted photoinitiator absorption spectra. This is otherwise only possible in PC-based measurement devices. The resulting repeatability of such a measurement with its standard deviation of 2% is at a high level and is not substantially worse that the results of < 1% obtained with a broadband radiometer.

Calibration

The most important criterion of spectral-radiometric measurements is the validity of the calibration, since these measurement devices can only be used after they have been calibrated. Typical calibration standards are quartz halogen lamps, type FEL 1000 W, in the spectral range 250 – 2500 nm and deuterium lamps in the spectral range 20 – 400 nm. The calibration distance is 50 – 70 cm, which is why spectral irradiances of between 0.5 mW/m²/nm and 10 mW/m²/nm are obtained for calibrations below 400 nm. There are seven orders of magnitude between the use of the measurement device and its calibration. No typical calibration standards can be obtained for the measurement device for measurement device dynamics lying between 10^4 and 10^5. A possibility would be the reduction of the calibration distance which, however, would not allow a sufficient signal-noise ratio to be attained. In order to enable calibration at high irradiances, Hg-, Hg-Xe or Xe short-arc lamps can be used as calibration sources. The spectral irradiance attained by a HBO 1000 W at a distance of 10 cm is shown in Figure 6 together with the spectral irradiance of an Hg-Xe calibration lamp [4].

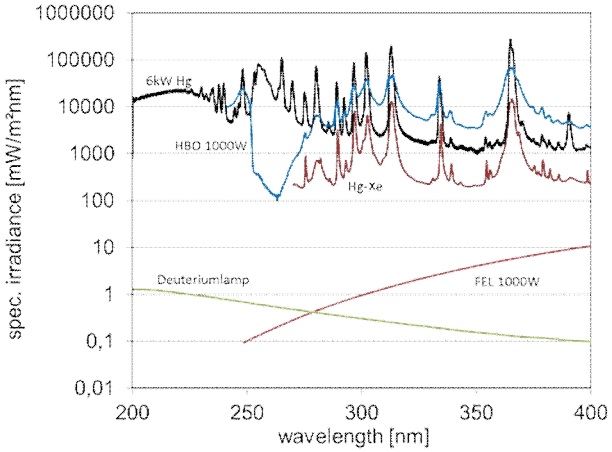

Figure 6. spectral irradiances of calibration lamps (deuterium, FEL 1000 W, Hg-Xe) and production lamps (HBO 1000W, 6 kW Hg).

The challenge for the calibrator is to transfer the partial irradiance of suitable UV lamps to mobile spectral radiometers. The complexity of a spectral calibration at a higher irradiances is, however, justified by the universal applicability of the spectral radiometer.

If validly calibrated, spectral-radiometric measurements of lamps with different doping contents (Hg, Ga, Fe) or UV LEDs are possible, the irradiance of which can be measured in conformity with standards and thus transferred. In this way, laborious comparisons of measurement devices can be dispensed with.

Summary

Spectral radiometers, in the same way as broadband radiometers, enable the measurement of irradinaces in UV curing systems. In addition, they also enable a comparison of radiation measurements since the calibration is also valid for different lamps and standardized irradiance readings can be taken.

Above all, this allows the deliberate oversizing of the systems to be reduced since the irradiances required to cure the paints and varnishes can be individually and precisely measured. This also leads to a reduction in the electrical power consumption of the systems. Moreover, the use of spectral radiometers means that complex comparisons of measurement devices can be dispensed with, something that is unavoidable in the case of broadband radiometers.

Special requirements must be taken into account when developing a spectral radiometer as a mobile device, e.g. a small overall height, the possibility of using it under harsh ambient conditions and its ease of use.

References

[1] C. Decker, "Kinetic Study and New Applications of UV Radiation Curing," *Macromolecular Rapid Communications* **23**, 1067–1093 (2003).

[2] DIN 5031-7:1984 *Radiation Physics in the Optical Segment and Light Technology – Naming Wavelength Ranges*.

[3] DIN 5031-11:2011 *Radiometer for measuring Actinic Radiation Parameters – Terminology, Properties and their Identification*.

[4] S. Nevas, P. Sperfeld, and Hg-Xe, "Development of a New Transfer Standard for High UV Irradiances," *Mapan Journal of Metrology Society of India* **25**, 53–62 (2010).

New design of UV detector heads for accurate and fast safety measurements

Anton Gugg-Helminger and Ralf Zuber

Gigahertz-Optik GmbH, Tuerkenfeld, Germany

Introduction

Optical radiation from artificial and natural light sources can affect a photo-biological reaction on human skin and eye with the risk of damage due to overexposure [1]. Regulations, standards and guidelines that include effective limit values are published for safety equipment and occupational safety in the workplace [2]. Worldwide accepted safety equipment needs manufacturers who design and classify their products according to the international standards. Workplace safety tends to be a national issue, requiring health hazard protection of employees including published exposure limit values, threat analysis, and precautionary measures.

The most current regulations are EN 62471:2009-02 for Equipment Safety; 2006/25/EC Guideline; DIN EN 60335-2-27 and DIN EN 14255 for Safety of Workplaces.

New design of the detector heads for safety measurement

Within the above mentioned regulations, the actinic curves are defined. There are in total three actinic curves to be used in the UV region, shown in Figs. 1 – 3.

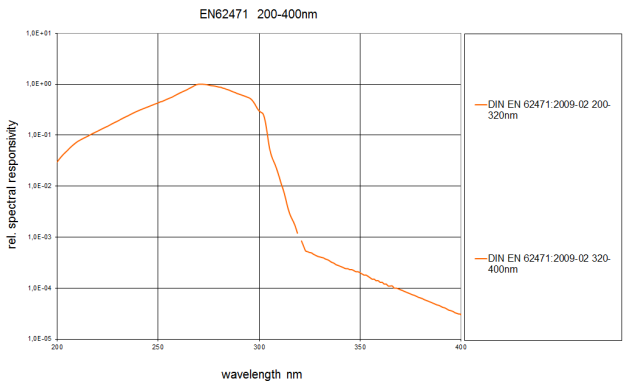

Figure 1. The UV Hazard actinic curve for UV safety weighting function.

An accurate measurement of radiation weighted according to the given action spectra requires a spectroradiometer based on a double monochromator. The wide dynamic range of more than four decades within the actinic weighting function prevents sufficient measurement accuracy with a single monochromator.

The very specific shape of the curve cannot be realized with a single integral detector head. With this knowledge, we decided to separate the discrete wavelength regions of the actinic curves.

Referring to the task of additional information within the spectral range 250 – 400 nm, we separate the UV hazard curve in Fig. 1 into two ranges; 250 – 320 nm and 320 – 400 nm. The UVA curve in Fig. 2 we realize with an additional detector head. The curve in Fig. 3 we realize with three separate detector heads. We also take into account not to measure radiation at the wavelengths above 400 nm, for example, due to the intensive line at 404 nm in the fluorescent lamps.

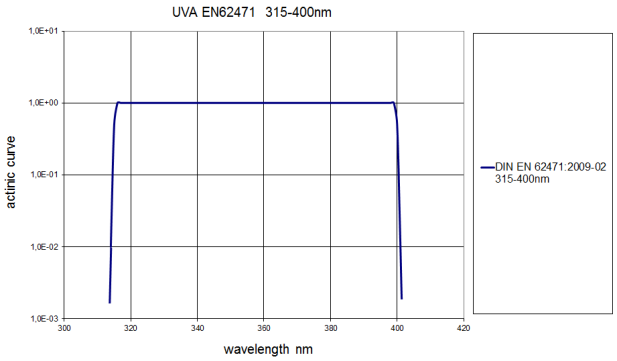

Figure 2. The UVA radiometric curve for UV safety weighting function.

The latest design model X13 (X_one_three) light hazard meter conforms to the 2006/25/EG, DIN EN 62471 and EN 14255-1 measurement criteria for the evaluation of hazard exposure. It is a supplemental or an alternative measurement method to the double grating monochromator spectroradiometer, the most accurate UV radiometric instrument for this application. A double monochromator based instrument is expensive, laboratory based, delicate and is not designed for mobile operation. These are the reasons why we developed a portable, hand-held and lower cost solution with our X13 light hazard meter.

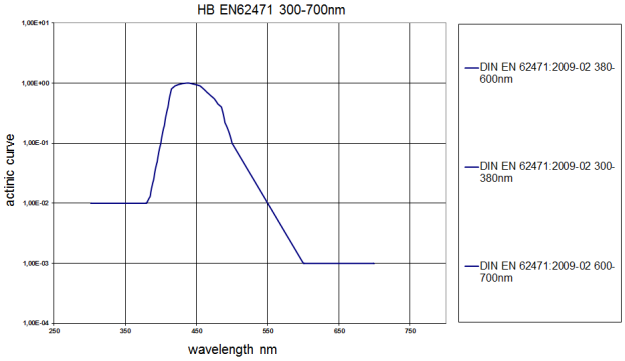

Figure 3. The Blue Light Hazard actinic curve for UV and visible safety weighting functions.

The complete X13 instrument consists of a compact X13 meter, an XD-45-HUV UV Hazard Detector and an XD HB Blue Light Hazard Detector. It is designed specifically for the evaluation of the potential health risk due to exposure from UV and Blue Light for workplace safety and product classification. It's simple use and

price level supports the needs of lamp distributors, light source systems and luminaire manufacturers, institutional and industrial safety engineers, hygienists and others required to perform routine and periodical health hazard optical radiation measurements independently without third party testing laboratories. The light hazard meter is calibrated in our calibration laboratory for optical radiation measurement units.

Figure 4. Detector head with 80° limitation.

The XD-45-HUV irradiance detector is specially designed for the evaluation of light exposure hazard values for artificial light sources. The three-sensor design of this unique device covers the requirements for skin and eye risk assessment.

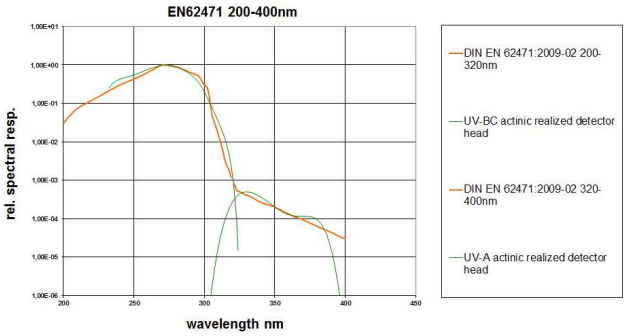

Figure 5. Actinic curve for the UV safety weighting function and the relative spectral responsivities of the detector heads realized.

The ICNIRP spectral sensitivity required for skin and eye risk evaluation is formed using two filtered sensors. This prevents the typical cross-talk and the limited sensitivity dynamics between the UV-A, UV-B and UV-C spectral ranges of a single filtered sensor solution. Also, a UV-A sensor for the evaluation of UV-A (315 – 400 nm) human eye risk is integrated. All three detector heads are mounted behind a 20-mm diameter cosine diffuser. For measurements of eye dependent irradiance values, a front adapter is supplied to limit the detector field-of-view to 80 degrees (see Fig. 4) The spectral responsivities of the detector heads realized for the UV-type are shown in Figs. 5 and 6.

The calibration of the detectors with ICNIRP (W/m²) and UVA (W/m²) sensitivities is performed by our calibration laboratory for optical radiation measurements quantities (Dakks-D-K-15047-01-00). As with all light detectors supplied by us, the calibration of the detector sensitivity includes the relative spectral sensitivity data. Having this data available allows the measurement uncertainty of each individual sensor to be calculated for light sources different from the reference lamp used for calibration. This includes a wide range of UV lamps as well as simulated UV LED sources. In measurements where the type of light source is known, source specific calibration correction factors are supplied to improve the measurement uncertainty.

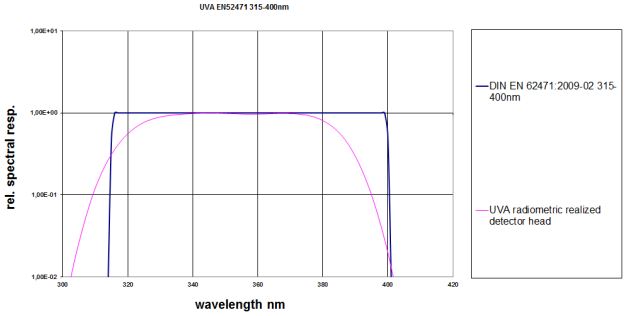

Figure 6. Actinic curve for the UV safety radiometric function and the relative spectral responsivity of the detector head realized.

The XD-45-HB irradiance detector is specially designed for the evaluation of blue light exposure hazard values for artificial light sources. It is designed starting from 300 nm. The four sensor design of this unique device covers the requirements for eye risk assessment.

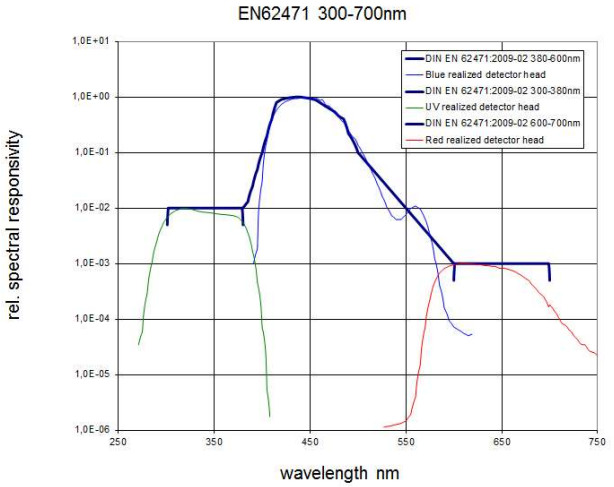

Figure 7. Actinic curve for the blue light hazard safety functions and the relative spectral responsivities of the detector heads realized.

The Blue Light Hazard spectral sensitivity required for eye risk evaluation is formed by three filtered sensors for the BLUEUVA300-400, BLUEBlue400-600 and BLUERED600-700 spectral ranges. The EN 62471 conformal $B(\lambda)$ detector is useful for evaluation of any type light source that contains UV-A and deep red light

components. Also, a $V(\lambda)$ photometric sensor for the evaluation of illuminance in lx is integrated to establish the 500 lx reference distance protocol for the illuminance and/or radiance qualification. All four filtered sensors are mounted behind the 20-mm diameter cosine diffuser. The realized detector heads for the blue light hazard meter are shown in Fig. 7.

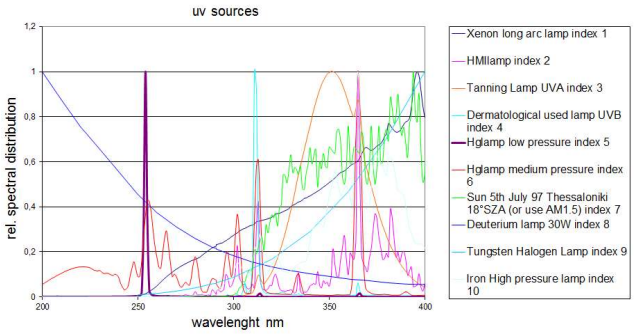

Figure 8. Selection of UV sources used for the calculation of the calibration correction factors.

The calibration of the $B(\lambda)$ (W/m²) and Ev (lx) detector sensitivities is performed by our calibration laboratory with the same features as above.

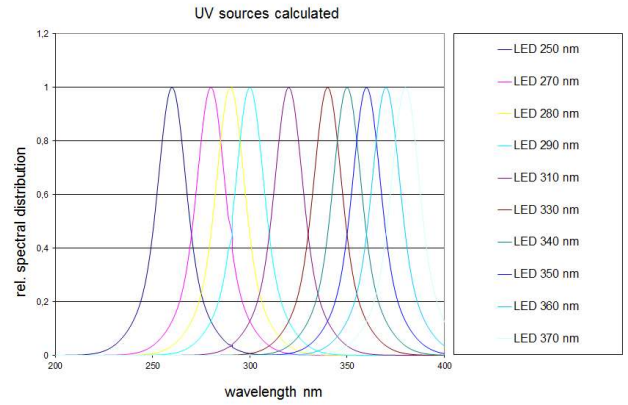

Figure 9. Selection of simulated UV sources used for the calculation of the calibration correction factors.

By looking at the relative responsivities of the realized single detector heads, we can see that even with the separation of the different wavelength ranges, the detectors do not match the weighting functions exactly. Therefore a spectral mismatch correction is needed. We installed a library of different sources for the different detector heads. We have following values in our library:

- UV Sources Library with $a(Z)$ Correction Values [3] for XD-45-HUV,
- UV LED's Library with $a(Z)$ Correction Values for XD-45-HUV,
- Technical Source Library with $a(Z)$ Correction Values for XD-45-HB,
- White & Monochromatic LED Library with $a(Z)$ Correction Values for XD-45-HB.

With this library, we can either check how well the realized detector matches the given curve and on the other hand, how accurate it will be for measuring an unknown light source without using a correction.

Table 1. Correction factors for XC-45-HUV detector.

Irradiation Source	UVA radiometric realized detector head	UV-BC actinic realized detector head	UV-A actinic realized detector head
Xenon long arc lamp index 1	0,87	0,99	0,99
HMIlamp index 2	1,00	0,86	1,00
Tanning Lamp UVA index 3	1,11	1,33	1,07
Dermatological used lamp UVB index 4	1,61	1,70	1,46
Hglamp low pressure index 5	1,25	1,28	1,30
Hglamp medium pressure index 6	1,22	1,05	1,20
Sun 5th July 97 Thessaloniki 18°SZA (or use AM1.5) index 7	0,91	1,43	1,00
Deuterium lamp 30W index 8	0,97	0,99	1,00
Tungsten Halogen Lamp index 9	0,82	0,98	0,95
Iron High pressure lamp index 10	0,98	0,88	1,01
LED 250 nm	1,00	1,17	1,00
LED 270 nm	1,29	1,04	1,16
LED 280 nm	1,10	0,95	1,05
LED 290 nm	1,09	0,87	1,02
LED 310 nm	0,89	0,96	0,86
LED 330 nm	1,13	1,09	1,12
LED 340 nm	1,16	1,34	1,06
LED 350 nm	1,14	1,00	1,01
LED 360 nm	1,07	1,00	1,09
LED 370 nm	0,86	1,00	1,10

a(Z) values in blue are out of the range from 0.5 up to 2 and set to 1.00 (= no correction possible)
a(Z) values in green are within the range from 0.9 up to 1.1
a(Z) values in red are in the range from 0.8 up to 1.25
a(Z) values in black are in the range from 0.5 up to 2

Some of the sources in the library used for characterising the UV detector heads are shown in Figs. 8 and 9. Calibration correction factors calculated for the sources are listed in Table 1. The correction factors for each source and detector head are given.

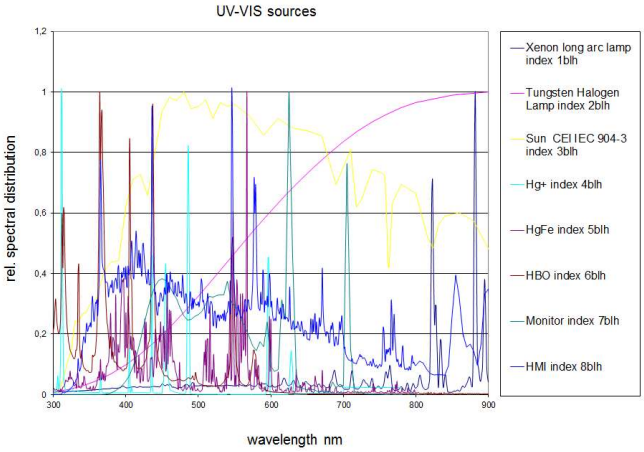

Figure 10. Selection of UV-VIS sources used for the calculation of the calibration correction factor.

Figure 10 shows spectra of suitable sources used for characterizing the blue light hazard detector head. Corresponding correction factors are listed in Table 2. These tables are stored into the read out of the meter and can be selected at each measurement.

As we can see from the calibration correction factors, the spectral mismatch factor is for most of the sources very close to unity. If the user knows the type of the lamp, he can select the source and get corrected values.

Table 2. Correction factors for the blue light hazard detector.

Irradiation Source	UV realized detector head	Blue realized detector head	Red realized detector head	Photometric realized detector head
Xenon long arc lamp index 1blh	1,00	0,98	1,04	0,99
Tungsten Halogen Lamp index 2blh	0,99	1,00	1,02	1,00
Sun CEI IEC 904-3 index 3blh	0,95	0,99	1,10	0,98
Hg+ index 4blh	0,98	1,00	1,00	1,01
HgFe index 5blh	1,09	0,97	1,54	0,98
HBO index 6blh	0,94	0,95	1,00	0,97
Monitor index 7blh	1,00	1,00	1,38	0,97
HMI index 8blh	0,93	0,96	1,19	0,99

a(Z) values in blue are out of the range from 0.5 up to 2 and set to 1.00 (= no correction possible)
a(Z) values in green are within the range from 0.9 up to 1.1
a(Z) values in red are in the range from 0.8 up to 1.25
a(Z) values in black are in the range from 0.5 up to 2

Conclusions

The introduced detector heads allow fast, precise and low cost measurements of the most existing UV sources. Its innovative multiple integral detector design allows it to imitate the UV hazard actinic curve, the UVA radiometric curve and the Blue Light Hazard actinic curve. This technology is able to replace the expensive and immobile monochromators in some applications, especially at safety measurement tasks where a high amount of measurements is required. Thereby it fits the most current regulations like EN 62471:2009-02 for Equipment Safety; 2006/25/EC Guideline; DIN EN 60335-2-27 and DIN EN 14255 for Safety of Workplaces.

References

[1] *Amtsblatt der Europäischen Union* (2005/C 172 E/02) p. 1 (4).

[2] *Expositionsgrenzwerte für künstliche optische Strahlung*, BG-Information BGI 5006 (Berufsgenossenschaft der Feinmechanik und Elektrotechnik, Oktober 2004) pp. 12f, 20f.

[3] "Characterizing the Performance of Integral Measuring UVMeters," ***UVNews* 6**, November 2000, p. A-10.

EUV calibration and irradiation tests of CMOS APS prototypes for EUI, the Extreme Ultraviolet Imager on-board Solar Orbiter

A. BenMoussa[1], B. Giordanengo[1], S. Gissot[1], G. Meynants[2], A. Gottwald[3] and U. Schühle[4]

1. Solar Terrestrial Center of Excellence (STCE), Royal Observatory of Belgium, Brussels, Belgium
2. CMOSIS nv, Antwerpen, Belgium
3. Physikalisch-Technische Bundesanstalt (PTB), Berlin, Germany
4. Max-Planck-Institut für Sonnensystemforschung, Katlenburg-Lindau, Germany

Abstract

For the Extreme Ultraviolet Imager (EUI) of the Solar Orbiter mission, planned to be launched in 2017, a complementary metal oxide semiconductor (CMOS) active pixel sensor (APS) prototypes have been developed. A set of measurements and irradiation tests were carried out to evaluate their EUV performance characteristics and to investigate their expected degradation under the space environment of Solar Orbiter.

Introduction

The Solar Orbiter mission is the next major space observatory of the European Space Agency (ESA) for solar and heliospheric physics studies. The Extreme Ultraviolet Imager (EUI) [1] on-board Solar Orbiter consists of a suite of two high-resolution imagers (HRI) and one dual-band full Sun imager (FSI) telescopes that will provide extreme ultraviolet (EUV, at 17.4 and 30.4 nm) and Lyman-α (hydrogen spectral line at 121.6 nm) images of the solar atmospheric layers. For the EUI instruments, a project has been initiated to develop a dedicated CMOS APS with low readout noise and high sensitivity in the EUV range. To be sensitive to the EUV range, i.e., in the 15-30 nm range, a backside illumination (BSI) approach is proposed. A set of radiometric calibration campaigns in the visible and EUV ranges have been carried out before and after the irradiation tests to characterize and to assess the maturity of the CMOS APS technology.

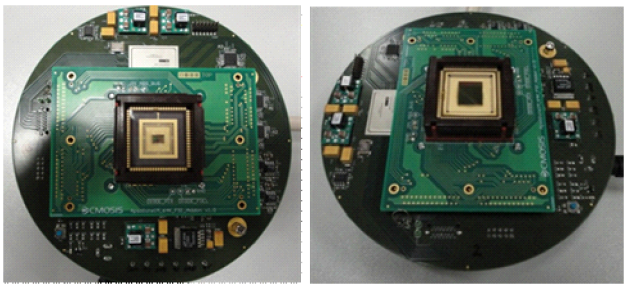

Figure 1. Photography of the prototype sensors, left: 256 x 256 pixels area. Right: 1024 x 1024 pixels format mounted in their vacuum compatible printed circuit boards and protected by a cover glass.

Detector design and operation

The 10x10 μm^2 pixel structure is based on the 4 transistors photodiode pixel design. The EUV sensitivity is achieved with backside illumination on a silicon-on-insulator (SOI) material in 0.18 μm CMOS process. The epitaxial Si layer is thinned down to either 2.75 or 2.6 μm depending on the prototypes to gain further sensitivity in the EUV range. A particularity of the detector is that it applies a so-called 'dual-transfer' scheme to achieve high dynamic range (DR) and to minimize the noise contribution from the analog chain. The approach is to readout the pixel through a high gain (HG) and low gain (LG) path. The associated capacitance nodes determine the sensitivity of the pixel path, i.e. the smaller the capacitance, the higher the conversion gain (volts per electron). As a result, pixel can achieve extremely low readout noise producing a high conversion gain. The sensor architecture details and operation are reported elsewhere [2-3].

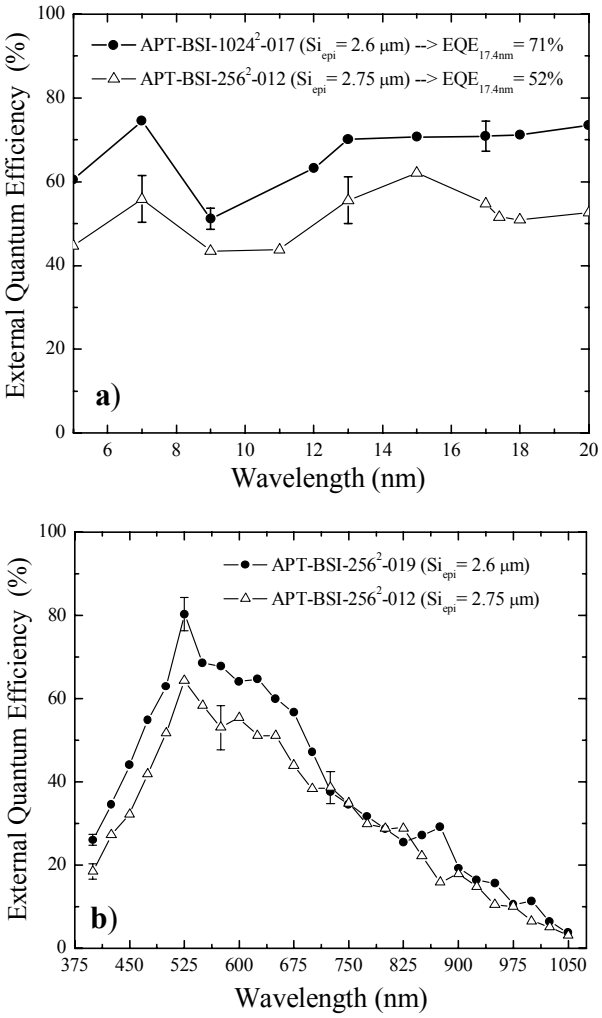

Figure 2. EQE of CMOS APS prototypes a) from 5 to 20 nm and b) from 400 to 1050 nm.

Calibration in the EUV range

The synchrotron radiation calibration campaigns were carried out at the soft X-ray grazing incidence radiometry beamline at the PTB/BESSY II [4]. The External Quantum Efficiency (EQE) was measured between 5 and 20 nm wavelength. As shown in Fig. 2, the detector prototypes are sensitive in the EUV range reaching the EUI requirement of EQE > 50% at 17.4 nm.

Note that the EQE includes also the fill factor, which is assumed to be 100% for BSI detectors.

As shown in Fig. 2, the different SOI thicknesses (epitaxial Si layer) have a significant impact on the EQE in the EUV and in the NUV-VIS ranges.

The photon transfer curve (PTC) [5] measurements were performed at 17.4 nm using two different detector column gain settings for each path. As shown in Fig. 3, there is a good matching between the HG and LG curves. The detector noise (expressed in photon) measured from the HG path is independent of the gain setting due to the high quantum yield at 17.4 nm where 1 absorbed photon generates almost 20 electrons. At this wavelength and flux, the detector has a readout noise (RN) inferior to 5 electrons rms equivalent to less than one photon and a saturated full well charge (FWC) of near 7000 photons (i.e. 90 000 electrons). In the EUV range, the detector is left essentially photon shot noise limited, resulting in a lower detection limit and, thus, a larger dynamic range (DR).

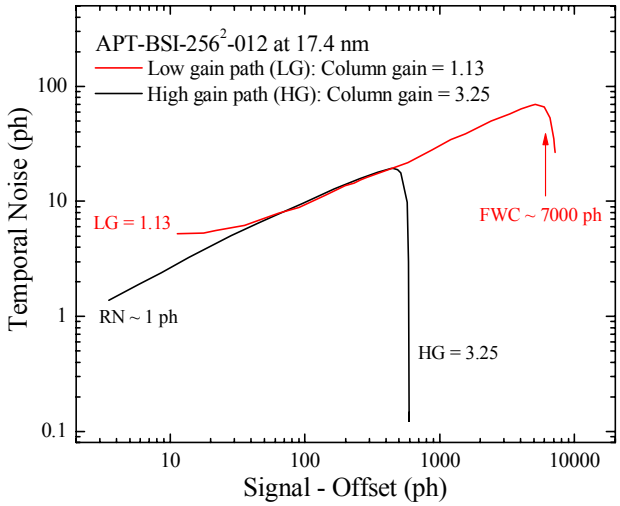

Figure 3. PTC at 17.4 nm for the HG and LG paths.

Irradiation damage tests

In space environment, ionization and atomic displacement are the two main types of interaction of radiation with materials. Energetic particles or photons passing through matter lose energy through a variety of interactions and scattering effects [6]. Gamma-rays (Co-60), heavy ions, and proton sources have been used, at room temperature, for the irradiation damage evaluation of the detector prototypes. The irradiations were carried out mainly at the Cyclotron Research Center (CRC) facility in Louvain-La-Neuve (Belgium). The ESA specifications (ECSS) were applied [7-8]. During each irradiation test, three detectors were tested unbiased (except during the heavy ions tests) as well as during the annealing periods. The detectors were characterized in the EUV range before and after the irradiation tests and annealing [9].

The most significant radiation damage measured is an increase in dark current (DC) associated with an increase in pixel noise and a decrease in EQE. As an example Fig. 4 shows the DC measured at around 30°C as a function of the total ionizing dose (TID) and during the annealing.

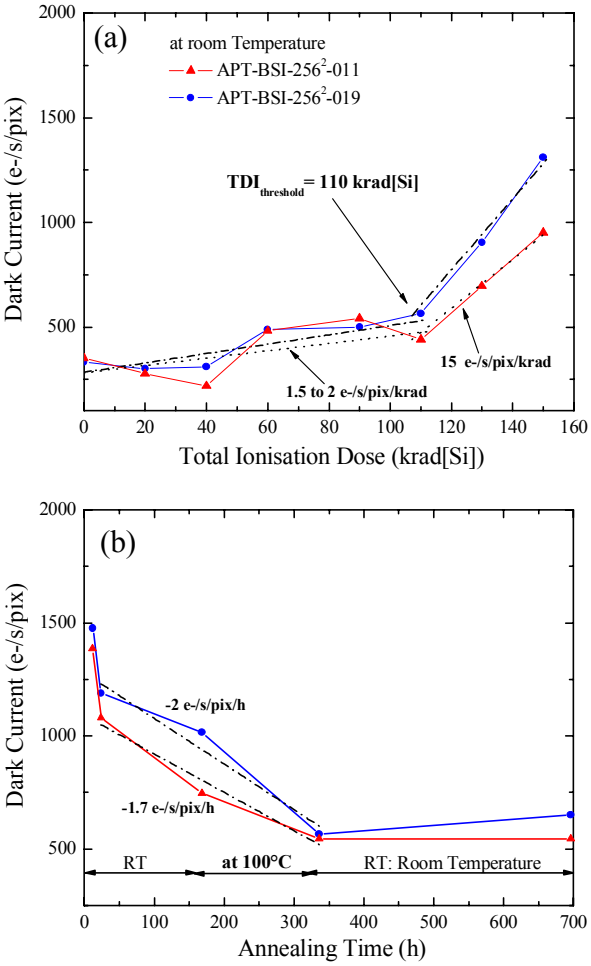

Figure 4. Dark current at room temperature (a) as a function of the total ionizing dose and (b) after irradiation, as a function of elapsed time during annealing (in hours) at room temperature and at 100°C.

As seen in Fig. 4 (a), the DC increases slightly with the gamma-ray dose up to 110 krad(Si). Below this TID threshold value, no significant DC increase can be observed. The high TID threshold value is probably associated to the scaling of technology i.e. 0.18 µm CMOS process. After irradiation and 24 hours at room temperature, the DC decays exponentially with time and the detector is gradually recovered . After two weeks, the DC remains almost constant but does not return completely to its pre-irradiated value.

Table 1 summarizes all relevant detector parameter values before and after irradiation and annealing tests. All measurements were performed with column gain settings as follows: HG=3.25 and LG=1.13.

In contrast to the degradation of the EQE after TID and proton irradiations the EQE after heavy ion irradiation remains unaffected within the error bars. Moreover, during the heavy ion irradiation (single event effect) no latch up has been detected on the three detectors up to a linear energy transfer (LET) of 67.7 MeV cm^2 mg^{-1}.

Table 1. Readout noise (RN), conversion gain (G), dark current (DC at room temperature) and the EQE (at 17.4 nm) before and after irradiation tests and annealing.

Parameters	RN_{HG} (e-)	G_{HG} (DN/e-)	G_{LG} (DN/e-)	DC_{HG} (e-/s/pix)	EQE (@17.4nm)
Gamma rays (APT-64k-BSI-011, TID=150 krad(Si))					
Pre-irradiation	3.7	0.590	0.034	496	52% (Si=2.75 µm)
Post-irradiation	6.8	0.608	0.033	700	32%
Heavy Ions (APT-64k-BSI-020, 459 MeV, LET of 67.7 MeV cm^2 mg^{-1})					
Pre-irradiation	4.0	0.613	0.034	1000	62% (Si=2.6 µm)
Post-irradiation	4.1	0.617	0.033	18000	62%
Proton (APT-64k-BSI-017, 15 MeV, 4 10^{11} p cm^{-2})					
Pre-irradiation	3.3	0.578	0.036	290	62% (Si=2.6 µm)
Post-irradiation	8.0	0.601	0.033	98010	22%

Conclusions

Backside illuminated CMOS APS prototype devices have been fully characterized at visible and EUV wavelengths before and after irradiation tests. The detectors show low read noise (RN < 5e- rms), high full well capacity (FWC > 80,000 e-) with good EUV sensitivity, i.e. EQE > 50% at 17.4 nm, making this detector a good candidate for the EUI instruments. The radiation hardness has been investigated thanks to exposure to gamma-rays, heavy ions, and protons, in order to reach the ESA Technology Readiness Level 5, i.e. the component validation in the relevant environment. Although there is room for optimisation [2,9], the test campaigns give promising results for EUI flight model detector fabrication which imposes the use of large, thinned arrays for backside illumination, namely formats of 2048 x 2048 pixels for the two High Resolution Imagers and 3072 x 3072 pixels for the Full Sun Imager, all with a 10 µm pixel pitch.

Acknowledgement. This work is based on a development project financed by the Belgian Federal Science Policy Office (BELSPO) which is part of the EUI project (ref : EUI PEA C90343).

References

[1] http://eui.sidc.be/

[2] A. BenMoussa, B. Giordanengo, S. Gissot, G. Meynants, X. Wang, B. Wolfs, J. Bogaerts, U. Schühle, G. Berger, A. Gottwald, C. Laubis, U. Kroth and F. Scholze, "Characterization of backside-illuminated CMOS APS prototypes for the Extreme Ultraviolet Imager on-board Solar Orbiter," *IEEE Electron devices* (Submitted).

[3] X. Wang, B. Wolfs, J. Bogaerts, G. Meynants and A. BenMoussa, "High Dynamic Range (HDR) Back-side Illuminated (BSI) CMOS Image Sensor for Extreme UV Detection," *Proc. SPIE* **8298**, 82980B (2012).

[4] F. Scholze, B. Beckhoff, G. Brandt, R. Fliegauf, R. Klein, B. Meyer, D. Rost, D. Schmitz and M. Veldkamp, "The new PTB-beamlines for high accuracy EUV reflectrometry at BESSY II," *Proc. SPIE* **4146**, 72-82 (2000).

[5] J. Janesick, *Photon Transfer*, SPIE Press Book (2007).

[6] A. Homes-Siedle and L. Adams, *Handbook of radiation effects*, 2nd edition (oxford university press, 2002).

[7] ESCC Radiation Standards. "Total Dose Steady-State Irradiation Test Method" ESA/ESCC 22900. http://www.ecss.nl/

[8] ESCC Radiation Standards. "Single Event Effects Test Method and Guidelines" ESA/ESCC 25100. http://www.ecss.nl/

[9] A. BenMoussa, S. Gissot, B. Giordanengo, G. Meynants, X. Wang, B. Wolfs, J. Bogaerts, U. Schühle, G. Berger A. Gottwald, C. Laubis, U. Kroth and F. Scholze, "Irradiation damage tests of backside-illuminated CMOS APS prototypes for the Extreme Ultraviolet Imager on-board Solar Orbiter," *IEEE TNS* (Submitted).

UVNet Workshop on August 27 – 28, 2013 in Davos

The Thematic Network for Ultraviolet Measurement will arrange a two-day workshop on Tuesday and Wednesday, August 27 – 28, 2013. The workshop will be hosted by the Physikalisch-Meteorologisches Observatorium Davos, World Radiation Center, in Davos, Switzerland.

Part of the workshop will be dedicated to presenting results of the EMRP-project ENV03 "Traceability for surface spectral solar ultraviolet radiation." Information on this project can be found in the project website:

http://projects.pmodwrc.ch/env03/

In addition, there will be an opportunity to present results of other UV-related activities. On Wednesday, there will be a presentation of the new renovated premises of PMOD/WRC.

The calls for participation and abstracts will be announced via UVNet mailing list in February. The abstracts should be submitted by May 24, 2013. The registration deadline will be July 15, 2013. The price for the workshop is CHF 150, including a workshop dinner on Tuesday evening.

Further information will follow. If you already wish to know something, please contact Julian Gröbner (julian.groebner@pmodwrc.ch).

EMRP
European Metrology Research Programme
Programme of EURAMET

The EMRP is jointly funded by the EMRP participating countries within EURAMET and the European Union